EGTRIB Journal
JOURNAL OF
THE EGYPTIAN SOCIETY OF TRIBOLOGY
VOLUME 22, No. 1, January 2025, pp. 122 - 163 ISSN 2090 - 5882
(Received September 28. 2024, Accepted in final form October 25. 2024) jest.journals.ekb.eg

DYNAMIC MODELING AND COMPUTED TORQUE CONTROL OF A 5-DOF MANIPULATOR ROBOT CONSIDERING FRICTION

Elmoushi EL Sayed, Hassan Hassan A., Ayoub Nasser and Abdelwahab Sabreen A.

Production Technology Department, Faculty of Technology and Education, Helwan University, Cairo, Egypt.

ABSTRACT

This paper presents the methodology used to model, simulate, and control a five-degree-of-freedom robot manipulator using the Computed Torque Control (CTC) technique. It formulates the basic control equations for model-based control strategies. The robot dynamics are analyzed and obtained by modeling the manipulator using SolidWorks and then exporting the CAD files to the MATLAB/SimMechanics environment to generate the block diagram of the multi-body system. The system motion equation is obtained through the dynamic Lagrange-Euler equation, which depends on the system's kinetic energy and potential energy considering friction. Then, a manipulator controller is designed to control the end-effector position's task space, and CTC is used with linear PD and PID controllers with feedback. The simulation results show that PD-CTC is effective and significantly superior to PID-CTC in achieving the required response of joint position, angular velocity, angular acceleration, and torque to achieve the required end-effector position, velocity, and acceleration. This study provides valuable insights to researchers on how to easily create dynamic equations for control and simulation, and evaluate and modify the system before implementing the prototype.

KEYWORDS

Robot dynamics, PID/PD controllers, Computed torque control, MATLAB SimMechanics, Friction model.

INTRODUCTION

Modeling and controlling robot dynamics has become more difficult as robotic systems become more complex ,[1-3], because the robot manipulator is a nonlinear system, [4]. Modeling and simulating the dynamics of the manipulator is an essential part of the control and development process of robotic systems, simulating robot kinematics, analyzing dynamics, and designing control algorithms, [5]. To design the control algorithm, a model of the manipulator's kinematics or dynamics must be developed, [6]. Manipulator dynamics is concerned with deducing linear equations that clearly describe the relationship between the joint position, angular velocity, angular acceleration, torque or force required to achieve the desired position, velocity

and acceleration of the end-effector, [7], and the system geometry. Dynamic equations play an important role in developing the basic control equations for model-based control strategies, [8 - 10], achieving precise control of end-effectors, prototyping, [11], mechanical design, [5], motor selection, [12], and real-time control and simulation. The dynamic model of the moving manipulator represents the relationship between the joint torque and its motion. There are many modeling methods for deriving dynamic models of manipulators in the literature, including the Newton-Euler method, [13], the Kane's approach, [14], the d'Alembert method, the recursive Lagrange method, [15 - 16], and the Lagrange-Euler method, [7, 17 - 19]. In the literature, the Lagrange-Euler formula is widely used to model robots. The Lagrange-Euler formula is considered a simple formula from a conceptual and methodological standpoint. It is a formula that includes all linear and angular dynamics in one equation; it depends on the kinetic energy and potential energy of the system.

It is well known that most of the industrial manipulators are equipped with the simplest proportional-derivative (PD) or proportional-integral-derivative (PID) control, [20]. A PD/PID controller is a linear controller that uses feedback in the control mechanism to enhance the stability of the system that controls its variables [21], and it is the most accurate, stable, and common control technique for building manipulator controllers. There are also many control techniques used in the development of manipulator controllers in the literature, such as linear and nonlinear predictive controllers, [22], adaptive control, [23], sliding mode control [19], fuzzy control [24], and adaptive fuzzy control, [25]. The PD controller in the task space of the robot manipulator is the simplest control scheme, and the guaranteed (bounded) stability of the PD controller in the task space can be obtained, [26 - 27]. To obtain the asymptotic stability of the controller, model-based control should be implemented when designing the controllers via computed torque control (CTC), [4, 12, 28 - 29], which is a technique to eliminate nonlinearities and unmolded dynamics. CTC is a method to achieve precise control of the manipulator motion during the performance of a task by applying torque control to the end effector, [4]. The controller acts as a model-based inverse dynamic controller, [9], providing high-precision tracking performance but requiring a very accurate dynamic model, [30].

The CTC technique with a classical PD/PID controller (PD-CTC, PID-CTC) is used to eliminate nonlinear dynamics, enabling the system to operate with higher tracking accuracy, lower feedback gain, higher suitability of conformal control, and lower energy consumption compared with model-free methods, [4, 12, 28]. The system dynamics can be approximated as a linear system while the manipulator performs tasks at low speeds. Using a linear control scheme based on the linearity of the system is one of the simple design methods for controlling the robot manipulator, and the model-based PD/PID controller is an effective control method. To adjust the control gains, specific methods are used to adjust the PID parameters because the robot's dynamics are non-linear, [31]. Including the methods of Ziegler-Nichols, Cohen-Coon, and model-based, the robot's processor has 15 gains to adjust, and when one gain is adjusted, the other 14 gains need to be adjusted in turn due to the dynamic

coupling of the robot. To reduce the steady-state error, K_i must be increased, to get less overshot, K_P must be reduced; and to get less settling time, K_d should be reduced. The unified robot description format (URDF) is a unified format for describing robot kinematics, dynamics, and geometry, and is the most widely used format in academia and industry for modeling multi-body systems. A URDF model is an XML file that describes a robot in high format, it can be imported or exported using various tools to visualize or simulate the robot, [32]. It represents kinematic structure, dynamic parameters (mass, center of mass or center of gravity, and inertia matrix), visual representation (geometry, origin, and materials), and physical collision geometry (geometry, and origin).

This paper presents the dynamic and kinematic modeling of a 5-degree-of-freedom manipulator, its simulation, and control using the CTC method, and formulates the control equations in the task space for model-based control strategies. The mechanical structure of the robot manipulator is designed, the specifications of the materials used in the robot construction process are accurately added, the URDF model of the robot is exported through SolidWorks and imported into MATLAB® in the Simscape Multibody environment, and finally, the DC motor is modeled considering friction, the computed torque controller is designed, the PD and PID controllers are added, and the control results are compared.

This paper contains six sections; the first section is the introduction. The 2nd section presents the mechanical design of the robot manipulator in SolidWorks. In the 3rd section, the kinematic and dynamic analysis of the robot manipulator are introduced. The 4th section explained the PD/PID control in task space. The 5th section gave the results and discussion. The 6th section drawn the main conclusions; this was followed by the references.

1 MECHANICAL DESIGN OF ROBOT MANIPULATOR IN SOLIDWORKS SOFTWARE

To extract the dynamic equations of the 5-DOF manipulator, it is required to know the center of mass position of the rigid body specified as a vector of the form $[x\ y\ z]$. The vector describes the location of the center of mass of the rigid body, relative to the body frame in meters. Also, it is required to find out the moment of inertia for each link in the robot specified as a vector of the form $[I_{xx}\ I_{yy}\ I_{zz}\ I_{yz}\ I_{xz}\ I_{xy}]$. The vector is expressed in kilograms per square meter in relation to the body frame. The inertia tensor is a positive definite matrix as in Equation (1).

$$I = \begin{bmatrix} i_{xx} & i_{xy} & i_{xz} \\ i_{xy} & i_{yy} & i_{yz} \\ i_{xz} & i_{yz} & i_{zz} \end{bmatrix} \quad (1)$$

The diagonal elements are the moments of inertia, and the off diagonals are products of inertia. Only six of these nine elements are unique (three moments and three products of inertia). Because of symmetry, the products of inertia of the robot linkages are frequently zero. A 5-DOF manipulator dynamic model thus entails 50 inertial parameters. Three parameters: center of mass for each link, 6 moments of inertia parameters for each link, and mass for each link. Because of friction and the

inertia of the motor armature, each joint could have additional parameters. Setting up numerical values for these many factors is a challenging task. Because there was no precise information about the moment of inertia or center of mass, the model was simulated in the SolidWorks software environment to obtain them, [19]. Information about the center of mass and moment of inertia were derived from the output of SolidWorks in the part (mass properties). A schematic model of the robot simulated in SolidWorks is shown in Fig. 1.

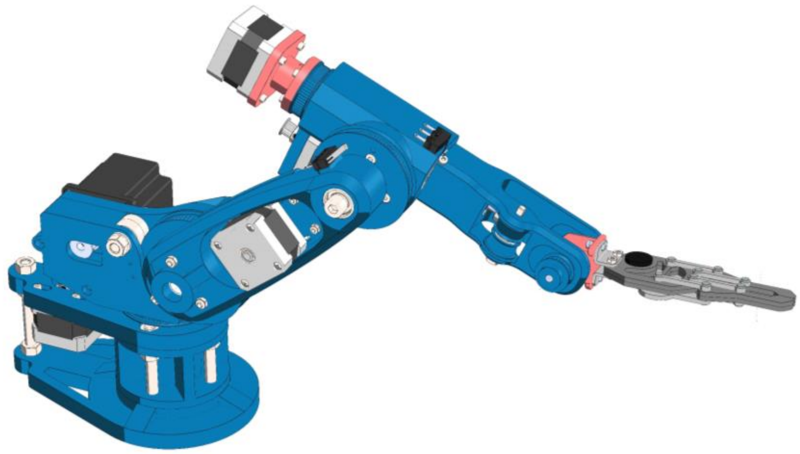

Fig. 1. Design of a 5-degree-of-freedom robotic manipulator in SolidWorks.

This robot simulation model comprises six parts, five links, and a base. All joints of the robot are revolute. Table 1 and Table 2 show the center of mass, and Table 2. Moment of inertia of the center of mass for all joints of the robotic arm.

Both tables contain information such as weight, moment of inertia about the center of mass of each link, and the center of mass of each link expressed in the base coordinate frame.

Table 1. Center of mass for all joints of the robotic arm.

Joints	Center of mass expressed in base coordinate frame m			Mass
	x	y	z	kg
Joint 1	-0.032346	0.01033	0.048135	1.0747
Joint 2	0.072502	-0.018534	0.051893	0.7287
Joint 3	0.023432	0.015484	0.0034787	0.6747
Joint 4	-0.018578	0.00149	-0.074565	0.5837
Joint 5	-0.019508	-0.064902	0.000009	0.1186

Table 2. Moment of inertia of the center of mass for all joints of the robotic arm.

Joints	Moment of inertial for the center of mass expressed in the base coordinate frame $kg.m^2$								
	I_{xx}	I_{xy}	I_{xz}	I_{yx}	I_{yy}	I_{yz}	I_{zx}	I_{zy}	I_{zz}
Joint 1	0.0031	0.0043	0.0019	0.0043	-0.005	0.0017	0.0019	0.0017	0.003
Joint 2	0.0021	0.0066	0.0048	0.0066	-0	-0.0028	0.0048	-0.0028	-0
Joint 3	0.4028	0.6201	0.7881	0.6201	-0.0276	-0.0616	0.7881	-0.0616	-0.2498
Joint 4	0.0034	0.0034	0.0002	0.0034	0	-0	0.002	-0	0
Joint 5	0.5892	0.0067	0.5842	0.0067	-0.0001	0	0.5842	0	-0.0076

2 KINEMATIC AND DYNAMIC ANALYSIS OF ROBOT MANIPULATOR

This section extracts the kinematic and dynamic equations used to control the manipulator arm. Dynamic modeling is essential for applying different control strategies for the manipulator.

3.1 Direct Kinematics of Robot Manipulator

Kinematics is a subfield of physics developed in classical mechanics that studies motion regardless of the forces that make it move. To obtain the kinematic equations and geometric properties of motion for the position variables of a manipulator arm mechanism, the Denavit-Hartenberg (D-H) convention, [33-34] was used, which is a systematic method for establishing the geometry of a series of links and joints to connect the reference frames to the links of the spatial-kinetic chain, it was developed to derive the forward kinematics of serial maneuvers. This is done by obtaining a simplified kinematic model of the robot as shown in Fig. 2. The link is determined through four parameters through the frames assigned to each link, starting from the fixed reference frame, and ending with the frame fixed at the end-effector. The frame assignments follow the D-H convention, which enables the location of each coordinate frame to be represented concerning each other, as shown in Table 3.

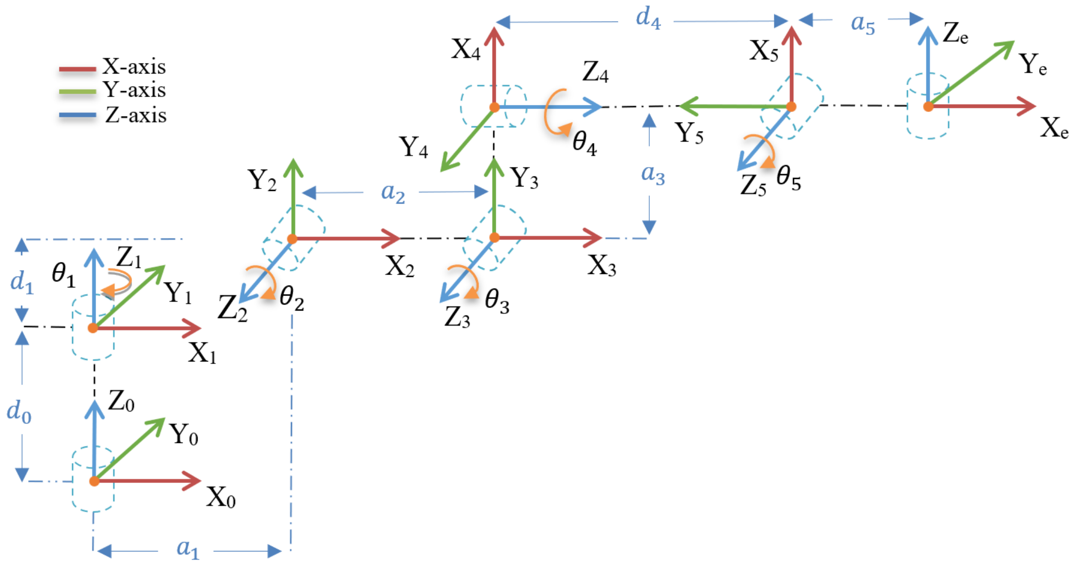

Fig. 2. Details of coordinate frames (D-H parameters) used for the 5-DOF manipulator.

Table 3. Kinematic parameters (D-H parameters) for the 5-DOF manipulator All lengths in m.

Link	Joint	a_i	α_i	d_i	θ_i
0	0-1	0	0	0.084	0
1	1-2	0.0375	pi/2	0.0513	θ_1
2	2-3	0.16	0	0	θ_2
3	3-4	0.015	pi/2	0	$\theta_3 + pi/2$
4	4-5	0	−pi/2	0.1384	θ_4
5	5-e	0.127	−pi/2	0	$\theta_5 - pi/2$

Where a_i (Link length) is the distance between the Z_{i-1} and Z_i axes along the X_i axis; for intersecting axes a_i is parallel to $Z_{i-1} \times Z_i$. α_i (Link twist) is the angle from the Z_{i-1} axis to the Z_i axis about the X_i axis. d_i (Link offset) is the distance from the origin of frame j-1 to the X_i axis along the Z_{i-1} axis. θ_i (Joint angle) is the angle between the X_{i-1} and X_i axes about the Z_{i-1} axis. The D-H representation results in a 4×4 homogeneous transformation matrix. This is done using the four parameters of this convention which describes each correlation with a coordinate transformation from the synchronous coordinate system to the previous coordinate system, as shown in Equation (2) [35].

$$ {}^{i-1}T_i = \left[\begin{array}{ccc|c} \cos\theta_i & -\sin\theta_i\cos\alpha_i & \sin\theta_i \sin\alpha_i & a_i\cos\theta_i \\ \sin\theta_i & \cos\theta_i\cos\alpha_i & -\cos\alpha_i\sin\alpha_i & a_i\sin\theta_i \\ 0 & \sin\alpha_i & \cos\alpha_i & d_i \\ \hline 0 & 0 & 0 & 1 \end{array}\right] \quad (2) $$

Where R is the 3×3 sub-matrix in the upper left that represents the rotation from frame $i-1$ to frame i and T is the 3×1 submatrix in the upper right that represents the translation (or displacement) from frame $i-1$ to frame i. The forward kinematic solution provides the coordinate frame, or posture, of the last link for an n-axis rigid-

link manipulator. For a 5-axis robot, the overall manipulator transform ${}^{0}T_n$ is frequently written as T_n or T_5 for a 5-axis robot, as shown in Equations (3) and (4).

$$ {}^{0}T_n(\theta_i) = {}^{0}T_1(\theta_1)\, {}^{1}T_2(\theta_2)\, {}^{2}T_3(\theta_3) \dots\dots\dots {}^{n-1}T_n(\theta_n) = \prod_{i=1}^{n} {}^{i-1}T_i(\theta_i) \quad (3) $$

Where n and ${}^{0}T_n$ represent the total number of degrees of freedom and the homogeneous matrix containing the position and orientation of the end-effector pose concerning the reference frame, respectively. θ_i with $i = 1, 2, \dots, n$ represents the angle position for each robot joint. The homogeneous matrix ${}^{i-1}T_i$ transforms the frame attached to link $i - 1$ into the frame attached to link i.

$$ {}^{0}T_e(\theta_i) = {}^{0}T_1(\theta_i)\, {}^{1}T_2(\theta_i)\, {}^{2}T_3(\theta_i)\, {}^{3}T_4(\theta_i)\, {}^{4}T_5(\theta_i)\, {}^{5}T_e(\theta_i) \quad (4) $$

Where ${}^{0}T_e$ is the homogeneous transformation describing the position of the end-effector frame with respect to the world coordinate system 0. ${}^{0}T_1, {}^{1}T_2, {}^{2}T_3, {}^{3}T_4, {}^{4}T_5, {}^{5}T_e$ are transformation matrices that describe the translation and rotation of reference frames for the 5-DOF manipulator.The above parameters in Table 3 are used for kinematic modeling of the robot. This is done by substituting the values of those parameters $a_i, \alpha_i, d_i, \theta_i$ for each joint into Equation (2), as shown below:

$$ {}^{0}T_1 = \begin{bmatrix} 1 & 0 & 0 & 0 \\ 0 & 1 & 0 & 0 \\ 0 & 0 & 1 & 0.084 \\ 0 & 0 & 0 & 1 \end{bmatrix} \quad (5) $$

Where ${}^{0}T_1$ is the transformation matrix that results from the shift between Joint 0 and Joint 1 by setting the D-H parameters for Link 0 from Table 3.

$$ {}^{1}T_2 = \begin{bmatrix} \cos\theta_1 & 0 & \sin\theta_1 & 0.0375\cos\theta_1 \\ \sin\theta_1 & 0 & -\cos\theta_1 & 0.0375\sin\theta_1 \\ 0 & 1 & 0 & 0.0513 \\ 0 & 0 & 0 & 1 \end{bmatrix} \quad (6) $$

Where ${}^{1}T_2$ is the transformation matrix results from the shift between Joint 1 and Joint 2 by setting the D-H parameters for Link 1 from Table 3.

$$ {}^{2}T_3 = \begin{bmatrix} \cos\theta_2 & -\sin\theta_2 & 0 & 0.16\cos\theta_1 \\ \sin\theta_2 & \cos\theta_2 & 0 & 0.16\sin\theta_1 \\ 0 & 0 & 1 & 0 \\ 0 & 0 & 0 & 1 \end{bmatrix} \quad (7) $$

Where ${}^{2}T_3$ is the transformation matrix that results from the shift between Joint 2 and Joint 3 by setting the D-H parameters for Link 2 from Table 3.

$$ {}^{3}T_4 = \begin{bmatrix} \cos(\theta_3 + \frac{\pi}{2}) & 0 & \sin(\theta_3 + \frac{\pi}{2}) & 0.015\cos(\theta_3 + \frac{\pi}{2}) \\ \sin(\theta_3 + \frac{\pi}{2}) & 0 & -\cos(\theta_3 + \frac{\pi}{2}) & 0.015\cos(\theta_3 + \frac{\pi}{2}) \\ 0 & 1 & 0 & 0 \\ 0 & 0 & 0 & 1 \end{bmatrix} \quad (8) $$

Where ${}^{3}T_4$ is the transformation matrix that results from the shift between Joint 3 and Joint 4 by setting the D-H parameters for Link 3 from Table 3.

$$ {}^{4}T_5 = \begin{bmatrix} \cos(\theta_4) & 0 & -\sin(\theta_4) & 0 \\ \sin(\theta_4) & 0 & \cos(\theta_4) & 0 \\ 0 & -1 & 0 & 0.1384 \\ 0 & 0 & 0 & 1 \end{bmatrix} \quad (9) $$

Where ${}^{4}T_5$ is the transformation matrix that results from the shift between Joint 4 and Joint 5 by setting the D-H parameters for Link 4 from Table 3.

$$
{}^{5}T_e = \begin{bmatrix} \cos(\theta_5 - \frac{\pi}{2}) & 0 & -\sin(\theta_5 - \frac{\pi}{2}) & 0.127\cos(\theta_3 - \frac{\pi}{2}) \\ \sin(\theta_5 - \frac{\pi}{2}) & 0 & \cos(\theta_5 - \frac{\pi}{2}) & 0.127\sin(\theta_3 - \frac{\pi}{2}) \\ 0 & -1 & 0 & 0 \\ 0 & 0 & 0 & 1 \end{bmatrix} \quad (10)
$$

Where ${}^{5}T_e$ is the transformation matrix that results from the shift between Joint 5 and Joint e by setting the D-H parameters for Link 5 from Table 3. By applying Equation (4) using the above values of transformation matrices, the correlation transformations can be linked (multiplied together) to get the transformation that connects the base frame (0) to the respondent end frame (e).

$$
{}^{0}T_e(\theta_i) = \begin{bmatrix} r_{xx} & r_{xy} & r_{xz} & p_x \\ r_{yx} & r_{yy} & r_{yz} & p_y \\ r_{zx} & r_{zy} & r_{zz} & p_z \\ 0 & 0 & 0 & 1 \end{bmatrix} \quad (11)
$$

Where ${}^{0}T_e$ is the transformation matrix that results from the shift between Joint 0 and Joint e. The transformation given by Equation (11) is a function of all the fifth common variables, and the Cartesian position and direction of the last link can be calculated using the above equation. The first three columns in the matrices represent the orientation of the end-effector, whereas the last column represents the position of the end-effector. The orientation and position of the end-effector can be calculated in terms of joint angles as in Equations (12) to (23).

$$r_{xx} = s_{145} + c_{1235} - c_{15}s_{23} - c_{124}s_{35} - c_{134}s_{25} \quad (12)$$

$$r_{yx} = c_{235}s_1 - c_1s_{45} - c_5s_{123} - c_{24}s_{135} - c_{34}s_{125} \quad (13)$$

$$r_{zx} = c_{25}s_3 + c_{35}s_2 + c_{234}s_5 - c_4s_{235} \quad (14)$$

$$r_{xy} = -c_4s_1 - c_{12}s_{34} - c_{13}s_{24} \quad (15)$$

$$r_{yy} = c_{14} - c_2s_{134} - c_3s_{124} \quad (16)$$

$$r_{zy} = c_{2+3}s_4 \quad (17)$$

$$r_{xz} = c_5s_{14} - c_{123}s_5 + c_1s_{235} - c_{1245}s_3 - c_{1345}s_2 \quad (18)$$

$$r_{yz} = s_{1235} - c_{23}s_{15} - c_{15}s_4 - c_{245}s_{13} - c_{345}s_{12} \quad (19)$$

$$r_{zz} = c_{2345} - c_3s_{25} - c_2s_{35} - c_{45}s_{23} \quad (20)$$

$$p_x = 0.0375c_1 + 0.16c_{12} - 0.1384c_1s_{23} + 0.127s_{145} + 0.1384c_{123} - 0.015c_{12}s_3 - 0.015c_{13}s_2 + 0.127c_{1235} - 0.127c_{15}s_{23} - 0.127c_{124}s_{35} - 0.127c_{134}s_{25} \quad (21)$$

$$p_y = 0.015s_1 + 0.16c_2s_1 - 0.015c_2s_{13} - 0.015c_3s_{12} - 0.127c_1s_{45} - 0.1384s_{123} + 0.1384c_{23}s_1 + 0.127c_{235}s_1 - 0.127c_5s_{123} - 0.127c_{24}s_{135} - 0.127c_{34}s_{125} \quad (22)$$

$$p_z = 0.16s_2 + 0.015c_{23} + 0.1384c_2s_3 + 0.1384c_3s_2 - 0.015s_{23} + 0.127c_{25}s_3 + 0.127c_{35}s_2 + 0.127c_{234}s_5 - 0.127c_4s_{235} + 0.1353 \quad (23)$$

where c_i and s_i are representative of $cos\theta_i$ and $sin\theta_i$, respectively.

3.2 Jacobian Matrix of Robot

Differential kinematics is what gives the relationship between the joint velocities and the corresponding end-effector linear and angular velocity as in Equation (24), [36 - 37]. This mapping is described by a geometric Jacobian matrix, which depends on the manipulator configuration.

$$v_e = \begin{bmatrix} \dot{p}_e \\ \omega_e \end{bmatrix} = \begin{bmatrix} J_P(q) \\ J_O(q) \end{bmatrix} . \dot{q} = J(q). \dot{q} \quad (24)$$

Where v_e is a (6×1)vector of the linear and angular velocity of the end-effector, and $\dot{q}$ is a $(n \times 1)$ vector of the joint velocities. J is the robot Jacobian matrix and has a

size of $(6 \times n)$ matrix. n depends on the number of the manipulator's joints.The linear velocity and angular velocity of the end-effector of the robot can be calculated as in Equation (25). This expression allows the Jacobian to be calculated simply and systematically based on the forward kinematic relationships. It is possible through the Jacobin equation to calculate the speed of any point on the processor and not just calculate the speed of the end-effector. This will be important when we need to calculate the velocity of the center of mass of different links to derive the dynamic equations of motion.

$$J = \begin{bmatrix} J_{v_i} \\ J_{\omega_i} \end{bmatrix} = \begin{bmatrix} \frac{\partial p_e(q)}{\partial q_i} \\ z_{i-1} \end{bmatrix} \quad (25)$$

Using the Cartesian coordinates $x, y,$ and z, the values of $x, y,$ and z can be found in the forward kinematics in the fourth column of the point that is expressed in the same frame, and taking the differentiation of that and the Jacobian matrix if this vector was expressed in frame 0, then the position p_e now is x, y and z of the end-effector, the point of influence terminal and the differential are taken concerning q_1, q_2, q_nwhich is also the Jacobian associated with linear motion. It's important to make sure that everything about all these vectors describing the Jacobian is expressed in the same frame, so this is a vector representation of Jacobian, and if the homogeneous transformation shift is calculated, then $z_1, z_2, z_n,$ and p_e can be extracted, and the simple differentiation can be done as shown in Equations (26) and (28) to find the Jacobian matrix.

$$J_v = \begin{bmatrix} \dot{x} \\ \dot{y} \\ \dot{z} \end{bmatrix} = p_e = \frac{\partial p}{\partial q_1} . \dot{q}_1 + \frac{\partial p}{\partial q_2} . \dot{q}_2 + \cdots + \frac{\partial p_e}{\partial q_n} . \dot{q}_n \quad (26)$$

$$J_v = \begin{bmatrix} \frac{\partial p_e}{\partial q_1} & \frac{\partial p_e}{\partial q_2} & \cdots & \frac{\partial p_e}{\partial q_n} \end{bmatrix} \quad (27)$$

$$J = \begin{bmatrix} \frac{\partial p_e}{\partial q_1} & \frac{\partial p_e}{\partial q_2} & \frac{\partial p_e}{\partial q_3} & \cdots & \frac{\partial p_e}{\partial q_n} \\ z_0 & z_1 & z_2 & \cdots & z_n \end{bmatrix} \quad (28)$$

The Jacobian can be expressed in frame 0 as shown in Equation (29).

$$J^0 = \begin{bmatrix} \frac{\partial^0 p_e}{\partial q_1} & \frac{\partial^0 p_e}{\partial q_2} & \frac{\partial^0 p_e}{\partial q_3} & \cdots & \frac{\partial^0 p_e}{\partial q_n} \\ z_0 & z_1 & z_2 & \cdots & z_n \end{bmatrix} \quad (29)$$

This Jacobian computation already exists within the homogeneous transformation, it is calculated at the same time when calculating the forward kinematics $x, y,$ and z, by deducing the z rays in the frame 0 and filling in the Jacobian matrix, and for the J_v part where this differentiation will be used to get on the Jacobian of the robotic arm, so the Jacobian matrix of the robotic arm is got once the homogeneous transformation is computed from e frame to frame 0. So, $x, y,$ and z are taken and are derived concerning q_1, which will give the first column, this column corresponds to the contribution of the first joint, so the differentiation is done for the first column related to q_1, the second column related to q_2, the third column related to q_3, the fourth column related to q_4, and the fifth column related to q_5, x_p is copied from x, y and z in the homogeneous transformation if the manipulator is working within Cartesian coordinates. Applying Equation (28) to the manipulators with 5-DOF, because all joints of the robot are revolute, the Jacobian matrix of the robot can be calculated as shown in Equation (30) [36].

$$J=\begin{bmatrix} \frac{\partial p_e}{\partial q_1} & \frac{\partial p_e}{\partial q_2} & \frac{\partial p_e}{\partial q_3} & \frac{\partial p_e}{\partial q_4} & \frac{\partial p_e}{\partial q_5} \\ z_0 & z_1 & z_2 & z_3 & z_4 \end{bmatrix} \quad (30)$$

Where z_0, z_1, z_2, z_3, z_4 are the first three elements of the third column of the $^0T_1$, $^0T_2$, $^0T_3$, $^0T_4$, $^0T_5$ matrixes obtained by successive multiplication of Equations (4) to (9) matrixes, respectively, and $\partial p_e/\partial q_1, \partial p_e/\partial q_2, \partial p_e/\partial q_3, \partial p_e/\partial q_4, \partial p_e/\partial q_5$ are the partial derivation of x, y, and z. The partial derivation of x, y, and z can be found in the forward kinematics as the first three elements of the fourth column of the ^0T_e matrix. Computation of the unit vectors of revolute joint axes given as in Equations (9) and (10). While Equations from (21) to (23) represent the x, y, z values of the position of the end-effector of the manipulator, with $z_0 = [0, 0, 1]^T$.

$$z_1 = \begin{bmatrix} s_1 \\ -c_1 \\ 0 \end{bmatrix} \quad (31)$$

$$z_2 = \begin{bmatrix} s_1 \\ -c_1 \\ 0 \end{bmatrix} \quad (32)$$

$$z_3 = \begin{bmatrix} c_{2+3}c_1 \\ c_{2+3}s_1 \\ s_{2+3} \end{bmatrix} \quad (33)$$

$$z_4 = \begin{bmatrix} c_4s_1 + c_{12}s_{34} + c_{13}s_{24} \\ c_2s_{134} - c_{14} + c_3s_{124} \\ -c_{2+3}s_4 \end{bmatrix} \quad (34)$$

$$\begin{aligned} x = {} & 0.0375c_1 + 0.16c_1c_2 - 0.1384c_1s_{23} + 0.127s_{145} + 0.1384c_{123} - 0.015c_{12}s_3 \\ & - 0.015c_{13}s_2 + 0.127c_{1235} - 0.127c_{15}s_{23} - 0.127c_{124}s_{35} \\ & - 0.127c_{134}s_{25} \end{aligned} \quad (35)$$

$$\begin{aligned} y = {} & 0.0375s_1 + 0.16c_2s_1 - 0.015c_2s_{13} - 0.015c_3s_{12} - 0.127c_1s_{45} - 0.1384s_{123} \\ & + 0.1384c_{23}s_1 + 0.127c_{235}s_1 - 0.127c_5s_{123} - 0.127c_{24}s_{135} \\ & - 0.127c_{34}s_{125} \end{aligned} \quad (36)$$

$$\begin{aligned} z = {} & 0.16s_2 - 0.015c_{23} + 0.1384c_2s_3 + 0.1384c_3s_2 - 0.015s_{23} + 0.127c_{25}s_3 \\ & + 0.127c_{35}s_2 + 0.127c_{234}s_5 - 0.127c_4s_{235} + 0.1353 \end{aligned} \quad (37)$$

A simple derivation of x, y, and z is done using MATLAB using gradient command to calculate both $\dot{x}, \dot{y}$, and $\dot{z}$ as shown in the Equations (38) to 40).

$$\dot{x} = \begin{bmatrix} \frac{\partial p_x}{\partial q_1} & \frac{\partial p_x}{\partial q_2} & \frac{\partial p_x}{\partial q_3} & \frac{\partial p_x}{\partial q_4} & \frac{\partial p_x}{\partial q_5} \end{bmatrix}$$

$$\begin{aligned} \partial p_x/\partial q_1 = {} & 0.015c_2s_{13} - 0.16c_2s_1 - 0.0375s_1 + 0.015c_3s_{12} + 0.127c_1s_{45} \\ & + 0.1384s_{123} - 0.1384c_{23}s_1 - 0.127c_{235}s_1 + 0.127c_5s_{123} \\ & + 0.127c_{24}s_{135} + 0.127c_{34}s_{125} \\ \partial p_x/\partial q_2 = {} & -c_1[0.16s_2 + 0.015c_{23} + 0.1384c_2s_3 + 0.1384c_3s_2 - 0.015s_{23} \\ & + 0.127c_{25}s_3 + 0.127c_{35}s_2 + 0.127c_{234}s_5 + 0.127c_4s_{235}] \\ \partial p_x/\partial q_3 = {} & -c_1[0.015c_{23} + 0.1384c_2s_3 + 0.1384c_3s_2 - 0.015s_{23} + 0.127c_{25}s_3 \\ & + 0.127c_{35}s_2 + 0.127c_{234}s_5 + 0.127c_4s_{235}] \\ \partial p_x/\partial q_4 = {} & 0.127s_5[c_4s_1 + c_{12}s_{34} + c_{13}s_{24}] \\ \partial p_x/\partial q_5 = {} & 0.127c_5s_{14} - 0.127c_{123}s_5 + 0.127c_1s_{235} - 0.127c_{124}s_3 \\ & - 0.127c_{1345}s_2 \end{aligned} \quad (38)$$

$$\dot{y} = \begin{bmatrix} \frac{\partial p_y}{\partial q_1} & \frac{\partial p_y}{\partial q_2} & \frac{\partial p_y}{\partial q_3} & \frac{\partial p_y}{\partial q_4} & \frac{\partial p_y}{\partial q_5} \end{bmatrix}$$

$$\begin{aligned} \partial p_y/\partial q_1 = {} & 0.0375c_1 + 0.16c_{12} - 0.1384c_1s_{23} + 0.127s_{145} + 0.1384c_{123} \\ & - 0.0375c_{12}s_3 - 0.0375c_{13}s_2 + 0.127c_{1235} - 0.127c_{15}s_{23} \\ & - 0.127c_{124}s_{35} - 0.127c_{134}s_{25} \\ \partial p_y/\partial q_2 = {} & -s_1[0.16s_2 + 0.015c_{23} + 0.1384c_2s_3 + 0.1384c_3s_2 - 0.015s_{23} \\ & + 0.127c_{25}s_3 + 0.127c_{35}s_2 + 0.127c_{234}s_5 - 0.127c_4s_{235}] \end{aligned} \quad (39)$$

$$\partial p_y/\partial q_3 = -s_1[0.015c_{23} + 0.1384c_2s_3 + 0.1384c_3s_2 - 0.015s_{23} + 0.127c_{25}s_3 + 0.127c_{35}s_2 + 0.127c_{234}s_5 - 0.127c_4s_{235}]$$
$$\partial p_y/\partial q_4 = 0.127s_5[c_2s_{134} - c_{14} + c_3s_{124}]$$
$$\partial p_y/\partial q_5 = 0.127s_{1235} - 0.127c_{23}s_{15} - 0.127c_{15}s_4 - 0.127c_{245}s_{13} - 0.127c_{345}s_{12}$$

$$\dot{z} = \begin{bmatrix} \frac{\partial p_z}{\partial q_1} & \frac{\partial p_z}{\partial q_2} & \frac{\partial p_z}{\partial q_3} & \frac{\partial p_z}{\partial q_4} & \frac{\partial p_z}{\partial q_5} \end{bmatrix}$$
$$\partial p_z/\partial q_1 = 0$$
$$\partial p_z/\partial q_2 = 0.16c_2 - 0.1384c_{23} - 0.0375c_2s_3 - 0.0375c_3s_2 - 0.1384s_{23} - 0.127c_5s_{23} + 0.127c_{235} - 0.127c_{24}s_{35} - 0.127c_{34}s_{25} \quad \textbf{(40)}$$
$$\partial p_z/\partial q_3 = 0.1384c_{23} - 0.0375c_2s_3 - 0.0375c_3s_2 - 0.1384s_{23} - 0.127c_5s_{23} + 0.127c_{235} - 0.127c_{24}s_{35} - 0.127c_{34}s_{25}$$
$$\partial p_z/\partial q_4 = 0.127c(2+3)s_{45}$$
$$\partial p_z/\partial q_5 = 0.127c_{2345} - 0.127c_3s_{25} - 0.127c_2s_{35} - 0.127c_{45}s_{23}$$

The Jacobian matrix of the 5-link robot is shown below. The robot dynamic equations can be obtained using Equation (41).

$$\mathrm{J} = \begin{bmatrix} \mathrm{J}_{v_i} \\ \cdots \\ \mathrm{J}_{\omega_i} \end{bmatrix} = \begin{bmatrix} \mathrm{J}_{11} & \mathrm{J}_{12} & \mathrm{J}_{13} & \mathrm{J}_{14} & \mathrm{J}_{15} \\ \mathrm{J}_{21} & \mathrm{J}_{22} & \mathrm{J}_{23} & \mathrm{J}_{24} & \mathrm{J}_{25} \\ \mathrm{J}_{31} & \mathrm{J}_{32} & \mathrm{J}_{33} & \mathrm{J}_{34} & \mathrm{J}_{35} \\ \cdots & \cdots & \cdots & \cdots & \cdots \\ \mathrm{J}_{41} & \mathrm{J}_{42} & \mathrm{J}_{43} & \mathrm{J}_{44} & \mathrm{J}_{45} \\ \mathrm{J}_{51} & \mathrm{J}_{52} & \mathrm{J}_{53} & \mathrm{J}_{54} & \mathrm{J}_{55} \\ \mathrm{J}_{61} & \mathrm{J}_{62} & \mathrm{J}_{63} & \mathrm{J}_{64} & \mathrm{J}_{65} \end{bmatrix} \quad \textbf{(41)}$$

Where v_i is the linear velocity of link i, ω_i is the angular velocity of link i, J_{v_i} and J_{ω_i} are the upper and lower halves of the Jacobian matrix and depend upon the linear and angular velocities, and c_i and s_i are representative of $cos\theta_i$ and $sin\theta_i$, respectively. All values for the elements of Jacobian matrix appear in Equation (42). The Jacobian matrix was calculated for the robot using the MATLAB according to Equation (29).

$$\mathrm{J}_{11} = 0.015c_2s_{13} - 0.16c_2s_1 - 0.0375s_1 + 0.015c_3s_{12} + 0.127c_1s_{45} + 0.1384s_{123} - 0.1384c_{23}s_1 - 0.127c_{235}s_1 + 0.127c_5s_{123} + 0.127c_{24}s_{135} + 0.127c_{34}s_{125}$$
$$\mathrm{J}_{12} = -c_1[0.16s_2 + 0.015c_{23} + 0.1384c_2s_3 + 0.1384c_3s_2 - 0.015s_{23} + 0.127c_{25}s_3 + 0.127c_{35}s_2 + 0.127c_{234}s_5 + 0.127c_4s_{235}]$$
$$\mathrm{J}_{13} = -c_1[0.015c_{23} + 0.1384c_2s_3 + 0.1384c_3s_2 - 0.015s_{23} + 0.127c_{25}s_3 + 0.127c_{35}s_2 + 0.127c_{234}s_5 + 0.127c_4s_{235}]$$
$$\mathrm{J}_{14} = 0.127s_5[c_4s_1 + c_{12}s_{34} + c_{13}s_{24}]$$
$$\mathrm{J}_{15} = 0.127c_5s_{14} - 0.127c_{123}s_5 + 0.127c_1s_{235} - 0.127c_{124}s_3 - 0.127c_{1345}s_2$$
$$\mathrm{J}_{21} = 0.0375c_1 + 0.16c_{12} - 0.1384c_1s_{23} + 0.127s_{145} + 0.1384c_{123} - 0.0375c_{12}s_3 - 0.0375c_{13}s_2 + 0.127c_{1235} - 0.127c_{15}s_{23} - 0.127c_{124}s_{35} - 0.127c_{134}s_{25} \quad \textbf{(42)}$$
$$\mathrm{J}_{22} = -s_1[0.16s_2 + 0.015c_{23} + 0.1384c_2s_3 + 0.1384c_3s_2 - 0.015s_{23} + 0.127c_{25}s_3 + 0.127c_{35}s_2 + 0.127c_{234}s_5 - 0.127c_4s_{235}]$$
$$\mathrm{J}_{23} = -s_1[0.015c_{23} + 0.1384c_2s_3 + 0.1384c_3s_2 - 0.015s_{23} + 0.127c_{25}s_3 + 0.127c_{35}s_2 + 0.127c_{234}s_5 - 0.127c_4s_{235}]$$
$$\mathrm{J}_{24} = 0.127s_5[c_2s_{134} - c_{14} + c_3s_{124}]$$
$$\mathrm{J}_{25} = 0.127s_{1235} - 0.127c_{23}s_{15} - 0.127c_{15}s_4 - 0.127c_{245}s_{13} - 0.127c_{345}s_{12}$$
$$\mathrm{J}_{31} = 0$$
$$\mathrm{J}_{32} = 0.16c_2 - 0.1384c_{23} - 0.0375c_2s_3 - 0.0375c_3s_2 - 0.1384s_{23} - 0.127c_5s_{23} + 0.127c_{235} - 0.127c_{24}s_{35} - 0.127c_{34}s_{25}$$
$$\mathrm{J}_{33} = 0.1384c_{23} - 0.0375c_2s_3 - 0.0375c_3s_2 - 0.1384s_{23} - 0.127c_5s_{23} + 0.127c_{235} - 0.127c_{24}s_{35} - 0.127c_{34}s_{25}$$

$$J_{34} = 0.127c_{2+3}s_{45}$$
$$J_{35} = 0.127c_{2345} - 0.127c_3s_{25} - 0.127c_2s_{35} - 0.127c_{45}s_{23}$$
$$J_{41} = 0$$
$$J_{42} = s_1$$
$$J_{43} = s_1$$
$$J_{44} = c_{2+3}c_1$$
$$J_{45} = c_4s_1 + c_{1234} + c_{13}s_{24}$$
$$J_{51} = 0$$
$$J_{52} = -c_1$$
$$J_{53} = -c_1$$
$$J_{54} = c_{2+3}s_1$$
$$J_{55} = c_2s_{134} - c_{14} + c_3s_{124}$$
$$J_{61} = 1$$
$$J_{62} = 0$$
$$J_{63} = 0$$
$$J_{64} = s_{2+3}$$
$$J_{65} = -c_{2+3}s_4$$

3.3 Dynamics of Robotic Manipulator

Manipulator dynamics is concerned with the equations of motion and the motion of a manipulator that moves as a result of torque applied to each joint by motors or external forces. In robotics, the dynamic equations of motion for manipulators are utilized to set up the fundamental equations for control. Lagrange's method is a conceptually and methodologically simple formula. Lagrange is a formula that includes all linear and angular dynamics in one equation, the equation depends on the kinetic energy and the potential energy of the system. To obtain the dynamic equations of the robot the Lagrange method was used. In this method, dynamic equations can be expressed using Equation (43) [38].

$$M(q)\ddot{q} + C(q,\dot{q}) + G(q) = \tau \tag{43}$$

For the 5-DOF robot manipulator, $M(q)$ is a positive symmetrical 5×5 knowledge matrix called the inertia matrix or the mass matrix and is obtained using Equation (44). $C(q,\dot{q})$ is a matrix of 5×5 which represents the centrifugal force and Coriolis forces, meaning that the product of the existing velocities causes the two forces and is obtained using the Equation (45), and $G(q)$ is a 5×1 matrix which represents the gravity loading acting on each joint depending on the configuration, and is obtained using the Equation (46). In addition, τ is a 5×1 matrix related to the robot's torque of the joints, and $q, \dot{q}, \ddot{q}$ are 3×1 matrixes related to the position, velocity, and acceleration of the robot's joints respectively.

$$M(q) = \sum_{i=1}^{n} m_i J_{v_i}(q)^T J_{v_i}(q) + J_{\omega_i}(q)^T I_{c_i} J_{\omega_i}(q) \tag{44}$$

Where m_i is the mass of link i, J_{v_i} denotes the linear velocity of the center of mass of link i, I_{c_i} is the inertia tensor of link i concerning its center of mass, and J_{ω_i} denotes the angular velocity of the center of mass of link i.

$$C_{ij} = \sum_{i=1}^{n} C_{ijk}(q)\dot{q}k = \sum_{i=1}^{n} \frac{1}{2}\left(\frac{\partial b_{ij}}{\partial q_k} + \frac{\partial b_{ik}}{\partial q_j} + \frac{\partial b_{jk}}{\partial q_i}\right) \tag{45}$$

Where C_{ij} are the elements of the $C(q,\dot{q})$ matrix, C_{ijk} are called the Christoffel symbols, and d_{ij} are elements of the D(q) matrix. In this paper, the value of c will not be calculated and considered equal to zero because it is a function of velocity, and any

error in estimating the centrifugal force may lead to the emergence of negative feedback in velocity.

$$G(q) = -\sum_{i=1}^{n} J_{v_i}(q)^T m_i g \quad (46)$$

Where m_i is the mass of link i, J_{v_i} denotes the linear velocity of the center of mass of link i, g is the gravitational acceleration vector in the base frame, and $g = [0, 0, -9.80665]^T$because the z is the vertical axis that is in the robot.
Deriving the dynamic equations for the robot requires the Jacobian to be calculated for those specific points of the center of mass for each link, it is needed to calculate J_{v_i}, J_{ω_i}, and to calculate the p_{ci} ray that defines the center of mass for each link. Once those rays are calculated to the five links for the robot, the partial derivatives are found and the Jacobian is calculated. Using MATLAB, these rays were calculated based on the center of mass of all joints as shown in Table 1. Then those rays are found separately in the fourth column of Equation (47), to convert those rays into matrices as shown in Equations (38) to (52). After those rays are calculated and put into matrices, the transformation of those specific points of center of mass from frame 0 to frame C_5 is computed as ${}^0\mathrm{T}_{C_1}$, ${}^0\mathrm{T}_{C_2}$, ${}^0\mathrm{T}_{C_3}$, ${}^0\mathrm{T}_{C_4}$, ${}^0\mathrm{T}_{C_5}$.

$$\mathrm{Rot}_{z_{i-1}}(\theta_i) = \begin{bmatrix} \cos\theta_i & -\sin\theta_i & 0 & 0 \\ \sin\theta_i & \cos\theta_i & 0 & 0 \\ 0 & 0 & 1 & 0 \\ 0 & 0 & 0 & 1 \end{bmatrix} \quad (47)$$

$${}^1\mathrm{T}_C = \begin{bmatrix} c_1 & -s_1 & 0 & 0.0034c(\theta_1 + 2.8325) \\ s_1 & c_1 & 0 & 0.0034s(\theta_1 + 2.8325) \\ 0 & 0 & 1 & 0.0481 \\ 0 & 0 & 0 & 1 \end{bmatrix} \quad (48)$$

$${}^2\mathrm{T}_C = \begin{bmatrix} c_2 & -s_2 & 0 & 0.0725c(\theta_2 + 5.6192e^{-4}) \\ s_2 & c_2 & 0 & 0.0725s(\theta_2 + 5.6192e^{-4}) \\ 0 & 0 & 1 & 0.0519 \\ 0 & 0 & 0 & 1 \end{bmatrix} \quad (49)$$

$${}^3\mathrm{T}_C = \begin{bmatrix} c_3 & -s_3 & 0 & 0.0281c(\theta_3 + 0.5577) \\ s_3 & c_3 & 0 & 0.0281s(\theta_3 + 0.5577) \\ 0 & 0 & 1 & 0.0035 \\ 0 & 0 & 0 & 1 \end{bmatrix} \quad (50)$$

$${}^4\mathrm{T}_C = \begin{bmatrix} c_4 & -s_4 & 0 & 9.036e^{-5}c(\theta_4 + 0.5577) \\ s_4 & c_4 & 0 & 9.036e^{-5}s(\theta_4 + 0.5577) \\ 0 & 0 & 1 & 0.0746 \\ 0 & 0 & 0 & 1 \end{bmatrix} \quad (51)$$

$${}^5\mathrm{T}_C = \begin{bmatrix} c_5 & -s_5 & 0 & 0.0689c(\theta_5 - 1.5843) \\ s_5 & c_5 & 0 & 0.0689s(\theta_5 - 1.5843) \\ 0 & 0 & 1 & 8.7791e^{-6} \\ 0 & 0 & 0 & 1 \end{bmatrix} \quad (52)$$

The Jacobin for the end-effector is expressed as J_{v_i} and J_{ω_i}, i in Equations (53) and (54) refers to a certain link speed. To calculate J_{v_i} at the center of mass and express it as a function of each q, this specific ray of the center of mass is taken, then its partial derivatives are found up to the point q_i as shown in Equation (55), and J_{ω_i} is calculated as shown in Equation (56).

$$v_{c_i} = J_{v_i} \cdot \dot{q} \quad (53)$$

$$\omega_{c_i} = J_{\omega_i} \cdot \dot{q} \quad (54)$$

$$J_{v_i} = \begin{bmatrix} \frac{\partial p_{c_1}}{\partial q_1} & \frac{\partial p_{c_2}}{\partial q_2} & \frac{\partial p_{c_3}}{\partial q_3} & \frac{\partial p_{c_4}}{\partial q_{n_4}} & \frac{\partial p_{c_5}}{\partial q_5} \end{bmatrix} \quad (55)$$

$$J_{\omega_i} = [\bar{\varepsilon}_1 z_1 \quad \bar{\varepsilon}_2 z_2 \quad \bar{\varepsilon}_3 z_3 \quad \bar{\varepsilon}_4 z_4 \quad \bar{\varepsilon}_5 z_5] \quad (56)$$

Where J_{v_i} and J_{ω_i} are the matrices related to the contribution of the joint velocities to the linear velocity and angular velocity of the center of mass, respectively for the manipulator.

This column i and every column following it will be zero, the Jacobean matrix generated with this vector is referred to as p_{C_i} up to this point, and then those zero columns are added. To calculate both J_{v_i} and J_{ω_i} by applying Equations (55) and (56) for the manipulator, Once the ray p_{C_i} is obtained, the partial derivatives are found and the Jacobian is calculated for the J_{v_1}. The first column concerning q_1 is derived as shown in Equation (57). For the J_{v_2}, the first and second columns concerning q_1, and q_2 respectively are derived, as shown in Equation (58). For the J_{v_3}, the first, second, and third columns with concerning to q_1, q_2, and q_3, respectively are derived as shown in Equation (59). For the J_{v_4}, the first, second, third, and fourth columns concerning q_1, q_2, q_3, and q_4 respectively are derived as shown in Equation (60). Finally, the J_{v_5} is calculated by deriving the first, second, third, fourth, and fifth columns concerning q_1, q_2, q_3, q_4, and q_5, respectively, as shown in Equation (61). In Equation (62) z_0, z_1, z_2, z_3, z_4 are the first three elements of the third column of the ${}^0T_1$, ${}^0T_2$, ${}^0T_3$, ${}^0T_4$, ${}^0T_5$ matrixes obtained by successive multiplication of Equations from (5) to (10), with $z_0 = [0, 0, 1]^T$. Results were obtained using MATLAB software.

$$J_{v_1} = \begin{bmatrix} \frac{\partial\, {}^0T_{C_1}}{\partial q_1} & 0 & 0 & 0 & 0 \end{bmatrix}$$

$$J_{v_1} = \begin{bmatrix} 0.0340s(\theta_1 + 2.8325) & 0 & 0 & 0 & 0 \\ 0.0340c(\theta_1 + 2.8325) & 0 & 0 & 0 & 0 \\ 0 & 0 & 0 & 0 & 0 \end{bmatrix} \quad (57)$$

$$J_{v_2} = \begin{bmatrix} \frac{\partial\, {}^0T_{C_2}}{\partial q_1} & \frac{\partial\, {}^0T_{C_2}}{\partial q_2} & 0 & 0 & 0 \end{bmatrix}$$

$$J_{v_2} = \begin{bmatrix} J_{v(1,1)} & J_{v(1,2)} & 0 & 0 & 0 \\ J_{v(2,1)} & J_{v(2,2)} & 0 & 0 & 0 \\ 0 & 0.0725 & 0 & 0 & 0 \end{bmatrix} \quad (58)$$

$$J_{v(1,1)} = 0.0519c_1 - 0.0375s_1 - 0.0725s_1c(\theta_2 + 5.6192e^{-4})$$

$$J_{v(1,2)} = -0.0725c_1s(\theta_2 + 5.6192e^{-4})$$

$$J_{v(2,1)} = 0.0375c_1 + 0.0519s_1 + 0.0725c_1c(\theta_2 + 5.6192e^{-4})$$

$$J_{v(2,2)} = -0.0725s_1s(\theta_2 + 5.6192e^{-4})$$

$$J_{v_3} = \begin{bmatrix} \frac{\partial\, {}^0T_{C_3}}{\partial q_1} & \frac{\partial\, {}^0T_{C_3}}{\partial q_2} & \frac{\partial\, {}^0T_{C_3}}{\partial q_3} & 0 & 0 \end{bmatrix}$$

$$J_{v_3} = \begin{bmatrix} J_{v(1,1)} & J_{v(1,2)} & J_{v(1,3)} & 0 & 0 \\ J_{v(2,1)} & J_{v(2,2)} & J_{v(2,3)} & 0 & 0 \\ 0 & J_{v(3,2)} & J_{v(3,3)} & 0 & 0 \end{bmatrix} \quad (59)$$

$$J_{v(1,1)} = 0.0281s(\theta_3 - 2.5577)s_{12} - 0.0375s_1 - 0.16c_2s_1 - 0.0281c(\theta_3 - 2.5577)c_2s_1 - 0.0035c_1$$

$$\mathbf{J}_{v_{(1,2)}} = -2.0281s(\theta_2+\theta_3-2.5577)c_1+0.1600s_2$$
$$\mathbf{J}_{v_{(1,3)}} = -0.0281s(\theta_2+\theta_3-2.5577)c_1$$
$$\mathbf{J}_{v_{(2,1)}} = 0.0375c_1-0.0035s_1+0.16c_{12}+0.0281c(\theta_3-2.5577)c_{12} - 0.0281s(\theta_3-2.5577)c_1s_2$$
$$\mathbf{J}_{v_{(2,2)}} = -2.0281s(\theta_2+\theta_3-2.5577)s_1+0.16s_2$$
$$\mathbf{J}_{v_{(2,3)}} = -0.0281s(\theta_2+\theta_3-2.5577)s_1$$
$$\mathbf{J}_{v_{(3,2)}} = 2.8086c(\theta_2+\theta_3-2.5577)+0.16c_2$$
$$\mathbf{J}_{v_{(3,3)}} = 2.8086c(\theta_2+\theta_3-2.5577)$$

$$J_{v_4} = \begin{bmatrix} \frac{\partial\, {}^0\mathrm{T}_{\mathrm{C}_4}}{\partial q_1} & \frac{\partial\, {}^0\mathrm{T}_{\mathrm{C}_4}}{\partial q_2} & \frac{\partial\, {}^0\mathrm{T}_{\mathrm{C}_4}}{\partial q_3} & \frac{\partial\, {}^0\mathrm{T}_{\mathrm{C}_4}}{\partial q_4} & 0 \end{bmatrix}$$
$$\mathbf{J}_{v_4} = \begin{bmatrix} \mathbf{J}_{v_{(1,1)}} & \mathbf{J}_{v_{(1,2)}} & \mathbf{J}_{v_{(1,3)}} & \mathbf{J}_{v_{(1,4)}} & 0 \\ \mathbf{J}_{v_{(2,1)}} & \mathbf{J}_{v_{(2,2)}} & \mathbf{J}_{v_{(2,3)}} & \mathbf{J}_{v_{(2,4)}} & 0 \\ 0 & \mathbf{J}_{v_{(3,2)}} & \mathbf{J}_{v_{(3,3)}} & \mathbf{J}_{v_{(3,4)}} & 0 \end{bmatrix}$$
$$\mathbf{J}_{v_{(1,1)}} = 9.036e^{-5}c_1s(\theta_4+1.6029)-0.16c_2s_1-0.0375s_1+0.015c_2s_{13} + 0.015c_3s_{12}-0.0746s_{123}+0.0746c_{23}s_1 + 9.036e^{-5}c_2(\theta_4+1.6029)s_{13}+9.036e^{-5}c_3c(\theta_4+1.6029)s_{12}$$
$$\mathbf{J}_{v_{(1,2)}} = c_1 0.0746c_2s_3-0.015c_{23}-0.16s_2+0.0746c_3s_2+0.015s_{23} + 9.036e^{-5}c(\theta_4+1.6029)s_{23}-9.036e^{-5}c_{23}c(\theta_4+1.6029)$$
$$\mathbf{J}_{v_{(1,3)}} = 3c_1 0.0249c_2s_3-0.005c_{23}+0.0249c_3s_2+0.005s_{23} + 3.012e^{-5}c(\theta_4+1.6029)s_{23}-3.012e^{-5}c_{23}c(\theta_4+1.6029)$$
$$\mathbf{J}_{v_{(1,4)}} = 9.036e^{-5}c(\theta_4+1.6029)s_1+9.036e^{-5}c_{12}s_3s(\theta_4+1.6029) + 9.036e^{-5}c_{13}s_2s(\theta_4+1.6029)$$
$$\mathbf{J}_{v_{(2,1)}} = 0.0375c_1+0.16c_{12}+9.036e^{-5}s_1s(\theta_4+1.6029)+0.0746c_1s_{23} - 9.036e^{-5}c_{123}-0.015c_{12}s_3-0.015c_{13}s_2 - 9.036e^{-5}c_{12}c(\theta_4+1.6029)s_3-9.036e^{-5}c_{13}c(\theta_4+1.6029)s_2 \quad \textbf{(60)}$$
$$\mathbf{J}_{v_{(2,2)}} = s_1 0.0746c_2s_3-0.015c_{23}-0.16s_2+0.0746c_3s_2+0.015s_{23} + 9.036e^{-5}c(\theta_4+1.6029)s_{23}-9.036e^{-5}c_{23}c(\theta_4+1.6029)$$
$$\mathbf{J}_{v_{(2,3)}} = 3s_1 0.0249c_2s_3-0.005c_{23}+0.0249c_3s_2+0.005s_{23} + 3.012e^{-5}c(\theta_4+1.6029)s_{23}-3.012e^{-5}c_{23}c(\theta_4+1.6029)$$
$$\mathbf{J}_{v_{(2,4)}} = 9.036e^{-5}c_2s_{13}s(\theta_4+1.6029)-9.036e^{-5}c_1c(\theta_4+1.6029) + 9.036e^{-5}c_3s_{12}s(\theta_4+1.6029)$$
$$\mathbf{J}_{v_{(3,2)}} = 0.16c_2-0.0746c_{23}-0.015c_2s_3-0.015c_3s_2+0.0746s_{23} - 9.036e^{-5}c_2c(\theta_4+1.6029)s_3-9.036e^{-5}c_3c(\theta_4+1.6029)s_2$$
$$\mathbf{J}_{v_{(3,3)}} = 0.0746s_{23}-0.015c_2s_3-0.015c_3s_2-0.0746c_{23} - 9.036e^{-5}c_2c(\theta_4+1.6029)s_3-9.036e^{-5}c_3c(\theta_4+1.6029)s_2$$
$$\mathbf{J}_{v_{(3,4)}} = 9.036e^{-5}c(\theta_2+\theta_3)s(\theta_4+1.6029)$$

$$J_{v_5} = \begin{bmatrix} \frac{\partial\, {}^0\mathrm{T}_{\mathrm{C}_5}}{\partial q_1} & \frac{\partial\, {}^0\mathrm{T}_{\mathrm{C}_5}}{\partial q_2} & \frac{\partial\, {}^0\mathrm{T}_{\mathrm{C}_5}}{\partial q_3} & \frac{\partial\, {}^0\mathrm{T}_{\mathrm{C}_5}}{\partial q_4} & \frac{\partial\, {}^0\mathrm{T}_{\mathrm{C}_5}}{\partial q_5} \end{bmatrix}$$
$$\mathbf{J}_{v_5} = \begin{bmatrix} \mathbf{J}_{v_{(1,1)}} & \mathbf{J}_{v_{(1,2)}} & \mathbf{J}_{v_{(1,3)}} & \mathbf{J}_{v_{(1,4)}} & \mathbf{J}_{v_{(1,5)}} \\ \mathbf{J}_{v_{(2,1)}} & \mathbf{J}_{v_{(2,2)}} & \mathbf{J}_{v_{(2,3)}} & \mathbf{J}_{v_{(2,4)}} & \mathbf{J}_{v_{(2,5)}} \\ 0 & \mathbf{J}_{v_{(3,2)}} & \mathbf{J}_{v_{(3,3)}} & \mathbf{J}_{v_{(3,4)}} & \mathbf{J}_{v_{(3,5)}} \end{bmatrix} \quad \textbf{(61)}$$

$$
\begin{aligned}
\mathrm{J}_{v_{(1,1)}} = {} & 8.7791e^{-6}c_{14} - 0.0375s_1 - 0.16c_2s_1 + 0.015c_2s_{13} + 0.015c_3s_{12} \\
& + 0.0689c_1s_4c(\theta_5 - 1.5843) + 0.1384s_{123} - 0.1384c_{23}s_1 \\
& - 0.0689s(\theta_5 - 1.5843)s_{123} - 8.7791e^{-6}c_2s_{134} \\
& - 8.7791e^{-6}c_3s_{124} + 0.0689s(\theta_5 - 1.5843)c_{23}s_1 \\
& + 0.0689c_{24}s_{13}c(\theta_5 - 1.5843) + 0.0689c_{34}s_{12}c(\theta_5 - 1.5843)
\end{aligned}
$$

$$
\begin{aligned}
\mathrm{J}_{v_{(1,2)}} = {} & -0.16c_1s_2 + 0.015c_{23} + 1.384e^{-6}c_{23} + 1.384e^{-6}c_3s_2 - 0.015s_{23} \\
& + 8.7791e^{-6}s_{234} - 0.0689s(\theta_5 - 1.5843)c_2s_3 \\
& - 0.0689s(\theta_5 - 1.5843)c_3s_2 - 8.7791e^{-6}c_{23}s_4 \\
& + 0.0689c_{234}c(\theta_5 - 1.5843) - 0.0689c_4s_{23}c(\theta_5 - 1.5843)
\end{aligned}
$$

$$
\begin{aligned}
\mathrm{J}_{v_{(1,3)}} = {} & -0.015c_{123} + 8.7791e^{-6}c_{23} + 1.384e^{-6}c_3s_2 - 0.015s_{23} + 8.7791e^{-6}s_{234} \\
& - 0.0689s(\theta_5 - 1.5843)c_2s_3 - 0.0689s(\theta_5 - 1.5843)c_2s_3 \\
& - 8.7791e^{-6}c_{23}s_4 + 0.0689c_{234}c(\theta_5 - 1.5843) \\
& - 0.0689c_4s_{23}c(\theta_5 - 1.5843)
\end{aligned}
$$

$$
\begin{aligned}
\mathrm{J}_{v_{(1,4)}} = {} & 0.0689c(\theta_5 - 1.5843)(c_4s_1 + c_{12}s_4 + c_{13}s_{24}) - 8.7791e^{-6}s_{14} \\
& + 8.7791e^{-6}s(\theta_2 + \theta_3)c_{14}
\end{aligned}
$$

$$
\begin{aligned}
\mathrm{J}_{v_{(1,5)}} = {} & 0.0689s(\theta_5 - 1.5843)(c_{124}s_3 - s_{14} + c_{134}s_2) - 0.0689c(\theta_2 \\
& + \theta_3)c_1c(\theta_5 - 1.5843)
\end{aligned}
$$

$$
\begin{aligned}
\mathrm{J}_{v_{(2,1)}} = {} & 0.0375c_1 + 0.16c_{12} + 8.7791e^{-6}c_4s_1 - 0.1384c_1s_{23} \\
& + 0.0689s_{14}c(\theta_5 - 1.5843) + 0.1384c_{123} - 0.015c_{12}s_3 \\
& - 0.015c_{13}s_2 + 0.0689s(\theta_5 - 1.5843)c_1s_{23} + 8.7791e^{-6}c_{12}s_{34} \\
& + 8.7791e^{-6}c_{13}s_{24} - 0.0689s(\theta_5 - 1.5843)c_{123} \\
& - 0.0689c_{124}s_3c(\theta_5 - 1.5843) - 0.0689c_{134}s_2c(\theta_5 - 1.5843)
\end{aligned}
$$

$$
\begin{aligned}
\mathrm{J}_{v_{(2,2)}} = {} & -0.16s_{12} + 0.015c_{23} + 1.384e^{-6}c_{23} + 1.384e^{-6}c_3s_2 - 0.015s_{23} \\
& + 8.7791e^{-6}s_{234} - 0.0689s(\theta_5 - 1.5843)c_2s_3 \\
& - 0.0689s(\theta_5 - 1.5843)c_3s_2 - 8.7791e^{-6}c_{23}s_4 \\
& + 0.0689c_{234}c(\theta_5 - 1.5843) - 0.0689c_4s_{23}c(\theta_5 - 1.5843)
\end{aligned}
$$

$$
\begin{aligned}
\mathrm{J}_{v_{(2,3)}} = {} & -0.015s_1c_{23} + 8.7791e^{-6}c_{23} + 1.384e^{-6}c_3s_2 - 0.015s_{23} \\
& + 8.7791e^{-6}s_{234} - 0.0689s(\theta_5 - 1.5843)c_2s_3 \\
& - 0.0689s(\theta_5 - 1.5843)c_2s_3 - 8.7791e^{-6}c_{23}s_4 \\
& + 0.0689c_{234}c(\theta_5 - 1.5843) - 0.0689c_4s_{23}c(\theta_5 - 1.5843)
\end{aligned}
$$

$$
\begin{aligned}
\mathrm{J}_{v_{(2,4)}} = {} & 8.7791e^{-6}c_1s_4 + 0.0689c(\theta_5 - 1.5843)(c_2s_{134} - c_{14} + c_3s_{124}) \\
& + 8.7791e^{-6}s(\theta_2 + \theta_3)c_4s_1
\end{aligned}
$$

$$
\begin{aligned}
\mathrm{J}_{v_{(2,5)}} = {} & 0.0689s(\theta_5 - 1.5843)(c_1s_4 + c_{24}s_{13} + c_{34}s_{12}) - 0.0689c(\theta_2 + \theta_3)s_1c(\theta_5 \\
& - 1.5843)
\end{aligned}
$$

$$
\begin{aligned}
\mathrm{J}_{v_{(3,2)}} = {} & 0.16c_2 + 0.1384c_{23} - 0.015c_2s_3 - 0.015c_3s_2 - 0.1384s_{23} \\
& + 8.7791e^{-6}c_2s_{34} + 8.7791e^{-6}c_3s_{34} - 0.0689s(\theta_5 - 1.5843)c_{23} \\
& + 0.0689s(\theta_5 - 1.5843)s_{23} - 0.0689c_{24}s_3c(\theta_5 - 1.5843) \\
& - 0.0689c_{34}s_2c(\theta_5 - 1.5843)
\end{aligned}
$$

$$
\begin{aligned}
\mathrm{J}_{v_{(3,3)}} = {} & 0.1384c_{23} - 0.015c_2s_3 - 0.015c_3s_2 - 0.1384s_{23} + 8.7791e^{-6}c_2s_{34} \\
& + 8.7791e^{-6}c_3s_{34} - 0.0689s(\theta_5 - 1.5843)c_{23} \\
& + 0.0689s(\theta_5 - 1.5843)s_{23} - 0.0689c_{24}s_3c(\theta_5 - 1.5843) \\
& - 0.0689c_{34}s_2c(\theta_5 - 1.5843)
\end{aligned}
$$

$$
\mathrm{J}_{v_{(3,4)}} = -c(\theta_2 + \theta_3)(8.7791e^{-6}c_4 + 0.0689s_4c(\theta_5 - 1.5843))
$$

$$
\mathrm{J}_{v_{(3,5)}} = -0.689s(\theta_2 + \theta_3)c(\theta_5 - 1.5843) - 0.0689s(\theta_5 - 1.5843)c(\theta_2 + \theta_3)c_4
$$

$$
J_{\omega_i} = \begin{bmatrix} 0 & s_1 & s_1 & c_{2+3}c_1 & c_4s_1 + c_{1234} + c_{13}s_{24} \\ 0 & -c_1 & -c_1 & c_{2+3}s_1 & c_2s_{134} - c_{14} + c_3s_{124} \\ 1 & 0 & 0 & s_{2+3} & -c_{2+3}s_4 \end{bmatrix} \qquad \textbf{(62)}
$$

3.3.1 Gravity matrix

The robot arm consists of links and joints in the form of rigid bodies, therefore the dynamic properties of the rigid body occupy a central place in the robot's dynamics. Each link is located somewhere as in Fig. 1 and we have the center of mass, whenever the robot is moved up or down a different potential energy is obtained, the higher the height is the better, and therefore the height h is significant and can be calculated, then the potential energy of a specific link is calculated and added to the potential energy as shown in Equation (63). So, to calculate the potential energy the height h must be first calculated. A ray has already found, this ray is specific to the position of the center of mass through which the height is calculated. The gravity towards the bottom is known, so the gravitational ray has a negative sign. It will be multiplied by p_{c_i}. From this multiplication h can be calculated, and this gives m_i as it is shown in Equation (64).

$$U_i = m_i g_0 h_i + U_0 \tag{63}$$

$$U_i = m_i(-g^T p_{c_i}); U = \sum_i^n U_i \tag{64}$$

Where U_i is the total energy of the link, m_i is the mass of the link, g_0 is the gravitational constant, h_i is the height of the link at its center, and U_0 is the potential energy. So, gravity is the gradient of this magnitude, that is, the gravitational forces are found by calculating the partial derivative concerning q, and the partial derivative gives the columns of the Jacobian matrix. So, gravity is simply this negative sign multiplied by J_{v_i} multiplied by this ray $m_1 g, m_2 g,$ and up to $m_n g$ as shown in Equations (65) and (66) [38].

$$G(q) = -\sum_{i=1}^{n} J_{v_i}(q)^T m_i g \tag{65}$$

$$G(q) = -\begin{bmatrix} J_{v_1}^T & J_{v_2}^T & \cdots & J_{v_n}^T \end{bmatrix} \begin{bmatrix} m_1 g \\ m_2 g \\ m_n g \end{bmatrix}$$
$$G(q) = -\left[J_{v_1}^T(m_1 g) + J_{v_2}^T(m_2 g) + \cdots\cdots + J_{v_n}^T(m_n g)\right] \tag{66}$$

By applying Equation (66) to the robot arm with five degrees of freedom, Equation (67) is got in frame $\{0\}$ and $g = [0, 0, -9.80665]^T$.

$$G(q) = -\left[J_{v_1}^T(m_1 g) + J_{v_2}^T(m_2 g) + J_{v_3}^T(m_3 g) + J_{v_4}^T(m_4 g) + J_{v_5}^T(m_5 g)\right] \tag{67}$$

The calculation is done for vectors $m_1 g, m_2 g, m_3 g, m_4 g, m_5 g$ by multiplying $g = [0, 0, -9.80665]^T$ by the mass of each link represented in Table 1, and these vectors can be calculated as in the Equation (68) to (72).

$$m_1 g = [0; 0; -10.5392] \tag{68}$$
$$m_2 g = [0; 0; -7.14600] \tag{69}$$
$$m_3 g = [0; 0; -6.61660] \tag{70}$$
$$m_4 g = [0; 0; -5.72400] \tag{71}$$
$$m_5 g = [0; 0; -1.16310] \tag{72}$$

To calculate the gravity matrix of the robot, the value of $J_{v_1}^T, J_{v_2}^T, J_{v_3}^T, J_{v_4}^T, J_{v_5}^T$ calculated above is substituted into Equation (67) using the Jacobian at the center of mass. By solving this equation using the MATLAB program, we get the Equation (73). $G(q)$ is a 5×1 matrix representing the gravity loading acting on each joint depending on the configuration.

$$G(q)_{n\times 1} = \begin{bmatrix} g_1 \\ g_2 \\ g_3 \\ g_4 \\ g_5 \end{bmatrix}$$

$$\begin{aligned}
g_1 &= 0 \\
g_2 &= 0.1858c(\theta_2 + \theta_3 - 2.5577) + 0.5181c(\theta_2 + 5.6192e^{-4}) + 2.1606c_2 \\
&\quad - 0.2658c_{23} - 0.1033c_2s_3 - 0.1033c_3s_2 + 0.2658s_{23} \\
&\quad + 1.0211e^{-5}c_2s_{34} + 1.0211e^{-5}c_3s_{24} - 0.0801s(\theta_5 - 1.5843)c_{23} \\
&\quad + 0.0801s(\theta_5 - 1.5843)s_{23} - 5.1722e^{-4}c_2c(\theta_4 - 1.6029)s_3 \\
&\quad - 5.1722e^{-4}c_3c(\theta_4 - 1.6029)s_2 - 0.0801c_{24}s_3c(\theta_5 - 1.5843) \\
&\quad - 0.0801c_{34}s_3c(\theta_5 - 1.5843) \\
g_3 &= 0.1858c(\theta_2 + \theta_3 - 2.5577) - 0.2658c_{23} - 0.1033c_2s_3 - 0.1033c_3s_2 \\
&\quad + 0.2658s_{23} + 1.0211e^{-5}c_2s_{34} + 1.0211e^{-5}c_3s_{24} \\
&\quad - 0.1858s(\theta_5 - 1.5843)c_{23} + 0.1858s(\theta_5 - 1.5843)s_{23} \\
&\quad - 5.1722e^{-4}c_2c(\theta_4 - 1.6029)s_3 - 5.1722e^{-4}c_3c(\theta_4 - 1.6029)s_2 \\
&\quad - 0.081c_{24}s_3c(\theta_5 - 1.5843) - 0.081c_{34}s_2c(\theta_5 - 1.5843) \\
g_4 &= 5.1722e^{-4}c(\theta_2 + \theta_3)s(\theta_4 + 1.5843) - 1.9703e^{-21}c(\theta_2 + \theta_3)(3.8987e^{-21}c_4 \\
&\quad + 3.0601e^{-17}s_4c(\theta_5 - 1.5843)) \\
g_5 &= 0.0801s(\theta_2 + \theta_3)c(\theta_5 - 1.5843) - 0.0801s(\theta_5 - 1.5843)c(\theta_2 + \theta_3)c_4
\end{aligned} \tag{73}$$

3.3.2 Mass matrix

The mass matrix is simply those Jacobines J_{v_i}, J_{ω_i} multiplied by the transposed Jacobian $J_{v_i}{}^T, J_{\omega_i}{}^T$ multiplied by the scaled mass properties m_i, I_{c_i}. That's what so all, this mass matrix is to take the Jacobian associated with those specific points of the center of mass, and see their impact on the velocity, because they are capturing the effect of the velocity, and are scaled by m_i or I_{c_i} as in the Equation (74) [38].

$$M(q) = \sum_{i=1}^{n} m_i J_{v_i}(q)^T J_{v_i}(q) + J_{\omega_i}(q)^T I_{c_i} J_{\omega_i}(q) \tag{74}$$

Where m_i is the mass of link i, J_{v_i} denotes the linear velocity of the center of mass of link i, I_{c_i} is the inertia tensor of link i for its center of mass, and J_{ω_i} denotes the angular velocity of the center of mass of link i, $M(q)$ is a positive symmetrical $n \times n$ knowledge matrix called the inertia matrix or the mass matrix by applying Equation (74) to the robot arm with five degrees of freedom, Equation (75) is got. When thinking about this mass matrix, it is symmetrical, definite, positive, and has many properties, and these properties can be linked to the structure of the robot. m_{11} represents the inertia, the inertia is dependent on the position, so if that position is changed then the value of m_{11} will change, m_{11} represents the inertia at joint 1, m_{22} represents the inertia at joint 2, m_{nn} represents the perceived inertia around this axis, so all these diagonal elements represent the perceived effective inertia at each joint. m_{11} is independent of the first joint because of the motion of this joint around its axis. After the installation of all the other joints, the inertia around that axis does not change, but it is dependent on all the following joints, where m_{11} is dependent on q_1 to q_n, and q_2 is dependent on q_3 to q_n, and m_{nn} is constant. So m_{12} represents the correlation of the acceleration of joint 2 with joint 1, m_{21} is the opposite representing the correlation of joint 1 with joint 2. Matrix m is a definite and positive symmetrical matrix, because it is not physically possible to talk about an object having a mass equal to zero, so the object must have a mass, and the mass is always positive.

$$M(q) = m_1 {J_{v_1}}^T J_{v_1} + {J_{\omega_1}}^T I_{c_1} J_{\omega_1} + m_2 {J_{v_2}}^T J_{v_2} + {J_{\omega_2}}^T I_{c_2} J_{\omega_2} + m_3 {J_{v_3}}^T J_{v_3} + {J_{\omega_3}}^T I_{c_3} J_{\omega_3} + m_4 {J_{v_4}}^T J_{v_4} + {J_{\omega_4}}^T I_{c_4} J_{\omega_4} + m_5 {J_{v_5}}^T J_{v_5} + {J_{\omega_5}}^T I_{c_5} J_{\omega_5} \quad (75)$$

The values of the moment of inertia for the center of mass were taken from Table 2, and put in the form of a matrix as shown in Equation (76).

$$I_{c_1} = \begin{bmatrix} 0.0031 & 0.0043 & 0.0019 \\ 0.0043 & -0.0005 & 0.0017 \\ 0.0019 & 0.0017 & 0.003 \end{bmatrix} I_{c_2} = \begin{bmatrix} 0.0021 & 0.00660 & 0.0048 \\ 0.0066 & -0 & -0.0028 \\ 0.0048 & -0.0028 & -0 \end{bmatrix}$$
$$I_{c_3} = e^{-3} \begin{bmatrix} 0.4028 & 0.6201 & 0.7881 \\ 0.6201 & -0.0276 & -0.0616 \\ 0.7881 & -0.0616 & -0.2498 \end{bmatrix} I_{c_4} = \begin{bmatrix} 0.0034 & 0.0034 & 0.0002 \\ 0.0034 & 0 & -0 \\ 0.0002 & -0 & 0 \end{bmatrix} \quad (76)$$
$$`I_{c_5} = e^{-3} \begin{bmatrix} 0.5892 & 0.0067 & 0.5842 \\ 0.0067 & -0.0001 & 0 \\ 0.5842 & 0 & -0.0076 \end{bmatrix}$$

To calculate the mass matrix of the robot, the value of $J_{v_1}^T, J_{v_2}^T, J_{v_3}^T, J_{v_4}^T, J_{v_5}^T$ and $J_{\omega_1}^T, J_{\omega_2}^T, J_{\omega_3}^T, J_{\omega_4}^T, J_{\omega_5}^T$ computed above was substituted into Equation (75) using the Jacobian in the center of mass, and substituting for the inertia values from Equation (76), and the mass values from Table 1, by solving this equation using the MATLAB , the Equations (77) to (101) are got. $M(q)$ is a 5×5 matrix representing the mass affecting each link according to the configuration of the robotic arm.

$$\begin{aligned} m_{11} = {} & 0.004c(\theta_2 + 5.6192e^{-4}) - 0.0072s(2\theta_1) + 593(2.0329e^{-29}c_1 + \\ & 8.6736e^{-29}c_{12} + 4.7592e^{-33}c_4 s_1 - 7.5027e^{-29}c_1 s_{23} + 3.7355e^{-29}s_{14}c(\theta_5 - \\ & 1.5843) + 7.5027e^{-29}c_{123} - 8.1315e^{-30}c_{12}s_3 - 8.1315e^{-30}c_{13}s_2 + \\ & 3.7355e^{-29}s(\theta_5 - 1.5843)c_1 s_{23} + 4.7592e^{-23}c_{12}s_{34} + 4.7592e^{-33}c_{13}s_{24} - \\ & 3.7355e^{-29}s(\theta_5 - 1.5843)c_{123} - 3.7355e^{-29}c_{124}s_3 c(\theta_5 - 1.5843) - \\ & 3.7355e^{-29}c_{134}s_2 c(\theta_5 - 1.5843))^2 + 67471(6.5052e^{-27}c_1 - 6.0346e^{-28}s_1 + \\ & 2.7756e^{-26}c_{12} + 4.8721e^{-27}c(\theta_3 - 2.5577)c_{12} - 4.8721e^{-27}s(\theta_3 - \\ & 2.5577c_1 s_2)^2 + 4.8499e^{-6}c(\theta_2 + \theta_3)^2 + 58369(1.9594e^{-30}c_1 s(\theta_4 + 1.5843) - \\ & 3.4694e^{-27}c_2 s_1 - 8.1315e^{-28}s_1 + 3.2526e^{-28}c_2 s_{13} + 3.2526e^{-28}c_3 s_{12} - \\ & 1.6169e^{-27}s_{123} + 1.6169e^{-27}c_{23}s_1 + 1.9594e^{-30}c_2 c(\theta_4 + 1.5843)s_{13} + \\ & 1.9594e^{-30}c_3 c(\theta_4 + 1.5843)s_{12})^2 - 0.0026{c_1}^2 + 6747(6.0346e^{-28}c_1 + \\ & 6.5052e^{-27}s_1 + 2.775e^{-26}c_2 s_1 + 4.8721e^{-27}c(\theta_3 - 2.5577)c_2 s_1 - \\ & 4.8721e^{-27}s(\theta_3 - 2.5577)s_{12})^2 + (c_4 s_1 + c_{12}s_{34} + c_{13}s_{24})\big(5.8916e^{-4}c_4 s_1 - \\ & 6.7417e^{-5}c_{14} - 5.8418e^{-4}c(\theta_2 + \theta_3)s_4 + 5.8916e^{-4}c_{12}s_{34} + 5.8916e^{-4}c_{13}s_{24} + \\ & 6.7417e^{-6}c_2 s_{134} + 6.7417e^{-6}c_3 s_{124}\big) + (c_2 s_{134} - c_{14} + c_3 s_{124})(8.7259e^{8}c_{14} + \\ & 6.7417e^{-6}c_4 s_1 - 9.7093e^{-11}c(\theta_2 + \theta_3)s_4 + 6.7417e^{-6}c_{12}s_{34} + \\ & 6.7417e^{-6}c_{13}s_{24} - 8.7259e^{-8}c_2 s_{134} - 8.7259e^{-8}c_3 s_{124} + \\ & 58369(1.6169e^{-27}c_{123} - 3.4694e^{-27}c_{12} - 1.9594e^{-30}s_1 s(\theta_4 + 1.5843) - \\ & 1.6169e^{-27}c_1 s_{23} - 8.1315e^{-28}c_1 + 3.256e^{-28}c_{12}s_3 + 3.256e^{-28}c_{13}s_2 + \\ & 1.9594e^{-30}c_{12}c(\theta_4 + 1.5843)s_3 + 1.9594e^{-30}c_{13}c(\theta_4 + 1.5843)s_2)^2 + \\ & 0.0034c(\theta_2 + \theta_3)^2 {c_1}^2 + 593(4.7592e^{-33}c_{14} - 2.0329e^{-29}s_1 - 8.6736e^{-29}c_2 s_1 + \\ & 8.1315e^{-30}c_2 s_{13} + 8.1315e^{-30}c_3 s_{12} + 3.7355e^{-29}c_1 s_4 c(\theta_5 + 1.5843) + \\ & 7.5027e^{-29}s_{123} - 7.5027e^{-29}c_{23}s_1 - 3.7355e^{-29}s(\theta_5 + 1.5843)s_{123} - \\ & 4.7592e^{-33}c_2 s_{134} - 4.7592e^{-33}c_3 s_{124} + 3.7355e^{-29}s(\theta_5 + 1.5843)c_{23}s_1 + \\ & 3.7355e^{-29}c_{24}s_{13}c(\theta_5 + 1.5843) + 3.7355e^{-29}c_{34}s_{12}c(\theta_5 + 1.5843))^2 + \\ & 0.3830c(\theta_2 + 5.6192e^{-4})^2 + 0.0068c(\theta_2 + \theta_3)^2 c_1 s_1 - c(\theta_2 + \\ & \theta_3)s_4(5.8418e^{-4}c_4 s_1 - 9.7093e^{-10}c_{14} + 7.6194e^{-6}c(\theta_2 + \theta_3)s_4 + \\ & 5.8418e^{-4}c_{12}s_{34} + 5.8418e^{-4}c_{13}s_{24} + 9.7093e^{-10}c_2 s_{134} + 9.7093e^{-10}c_3 s_{124}) \times \\ & 3.2361e^{-4}c(\theta_2 + \theta_3)s(\theta_2 + \theta_3)c_1 - 3.2188e^{-7}c(\theta_2 + \theta_3)s(\theta_2 + \theta_3)s_1 + 0.0071 \end{aligned} \quad (77)$$

$$\begin{aligned} m_{12} = {} & 6.5921e^{-5}s(\theta_2 + \theta_3 - 2.5577) - 0.0072s(2\theta_1) - 0.0027s(\theta_2 + \\ & 5.6192e^{-4}) + 3.7554e^{-4}s_2 + 4.8499e^{-6}c(\theta_2 + \theta_3)^2 + 1.1437e^{-26}s(\theta_4 + \end{aligned} \quad (78)$$

$$1.6029)\Big(4.0422e^{-27}c_2s_3 - 8.1315e^{-28}c_{23} - 8.6736e^{-27}s_2 + 4.0422e^{-27}c_3s_2 + 8.1315e^{-28}c_2s_3 + 4.8984e^{-30}c(\theta_4 + 1.5843)s_{23} - 4.8984e^{-30}c_{23}c(\theta_4 + 1.5843)\Big) - 0.0026{c_1}^2 - 593(4.7592e^{-33}c_4 + 3.755e^{-29}s_4c(\theta_5 - 1.5843)(5.4210e^{-26}s_2 + 5.0822e^{-27}c_{23} + 4.6892e^{-26}c_{23} + 4.6892e^{-26}c_3s_2 - 5.0822e^{-27}s_{23} + 2.9745e^{-30}s_{234} - 2.3347e^{-26}s(\theta_5 - 1.5843)c_2s_3 - 2.3347e^{-26}s(\theta_5 - 1.5843)c_3s_2 - 2.9745e^{-30}c_{23}s_4 + 2.3347e^{-26}c_{234}c(\theta_5 - 1.5843) - 2.3347e^{-26}c_4s_{23}c(\theta_5 - 1.5843) + (c_4s_1 + c_{12}s_{34} + c_{13}s_{24})(5.8916e^{-4}c_4s_1 - 6.7417e^{-6}c_{14} - 5.8418e^{-4}c(\theta_2 + \theta_3)s_4 + 5.8916e^{-4}c_{12}s_{34} + 5.8916e^{-4}c_{13}s_{24} + 6.7417e^{-6}c_2s_{134} + 6.7417e^{-6}c_3s_{124}) + (c_2s_{134} - c_{14} + c_3s_{124})(8.7259e^{-8}c_{14} + 6.7417e^{-6}c_4s_1 - 9.7093e^{-10}c(\theta_2 + \theta_3)s_4 + 6.7417e^{-6}c_{12}s_{34} + 6.7417e^{-6}c_{13}s_{24} - 8.7259e^{-8}c_2s_{134} - 8.7259e^{-8}c_3s_{124}) + 3.4167c(\theta_2 + \theta_3)^2{c_1}^2 + 0.0068c(\theta_2 + \theta_3)^2c_1s_1 - c(\theta_2 + \theta_3)s_4\big(5.8418e^{-4}c_4s_1 - 9.7093e^{-10}c_{14} + 7.6194e^{-5}c(\theta_2 + \theta_3)s_4 + 5.8418e^{-4}c_{12}s_{34} + 5.8418e^{-4}c_{13}s_{24} + 9.7093e^{-10}c_2s_{134} + 9.7093e^{-10}c_3s_{124}\big) + 0.0032c(\theta_2 + \theta_3)s(\theta_2 + \theta_3)c_1 - 3.2188e^{-7}c(\theta_2 + \theta_3)s(\theta_2 + \theta_3)s_1 + 0.0029$$

$$m_{13} = 6.5921e^{-5}s(\theta_2 + \theta_3 - 2.5577) - 0.0072s(2\theta_1) + 4.8499e^{-6}c(\theta_2 + \theta_3)^2 - 593\Big(4.7592e^{-33}c_4 + 3.7355e^{-29}s_4c(\theta_5 + 1.5843)\Big)\Big(5.0822e^{-27}c_{23} + 4.6892e^{-26}c_2s_3 + 4.6892e^{-26}c_3s_2 - 5.0822e^{-27}s_{23} + 2.9745e^{-30}s_{234} - 2.3347e^{-26}s(\theta_5 + 1.5843)c_2s_3 - 2.3347e^{-26}s(\theta_5 + 1.5843)c_3s_2 - 2.9745e^{-30}c_{23}s_4 + 2.3347e^{-26}c_{234}c(\theta_5 + 1.5843) - 2.3347e^{-26}c_4s_{23}c(\theta_5 + 1.5843)\Big) - 0.0026{c_1}^2 + (c_4s_1 + c_{12}s_{34} + c_{13}s_{24})(5.8916e^{-4}c_4s_1 - 6.7417e^{-6}c_{14} - 5.8418e^{-4}c(\theta_2 + \theta_3)s_4 + 5.8916e^{-4}c_{12}s_{34} + 5.8916e^{-4}c_{13}s_{24} + 6.7417e^{-6}c_2s_{134} + 6.7417e^{-6}c_3s_{124}) + (c_2s_{134} - c_{14} + c_3s_{124})(8.7259e^{-8}c_{14} + 6.7417e^{-6}c_4s_1 - 9.7093e^{-10}c(\theta_2 + \theta_3)s_4 + 6.7417e^{-6}c_{12}s_{34} + 6.7417e^{-6}c_{13}s_{24}) - 8.7259e^{-8}c_2s_{134} - 8.7259e^{-8}c_3s_{124}) + 3.4167c(\theta_2 + \theta_3)^2{c_1}^2 + 3.4310e^{-25}s(\theta_4 + 1.6029)\Big(1.3474e^{-26}c_2s_3 - 2.7105e^{-27}c_{23} + 1.3474e^{-26}c_3s_2 + 2.7105e^{-27}s_{23} + 1.6328e^{-29}c(\theta_4 + 1.5843)s_{23} - 1.6328e^{-29}c_{23}c(\theta_4 + 1.5843)\Big) + 0.0068c(\theta_2 + \theta_3)^2c_1s_1 - c(\theta_2 + \theta_3)s_4\big(5.8916e^{-4}c_4s_1 - 9.7093e^{-10}c_{14} + 7.6194e^{-5}c(\theta_2 + \theta_3)s_4 + 5.8418e^{-4}c_{12}s_{34} + 5.8418e^{-4}c_{13}s_{24} + 9.7093e^{-10}c_2s_{134} + 9.7093e^{-10}c_3s_{124}\big) + 0.0032c(\theta_2 + \theta_3)s(\theta_2 + \theta_3)c_1 - 3.2188e^{-7}c(\theta_2 + \theta_3)s(\theta_2 + \theta_3)s_1 + 0.0029 \quad \textbf{(79)}$$

$$m_{14} = 3.9045e^{-8}s_4 - 1.9778e^{-6}c(\theta_4 + 1.5843) - 0.0072s(2\theta_1) + 4.8499e^{-6}c(\theta_2 + \theta_3)^2 - 8.4387e^{-6}c_2c(\theta_4 + 1.5843) + 4.7749e^{-9}c_2s_3 + 4.7749e^{-9}c_3s_2 + 1.6659e^{-7}c_2s_4 - 3.0647e^{-4}c_4c(\theta_5 - 1.5843) - 0.0026{c_1}^2 + 3.4167c(\theta_2 + \theta_3)^2{c_1}^2 - 7.6194e^{-5}c(\theta_2 + \theta_3)^2{c_4}^2 - 8.7259e^{-8}{c_1}^2{c_4}^2 + 5.8916e^{-4}{c_4}^2{s_1}^2 - 0.0013c_{24}c(\theta_5 - 1.5843) - 1.5618e^{-8}c_2s_{34} - 1.5618e^{-8}c_3s_{24} - 3.9327e^{-6}c(\theta_4 + 1.5843)s_{23} - 1.4410e^{-7}s_{234} + 0.0068c(\theta_2 + \theta_3)^2c_1s_1 - 1.3483e^{-5}c_1{c_4}^2s_1 + 5.6315e^{-4}c_2s_3c(\theta_5 - 1.5843)^2 + 5.6315e^{-4}c_3s_2c(\theta_5 - 1.5843)^2 + 0.0032c(\theta_2 + \theta_3)s(\theta_2 + \theta_3)c_1 - 3.2188e^{-7}c(\theta_2 + \theta_3)s(\theta_2 + \theta_3)s_1 + 3.9327e^{-6}c_{23}c(\theta_4 + 1.5843) + 1.4410e^{-7}c_{23}s_4 + 7.9113e^{-7} + 7.9113e^{-7}c_3c(\theta_4 + 1.5843)s_2 + 7.1747e^{-7}s(\theta_5 - 1.5843)s_{234} + 5.8916e^{-4}{c_1}^2{c_2}^2{s_3}^2{s_4}^2 + 5.8916e^{-4}{c_1}^2{c_3}^2{s_2}^2{s_4}^2 - 8.7259e^{-8}{c_2}^2{s_2}^2{s_3}^2{s_4}^2 - 8.7259e^{-8}{c_3}^2{s_1}^2{s_2}^2{s_4}^2 + 1.9419e^{-9}c(\theta_2 + \theta_3)c_{14}s_4 - 0.0012c(\theta_2 + \theta_3)c_4s_{14} - 1.1311e^{-5}c_{234}c(\theta_5 - 1.5843) + 1.2259e^{-4}c_{24}s_3c(\theta_5 - 1.5843) + 1.2259e^{-4}c_{34}s_2c(\theta_5 - 1.5843) - 7.1747e^{-7}s(\theta_5 - 1.5843)c_{23}s_4 + 1.1311e^{-5}c_4s_{23}c(\theta_5 - 1.5843) - 5.6315e^{-4}s(\theta_5 - 1.5843)c_4s_{23}c(\theta_5 - 1.5843) - 1.3483e^{-5}{c_1}^2c_2c_4s_{34} - \quad \textbf{(80)}$$

$$1.3483e^{-5}c_1{}^2c_{34}s_{24} + 1.3483e^{-5}c_{24}s_1{}^2s_{34} + 1.3483e^{-5}c_{34}s_1{}^2s_{24} + 5.6315e^{-4}s(\theta_5 - 1.5843)c_{234}c(\theta_5 - 1.5843) + 1.3483e^{-5}c_1c_2{}^2s_1s_3{}^2s_4{}^2 + 1.3483e^{-5}c_1c_3{}^2s_1s_4{}^2 - 0.0012c(\theta_2 + \theta_3)c_1c_2s_3s_4{}^2 - 0.0012c(\theta_2 + \theta_3)c_{13}s_2s_4{}^2 - 1.9419e^{-9}c(\theta_2 + \theta_3)c_2s_{13}s_4{}^2 - 1.9419e^{-9}c(\theta_2 + \theta_3)c_3s_{12}s_4{}^2 + 0.0012 + 2.6967e^{-5}c_{123}s_{123}s_4{}^2 + 0.0029$$

$$m_{15} = 4.8499e^{-6}c(\theta_2 + \theta_3)^2 - 0.0072s(2\theta_1) - 0.0026c_1{}^2 + 3.0647e^{-4}s(\theta_5 - 1.5843)s_4 + 3.4167c(\theta_2 + \theta_3)^2c_1{}^2 - 7.6194e^{-5}c(\theta_2 + \theta_3)^2s_4{}^2 - 8.7259e^{-8}c_1{}^2c_4{}^2 + 5.8916e^{-4}c_4{}^2s_1{}^2 + 5.6315e^{-4}s_{234} + 7.1747e^{-7}s(\theta_5 - 1.5843)c_2s_3 + 7.1747e^{-7}s(\theta_5 - 1.5843)c_3s_2 + 0.0013s(\theta_5 - 1.5843)c_2s_4 + 0.0068c(\theta_2 + \theta_3)^2c_1s_1 - 1.3483e^{-5}c_1c_4{}^2s_1 + 0.0032c(\theta_2 + \theta_3)s(\theta_2 + \theta_3)c_1 - 3.2188e^{-7}c(\theta_2 + \theta_3)s(\theta_2 + \theta_3)s_1 - 5.6315e^{-4}c_{23}s_4 - 1.2259e^{-4}s(\theta_5 - 1.5843)c_2s_{34} - 1.2259e^{-4}s(\theta_5 - 1.5843)c_3s_{24} - 1.1311e^{-5}s(\theta_5 - 1.5843)s_{234} + 5.8916e^{-4}c_1{}^2c_2{}^2s_3{}^2s_4{}^2 + 5.8916e^{-4}c_1{}^2c_3{}^2s_2{}^2s_4{}^2 - 8.7259e^{-8}c_2{}^2s_1{}^2s_3{}^2s_4{}^2 - 8.7259e^{-8}c_3{}^2s_1{}^2s_2{}^2s_4{}^2 + 1.9419e^{-9}c(\theta_2 + \theta_3)c_{14}s_4 - 0.0012c(\theta_2 + \theta_3)c_4s_{14} - 7.1747e^{-7}c_{234}c(\theta_5 - 1.5843) + 1.1311e^{-5}s(\theta_5 - 1.5843)c_{23}s_4 + 7.1747e^{-7}c_4s_{23}c(\theta_5 - 1.5843) - 1.3483e^{-5}c_1{}^2c_{24}s_{34} - 1.3483e^{-5}c_1{}^2c_{34}s_{24} + 1.3483e^{-5}c_{24}s_1{}^2s_{34} + 1.3483e^{-5}c_{34}s_1{}^2s_{24} + 1.3483e^{-5}c_1c_2{}^2s_1s_3{}^2s_4{}^2 + 1.3483e^{-5}c_1c_3{}^2s_1s_2{}^2s_4{}^2 - 0.0012c(\theta_2 + \theta_3)c_{12}s_3s_4{}^2 - 0.0012c(\theta_2 + \theta_3)c_{13}s_2s_4{}^2 - 1.9419e^{-9}c(\theta_2 + \theta_3)c_2s_{13}s_4{}^2 - 1.9419e^{-9}c(\theta_2 + \theta_3)c_3s_{12}s_4{}^2 + 0.0012c_1{}^2c_{23}s_{23}s_4{}^2 - 1.7452e^{-7}c_{23}s_1{}^2s_{23}s_4{}^2 + 0.0012c_{124}s_{134} + 0.0012c_{134}s_{124} + 2.6967e^{-5}c_{123}s_{123}s_4{}^2 + 0.0029 \quad \textbf{(81)}$$

$$m_{21} = 6.5921e^{-5}s(\theta_2 + \theta_3 - 2.5577) - 0.0072s(2\theta_1) - 0.0072s(\theta_2 + 5.6192e^{-4}) + 3.7554e^{-4}s_2 + 4.8499e^{-6}c(\theta_2 + \theta_3)^2 + 1.1437e^{-26}s(\theta_4 + 1.6029)\Big(4.0422e^{-4}c_2s_3 - 8.1315e^{-28}c_{23} - 8.6736e^{-27}s_2 + 4.0422e^{-27}c_3s_2 + 8.1315e^{-28}s_{23} + 4.8984e^{-30}c(\theta_4 + 1.5843)s_{23} - 4.8984e^{-3}c_{23}c(\theta_4 + 1.5843)\Big) - 0.0026c_1{}^2 - 593\Big(4.7592e^{-23}c_4 + 3.7355e^{-29}s_4c(\theta_5 - 1.5843)\Big)\Big(5.4210e^{-26}s_2 + 5.0822e^{-27}c_{23} + 4.6892e^{-26}c_2s_3 + 4.6892e^{-26}c_3s_2 - 5.0822e^{-27}s_{23} + 2.9745e^{-30}s_{234} - 2.3347e^{-26}s(\theta_5 - 1.5843)c_2s_3 - 2.3347e^{-26}s(\theta_5 - 1.5843)c_3s_2 - 2.9745e^{-30}c_{23}s_4 + 2.3347e^{-26}c_{234}c(\theta_5 - 1.5843) - 2.3347e^{-26}c_4s_{23}c(\theta_5 - 1.5843)\Big) + (c_4s_1 + c_{12}s_{34} + c_{13}s_{24})(5.8916e^{-4}c_4s_1 - 6.7417e^{-6}c_{14} - 5.8418e^{-4}c(\theta_2 + \theta_3)s_4 + 5.8916e^{-4}c_{12}s_{34} + 5.8916e^{-4}c_{13}s_{24} + 6.7417e^{-6}c_2s_{134} + 6.7417e^{-6}c_3s_{124} + c_2s_{134} - c_{14} + c_3s_{124})(8.7259e^{-8}c_{14} + 6.7417e^{-6}c_4s_1 - 9.7093e^{-10}c(\theta_2 + \theta_3)s_4 + 6.7417e^{-6}c_{12}s_{34} + 6.7417e^{-6}c_{13}s_{24} + 8.7259e^{-8}c_2s_{134} - 8.7259e^{-8}c_2s_{134} - 8.7259e^{-8}c_2s_{124}) + 3.4167c(\theta_2 + \theta_3)^2c_1{}^2 + 0.0068c(\theta_2 + \theta_3)^2c_1s_1 - c(\theta_2 + \theta_3)s_4)(5.8418e^{-4}c_4s_1 - 9.7093e^{-10}c_{14} + 7.6194e^{-4}c(\theta_2 + \theta_3)s_4 + 5.8418e^{-4}c_{12}s_{34} + 5.8418e^{-4}c_{13}s_{24} + 9.7093e^{-10}c_2s_{134} + 9.7093e^{-10}c_3s_{124}) + 0.0032c(\theta_2 + \theta_3)s(\theta_2 + \theta_3)c_1 - 3.288e^{-7}c(\theta_2 + \theta_3)s(\theta_2 + \theta_3)s_1 + 0.0029 \quad \textbf{(82)}$$

$$m_{22} = 1.4079e^{-4}c(2\theta_4) - 0.0072s(2\theta_1) + 0.0061c(\theta_3 - 2.5577) - 0.0087c_3 - 0.0034s_3 - 3.1236e^{-8}s_4 + 4.899e^{-6}c(\theta_2 + \theta_3)^2 + 3.3318e^{-7}s_{34} - 0.0026c_1{}^2 + 1.5823e^{-6}c(1.6029)c_4 - 1.5823e^{-6}s(1.6029)s_4 - 2.2622e^{-5}c(1.5843)s_5 + 2.2622e^{-5}s(1.5843)c_5 + 2.3829e^{-9}c(3.2058)c(2\theta_4) + 3.4167c(\theta_2 + \theta_3)^2c_1{}^2 - 7.6194e^{-5}c(\theta_2 + \theta_3)^2s_4{}^2 - 1.4079e^{-4}c(3.1687)c(2\theta_5) - 2.3829e^{-9}s(3.2058)s(2\theta_4) - 8.7259e^{-8}c_1{}^2c_4{}^2 - 1.4079e^{-4}s(3.1687)s(2\theta_5) + 5.8916e^{-4}c_4{}^2s_1{}^2 + 1.4079e^{-4}s(3.1687)c(2\theta_4)s(2\theta_5) - 1.6877e^{-5}c(1.6029)c_4s_3 + 0.0068c(\theta_2 + \theta_3)^2c_1s_1 + 2.4518e^{-4}c(1.5843)c_{45} - \quad \textbf{(83)}$$

$$
\begin{gathered}
0.0026c(1.5843)c_3s_5 + 0.0026c(1.5843)c_{35} + 1.6877e^{-5}s(1.5843)s_{34} + \\
2.4518e^{-4}s(1.5843)c_4s_5 - 1.3483e^{-5}c_1c_1{}^2s_1 + 0.0032c(\theta_2+\theta_3)(\theta_2+\theta_3)c_1 - \\
7.1747e^{-7}c(1.5843)s(2\theta_4)c_5 - 3.2188e^{-7}c(\theta_2+\theta_3)(\theta_2+\theta_3)s_1 - \\
7.1747e^{-7}s(1.5843)s(2\theta_4)s_5 + 1.4079e^{-4}c(3.1687)c(2\theta_4)c(2\theta_5) - \\
0.0026c(1.5843)c_{45}s_3 - 0.0026(1.5843)c_4s_{35} + 5.8916e^{-4}c_1{}^2c_2{}^2s_3{}^2s_4{}^2 + \\
5.8916e^{-4}c_1{}^2c_3{}^2s_2{}^2s_4{}^2 - 8.7259e^{-8}c_2{}^2s_1{}^2s_3{}^2s_4{}^2 - 8.7259e^{-8}c_3{}^2s_1{}^2s_2{}^2s_4{}^2 + \\
1.9419e^{-9}c(\theta_2+\theta_3)c_{14}s_4 - 0.0012c(\theta_2+\theta_3)c_4s_{14} - 1.3483e^{-5}c_1{}^2c_{24}s_{34} - \\
1.3483e^{-5}c_1{}^2c_{34}s_{24} + 1.3483e^{-5}c_{24}s_1{}^2s_{34} + 1.3483e^{-5}c_{34}s_1{}^2s_{24} + \\
1.3483e^{-5}c_1c_2{}^2s_1s_3{}^2s_4{}^2 + 1.3483e^{-5}c_1c_3{}^2s_1s_2{}^2s_4{}^2 - 0.0012c(\theta_2 + \\
\theta_3)c_{12}s_3s_4{}^2 - 0.0012c(\theta_2+\theta_3)c_{13}s_2s_4{}^2 - 1.9419e^{-9}c(\theta_2+\theta_3)c_2s_{13}s_4{}^2 - \\
1.9419e^{-9}c(\theta_2+\theta_3)c_3s_{12}s_4{}^2 + 0.0012c_1{}^2c_{23}s_3s_4{}^2 - 1.7452e^{-7}c_{23}s_1{}^2s_{23}s_4{}^2 + \\
0.0012c_{124}s_{134} + 0.0012c_{134}s_{124} + 2.6967e^{-5}c_{123}s_{123}s_4{}^2 + 0.0486
\end{gathered}
$$

$$
\begin{gathered}
m_{23} = 1.4079e^{-4}c(2\theta_4) - 0.0072s(2\theta_1) + 0.0030c(\theta_3 - 2.5577) - 0.0043c_3 - \\
0.0017s_3 - 3.1236e^{-8}s_4 + 4.8499e^{-6}c(\theta_2+\theta_3)^2 + 1.6659e^{-7}s_{34} - 0.0026c_1{}^2 + \\
1.5823e^{-6}c(1.6029)c_4 - 1.5823e^{-6}s(1.6029)s_4 - 2.2622e^{-5}c(1.6029)s_5 + \\
2.2622e^{-5}s(1.6029)c_5 + 2.3829e^{-9}c(3.2058)c(2\theta_4) + 3.4167c(\theta_2+\theta_3)^2c_{12} - \\
7.6194e^{-5}c(\theta_2+\theta_3)^2s_4{}^2 - 1.4079e^{-4}c(3.1687)c(2\theta_5) - \\
2.3829e^{-9}s(3.2058)s(2\theta_4) - 8.7259e^{-8}c_1{}^2c_4{}^2 - 1.4079e^{-4}s(3.1687)s(2\theta_5) + \\
5.8916e^{-4}c_4{}^2s_1{}^2 + 1.4079e^{-4}s(3.1687)c(2\theta_4)s(2\theta_5) - \\
8.4387e^{-6}c(1.6029)c_4s_3 + 0.0068c(\theta_2+\theta_3)^2c_1s_1 + 2.4518e^{-4}c(1.5843)c_{45} - \\
0.0013c(1.5843)c_3s_5 + 0.0013s(1.5843)c_{35} + 8.4387e^{-6}s(1.6029)s_{34} + \\
2.4518e^{-4}s(1.5843)c_4s_5 - 1.3483e^{-5}c_1c_4{}^2s_1 + 0.0032c(\theta_2+\theta_3)s(\theta_2+\theta_3)c_1 - \\
7.1747e^{-7}c(1.5843)c(2\theta_5)s(2\theta_4) - 3.2188e^{-7}c(\theta_2+\theta_3)s(\theta_2+\theta_3)s_1 - \\
1.1747e^{-7}s(1.5843)s(2\theta_4)s_5 + 1.4079e^{-4}c(3.1687)c(2\theta_4)c(2\theta_5) - \\
0.0013c(1.5843)c_{45}s_3 - 0.0013c(1.5843)c_4s_{35} + 5.8916e^{-4}c_1{}^2c_2{}^2s_3{}^2s_4{}^2 + \\
5.8916e^{-4}c_1{}^2c_3{}^2s_2{}^2s_4{}^2 - 8.7259e^{-8}c_2{}^2s_1{}^2s_3{}^2s_4{}^2 - 8.7259e^{-8}c_3{}^2s_1{}^2s_2{}^2s_4{}^2 + \\
1.9419e^{-9}c(\theta_2+\theta_3)c_{14}s_4 - 0.0012c(\theta_2+\theta_3)c_4s_{14} - 1.3483e^{-5}c_1{}^2c_{24}s_{34} - \\
1.3483e^{-5}c_1{}^2c_{34}s_{24} + 1.3483e^{-5}c_{24}s_1{}^2s_{34} + 1.3483e^{-5}c_{34}s_1{}^2s_{24} + \\
1.3483e^{-5}c_1c_2{}^2s_1s_3{}^2s_4{}^2 + 1.3483e^{-5}c_1c_3{}^2s_1s_2{}^2s_4{}^2 - 0.0012c(\theta_2 + \\
\theta_3)c_{12}s_3s_4{}^2 - 0.0012c(\theta_2+\theta_3)c_{13}s_4{}^2 - 1.9419e^{-9}c(\theta_2+\theta_3)c_2s_{13}s_4{}^2 - \\
1.9419e^{-9}c(\theta_2+\theta_3)c_3s_{12}s_4{}^2 + 0.0012c_1{}^2c_{23}s_{23}s_4{}^2 - 1.7352e^{-7}c_{23}s_1{}^2s_{23}s_4{}^2 + \\
0.0012c_{124}s_{134} + 0.0012c_{134}s_{124} + 2.6967e^{-5}c_{123}s_{123}s_4{}^2 + 0.0095
\end{gathered}
\tag{84}
$$

$$
\begin{gathered}
m_{24} = 4.8499e^{-6}c(\theta_2+\theta_3)^2 - 0.0072s(2\theta_1) - 0.0026c_1{}^2 - 593\Big(3.897e^{-29}c_4 + \\
3.0601e^{-25}s_4s(\theta_5 - 1.5843)\Big)\ (5.4210e^{-26}c_3 - 2.3347e^{-26}s(\theta_5 - 1.5843) + \\
4.6892e^{-26}) + (c_4s_1 + c_{12}s_{34} + c_{13}s_{24})\ (5.8916e^{-4}c_4s_1 - 6.7417e^{-6}c_{14} - \\
5.8916e^{-4}\,c(\theta_2+\theta_3)s_4 + 5.8916e^{-4}c_{12}s_{34} + 5.8916e^{-4}c_{13}s_{24} + \\
6.7417e^{-6}c_2s_{134} + 6.7417e^{-6}c_3s_{124}) + (c_2s_{134} - c_{14} + c_3s_{124})(8.7259e^{-8}c_{14} + \\
6.7417e^{-6}c_4s_1 - 9.7093e^{-10}c(\theta_2+\theta_3)s_4 + 6.7417e^{-6}c_{12}s_{34} + \\
6.7417e^{-6}c_{13}s_{24} - 8.7259e^{-8}c_2s_{134} - 8.7259e^{-8}c_3s_{124}) + 3.4167c(\theta_2 + \\
\theta_3)^2c_1{}^2 - 2.9278e^{-23}(\theta_4 - 1.6029)(8.6736e^{-26}c_3 - 4.0422e^{-26}) + \\
0.0068c(\theta_2+\theta_3)^2c_1s_1 - c(\theta_2+\theta_3)s_4\big(5.8916e^{-4}c_4s_1 - 9.7093e^{-10}c_{14} + \\
7.6194e^{-5}(\theta_2+\theta_3)s_4 + 5.8418e^{-4}c_{12}s_{34} + 5.8418e^{-4}c_{13}s_{24} + \\
9.7093e^{-10}c_2s_{134} + 9.7093e^{-10}c_3s_{124}\big) + 0.0032c(\theta_2+\theta_3)s(\theta_2+\theta_3)c_1 - \\
3.2188e^{-7}c(\theta_2+\theta_3)s(\theta_2+\theta_3)s_1 + 0.0029
\end{gathered}
\tag{85}
$$

$$
\begin{gathered}
m_{25} = 5.6315e^{-4}c_4 - 0.0072s(2\theta_1) + 1.2259e^{-4}c(\theta_5 - 1.5843) + \\
4.8499e^{-6}c(\theta_2+\theta_3)^2 - 0.0026c_{12} - 0.0013s_3c(\theta_5 - 1.5843) - 1.311e^{-5}s(\theta_5 - \\
1.5843)c_4 - 7.1747e^{-7}s_4c(\theta_5 - 1.5843) + 3.4167c(\theta_2+\theta_3)^2c_1{}^2 - \\
7.6194e^{-5}c(\theta_2+\theta_3)^2s_4{}^2 - 8.7259e^{-8}c_1{}^2c_4{}^2 + 5.8916e^{-4}c_4{}^2s_1{}^2 -
\end{gathered}
\tag{86}
$$

$$0.0013s(\theta_5 - 1.5843)c_{34} + 0.0068c(\theta_2 + \theta_3)^2 c_1 s_1 - 1.3483e^{-5} c_1 c_4^2 s_1 + 0.0032c(\theta_2 + \theta_3)s(\theta_2 + \theta_3)c_1 - 3.2188e^{-7} c(\theta_2 + \theta_3)s(\theta_2 + \theta_3)s_1 + 5.8916e^{-4} c_1^2 c_2^2 s_3^2 s_4^2 + 5.8916e^{-4} c_1^2 c_3^2 s_2^2 s_4^2 - 8.7259e^{-8} c_2^2 s_1^2 s_3^2 s_4^2 - 8.7259e^{-8} c_3^2 s_1^2 s_2^2 s_4^2 + 1.9419e^{-9} c(\theta_2 + \theta_3)c_{14} s_3 - 0.0012c(\theta_2 + \theta_3)c_4 s_{14} - 1.3483e^{-5} c_1^2 c_{24} s_{34} - 1.3483e^{-5} c_1^2 c_{34} s_{24} + 1.3483e^{-5} c_{24} s_1^2 s_{34} + 1.3483e^{-5} c_{34} s_1^2 s_{24} + 1.3483e^{-5} c_1 c_2^2 s_1 s_3^2 s_4^2 + 1.3483e^{-5} c_1 c_3^2 s_1 s_2^2 s_4^2 - 0.0012c(\theta_2 + \theta_3)c_{12} s_3 s_4^2 - 0.0012c(\theta_2 + \theta_3)c_{13} s_2 s_4^2 - 1.9419e^{-9} c(\theta_2 + \theta_3)c_2 s_1 s_3 s_4^2 - 1.9419e^{-9} c(\theta_2 + \theta_3)c_3 s_{12} s_4^2 + 0.0012c_1^2 c_{23} s_3 s_4^2 - 1.7452e^{-7} c_{23} s_1^2 s_{23} s_4^2 + 0.0012c_{124} s_{134} + 0.0012c_{134} s_{124} + 2.6967e^{-5} c_{123} s_{123} s_4^2 + 0.0029$$

$$m_{31} = 6.5921e^{-5} s(\theta_2 + \theta_3 - 2.5577) - 0.0072s(2\theta_1) + 4.8499e^{-6} c(\theta_2 + \theta_3)^2 - 593\left(4.7592e^{-33} c_4 + 3.7355e^{-29} s_4 c(\theta_5 - 1.5843)\right)\left(5.0822e^{-27} c_{23} + 4.6892e^{-26} c_2 s_3 + 4.6892e^{-26} c_3 s_2 - 5.0822e^{-27} s_{23} + 2.9745e^{-30} s_{234} - 2.3347e^{-26} s(\theta_5 - 1.5843)c_2 s_3 - 2.3347e^{-26} s(\theta_5 - 1.5843)c_3 s_2 - 2.9745e^{-30} c_{23} s_4 + 2.3347e^{-26} c_{234} c(\theta_5 - 1.5843) - 2.3347e^{-26} c_4 s_{23} c(\theta_5 - 1.5843)\right) - 0.0026c_1^2 + (c_4 s_1 + c_{12} s_{34} + c_{13} s_{24})(5.8916e^{-4} c_4 s_1 - 6.7417e^{-6} c_{14} - 5.8916e^{-4} e^{-7} c(\theta_2 + \theta_3)s_4 + 5.8916e^{-4} c_{12} s_{34} + 5.8916e^{-4} c_{13} s_{24} + 6.7417e^{-6} c_2 s_{134} + 6.7417e^{-6} c_3 s_{124}) + (c_2 s_{134} - c_{14} + c_3 s_{124})(8.7259e^{-8} c_{14} + 6.7417e^{-6} c_4 s_1 - 9.7093e^{-10} c(\theta_2 + \theta_3)s_4 + 6.7417e^{-6} c_{12} s_{34} + 6.7417e^{-6} c_{13} s_{24} - 8.7259e^{-8} c_2 s_{134} - 8.7259e^{-8} c_3 s_{124}) + 3.4167c(\theta_2 + \theta_3)^2 c_1^2 + 3.4310e^{-25} s(\theta_4 + 1.6029)(1.3474e^{-26} c_2 s_3 - 2.7105e^{-27} c_{23} + 1.3474e^{-26} c_3 s_2 + 2.7105e^{-27} s_{23} + 1.6328e^{-29} c(\theta_4 - 1.6029)s_{23} - 1.6328e^{-29} c_{23} c(\theta_4 - 1.6029) + 0.0068c(\theta_2 + \theta_3)^2 c_1 s_1 - c(\theta_2 + \theta_3)s_4(5.8418e^{-4} c_4 s_1 - 9.7093e^{-10} c_{14} + 7.6194e^{-5} c(\theta_2 + \theta_3)s_4 + 5.8418e^{-4} c_{12} s_{34} + 5.8418e^{-4} c_{13} s_{24} + 9.7093e^{-10} c_2 s_{134} + 9.7093e^{-10} c_3 s_{124} + 0.0032c(\theta_2 + \theta_3)s(\theta_2 + \theta_3)c_1 - 3.2188e^{-7} c(\theta_2 + \theta_3)s(\theta_2 + \theta_3)s_1 + 0.0029 \quad (87)$$

$$m_{32} = 1.4079e^{-4} c(2\theta_4) - 0.0072s(2\theta_1) + 0.0030c(\theta_3 - 2.5577) - 0.0043c_3 - 0.0017s_3 - 3.1236e^{-8} s_4 + 4.8499e^{-6} c(\theta_2 + \theta_3)^2 + 1.6659e^{-7} s_{34} - 0.0026c_1^2 + 1.5823e^{-6} c(1.6029)c_4 - 1.5823e^{-6} s(1.6029)s_4 - 2.2622e^{-5} c(1.6029)s_5 + 2.2622e^{-5} s(1.5843)c_5 + 2.3829e^{-9} c(1.6029)c(2\theta_4) + 3.4167c(\theta_2 + \theta_3)^2 c_1^2 - 7.6194e^{-5} c(\theta_2 + \theta_3)^2 s_4^2 - 1.4079e^{-4} c(3.1687)c(2\theta_5) - 2.3829e^{-9} s(3.2058)s(2\theta_4) - 8.7259e^{-8} c_1^2 c_4^2 - 1.4079e^{-4} s(3.1687)s(2\theta_5) + 5.8916e^{-4} c_4^2 s_1^2 + 1.4079e^{-4} s(3.1687)c(2\theta_4)s(2\theta_5) - 8.4387e^{-6} c(1.6029)c_4 s_3 + 0.0068c(\theta_2 + \theta_3)^2 c_1 s_1 + 2.4518e^{-4} c(1.5843)c_{45} - 0.0013c(1.5843)c_3 s_5 + 0.0013s(1.5843)c_{35} + 8.4387e^{-6} s(1.6029)s_{34} + 2.4518e^{-4} s(1.5843)c_4 s_5 - 1.3483e^{-5} c_1 c_4^2 s_1 + 0.0032c(\theta_2 + \theta_3)s(\theta_2 + \theta_3)c_1 - 7.1747e^{-7} c(1.5843)s(2\theta_1)c_5 - 3.2188e^{-7} c(\theta_2 + \theta_3)s(\theta_2 + \theta_3)s_1 - 7.1747e^{-7} s(1.5843)s(2\theta_4)s_5 + 1.4079e^{-4} c(3.1687)c(2\theta_4)c(2\theta_5) - 0.0013c(1.5843)c_{45} s_3 - 0.0013s(1.5843)c_4 s_{35} + 5.8916e^{-4} c_1^2 c_2^2 s_3^2 s_4^2 + 5.8916e^{-4} c_1^2 c_3^2 s_2^2 s_4^2 - 8.7259e^{-8} c_2^2 s_1^2 s_3^2 s_4^2 - 8.7259e^{-8} c_3^2 s_1^2 s_2^2 s_4^2 + 1.9419e^{-9} c(\theta_2 + \theta_3)c_{14} s_4 - 0.0012c(\theta_2 + \theta_3)c_4 s_{14} - 1.3483e^{-5} c_1^2 c_{24} s_{34} - 1.3483e^{-5} c_1^2 c_{34} s_{24} + 1.3483e^{-5} c_{24} s_1^2 s_{34} + 1.3483e^{-5} c_{34} s_1^2 s_{24} + 1.3483e^{-5} c_1 c_2^2 s_1 s_4^2 + 1.3483e^{-5} c_1 c_3^2 s_1 s_2^2 s_4^2 - 1.9419e^{-9} c(\theta_2 + \theta_3)c_3 s_{12} s_4^2 + 0.0012c_1^2 c_{23} s_{23} s_4^2 - 1.7452e^{-7} c_{23} s_1^2 s_{23} s_4^2 + 0.0012c_{124} s_{134} + 0.0012c_{134} s_{124} + 2.6967e^{-5} c_{123} s_{123} s_4^2 + 0.0095 \quad (88)$$

$$m_{33} = 1.407e^{-4} c(2\theta_4) + 2.3829e^{-9} c(2\theta_4 + 3.258) - 0.0072s(2\theta_1) + 1.5823e^{-6} c(\theta_4 + 1.6029) - 3.1236e^{-8} s_4 + 4.8499e^{-6} c(\theta_2 + \theta_3)^2 - 0.0026c_1^2 - 2.2622e^{-5} c(1.5843)s_5 + 2.2622e^{-5} s(1.5843)c_5 + 3.4167c(\theta_2 + \theta_3)^2 c_1^2 - \quad (89)$$

$$
\begin{gathered}
7.6194e^{-5}c(\theta_2+\theta_3)^2{s_4}^2 - 1.4079e^{-4}c(3.1687)c(2\theta_5) - 8.7259e^{-8}{c_1}^2{c_4}^2 - \\
1.4079e^{-4}s(3.1687)s(2\theta_5) + 5.8916e^{-4}{c_4}^2{s_1}^2 + \\
1.4079e^{-4}s(3.1687)c(2\theta_4)s(2\theta_5) + 0.0068c(\theta_2+\theta_3)^2c_1s_1 + \\
2.4518e^{-4}c(1.5843)c_{45} + 2.4518e^{-4}s(1.5843)c_4s_5 - 1.3483e^{-5}c_1{c_4}^2s_1 + \\
0.0032c(\theta_2+\theta_3)s(\theta_2+\theta_3)c_1 - 7.174e^{-7}c(1.5843)s(2\theta_4)c_5 - 3.2188e^{-7}c(\theta_2 + \\
\theta_3)s(\theta_2+\theta_3)s_1 - 7.174e^{-7}s(1.5843)s(2\theta_4)s_5 + \\
1.4079e^{-4}c(3.1687)c(2\theta_4)c(2\theta_5) + 5.8916e^{-4}{c_1}^2{c_2}^2{s_3}^2{s_4}^2 + \\
5.8916e^{-4}{c_1}^2{c_3}^2{s_2}^2{s_4}^2 - 8.7259e^{-8}{c_2}^2{s_1}^2{s_3}^2{s_4}^2 - 8.7259e^{-8}{c_3}^2{s_1}^2{s_2}^2{s_4}^2 + \\
1.9419e^{-9}c(\theta_2+\theta_3)c_{14}s_4 - 0.0012c(\theta_2+\theta_3)c_4s_{14} - 1.3483e^{-5}{c_1}^2c_{24}s_{34} - \\
1.3483e^{-5}{c_1}^2c_{34}s_{24} + 1.3483e^{-5}c_{24}{s_1}^2s_{34} + 1.3483e^{-5}c_{34}{s_1}^2s_{24} + \\
1.3483e^{-5}c_1{c_2}^2s_1{s_3}^2{s_4}^2 + 1.3483e^{-5}c_1{c_3}^2s_1{s_2}^2{s_4}^2 - 0.0012c(\theta_2 + \\
\theta_3)c_{12}s_3{s_4}^2 - 0.0012c(\theta_2+\theta_3)c_{13}s_2{s_4}^2 - 1.9419e^{-9}c(\theta_2+\theta_3)c_2s_{13}{s_4}^2 - \\
1.9419e^{-9}c(\theta_2+\theta_3)c_3s_{12}{s_4}^2 + 0.0012{c_1}^2c_{23}s_{23}{s_4}^2 - 1.7452e^{-7}c_{23}{s_1}^2s_{23}{s_4}^2 + \\
0.0012c_{124}s_{134} + 0.0012c_{134}s_{124} + 2.6967e^{-5}c_{123}s_{123}{s_4}^2 + 0.0095
\end{gathered}
$$

$$
\begin{gathered}
m_{34} = 3.9327e^{-6}s(1.6029+\theta_4) - 1.4410e^{-7}c_4 - 0.0072s(2\theta_1) + \\
4.8499e^{-6}c(\theta_2+\theta_3)^2 - 0.0026{c_1}^2 + 7.1747e^{-7}s(\theta_5-1.5843)c_4 - \\
1.1311e^{-5}s_4c(\theta_5-1.5843) + 3.4167c(\theta_2+\theta_3)^2{c_1}^2 - 7.6194e^{-5}c(\theta_2 + \\
\theta_3)^2{s_4}^2 - 8.7259e^{-8}{c_1}^2{c_4}^2 + 5.8916e^{-4}{c_4}^2{s_1}^2 + 0.0068c(\theta_2+\theta_3)^2c_1s_1 + \\
5.6315e^{-4}s(\theta_5-1.5843)s_4c(\theta_5-1.5843) - 1.348e^{-5}c_1{c_4}^2s_1 + 0.0032c(\theta_2 + \\
\theta_3)s(\theta_2+\theta_3)c_1 - 3.2188e^{-7}c(\theta_2+\theta_3)s(\theta_2+\theta_3)s_1 + 5.8916e^{-4}{c_1}^2{c_2}^2{s_3}^2{s_4}^2 + \\
5.8916e^{-4}{c_1}^2{c_3}^2{s_2}^2{s_4}^2 - 8.7259e^{-8}{c_2}^2{s_1}^2{s_3}^2{s_4}^2 - 8.7259e^{-8}{c_3}^2{s_1}^2{s_2}^2{s_4}^2 + \\
1.9419e^{-9}c(\theta_2+\theta_3)c_{14}s_4 - 0.0012c(\theta_2+\theta_3)c_4s_{14} - 1.3483e^{-5}{c_1}^2c_{24}s_{34} - \\
1.3483e^{-5}{c_1}^2c_{34}s_{24} + 1.3483e^{-5}c_{24}{s_1}^2s_{34} + 1.3483e^{-5}c_{34}{s_1}^2s_{24} + \\
1.3483e^{-5}c_1{c_2}^2{s_3}^2{s_4}^2 + 1.3483e^{-5}c_1{c_3}^2s_1{s_2}^2{s_4}^2 - 0.0012c(\theta_2+\theta_3)c_{12}s_3{s_4}^2 - \\
0.0012c(\theta_2+\theta_3)c_{13}s_2{s_4}^2 - 1.9419e^{-9}c(\theta_2+\theta_3)c_2s_{13}{s_4}^2 - 1.9419e^{-9}c(\theta_2 + \\
\theta_3)c_3s_{12}{s_4}^2 + 0.0012{c_1}^2c_{23}s_{23}{s_4}^2 - 1.7452e^{-7}c_{23}{s_1}^2s_{23}{s_4}^2 + 0.0012c_{124}s_{134} + \\
0.0012c_{134}s_{124} + 2.6967e^{-5}c_{123}s_{123}{s_4}^2 + 0.0029
\end{gathered}
\tag{90}
$$

$$
\begin{gathered}
m_{35} = 5.6315e^{-4}c_4 - 0.0072s(2\theta_1) + 1.2259e^{-4}c(\theta_5-1.5843) + \\
4.8499e^{-6}c(\theta_2+\theta_3)^2 - 0.0026{c_1}^2 - 1.1311e^{-5}s(\theta_5-1.5843)c_4 - \\
7.1747e^{-7}s_4c(\theta_5-1.5843) + 3.4167c(\theta_2+\theta_3)^2{c_1}^2 - 7.6194e^{-5}c(\theta_2 + \\
\theta_3)^2{s_4}^2 - 8.7259e^{-8}{c_1}^2{c_4}^2 + 5.8916e^{-4}{c_4}^2{s_1}^2 + 0.0068c(\theta_2+\theta_3)^2c_1s_1 - \\
1.3483e^{-5}c_1{c_4}^2s_1 + 0.0032c(\theta_2+\theta_3)s(\theta_2+\theta_3)c_1 - 3.2188e^{-7}c(\theta_2+\theta_3)s(\theta_2 + \\
\theta_3)s_1 + 5.8916e^{-4}{c_1}^2{c_2}^2{s_4}^2 + 5.8916e^{-4}{c_1}^2{c_3}^2{s_2}^2{s_4}^2 - \\
8.7259e^{-8}{c_2}^2{s_1}^2{s_3}^2{s_4}^2 - 8.7259e^{-8}{c_3}^2{s_1}^2{s_2}^2{s_4}^2 + 1.9419e^{-9}c(\theta_2+\theta_3)c_{14}s_4 - \\
0.0012c(\theta_2+\theta_3)c_4s_{14} - 1.3483e^{-5}{c_1}^2c_{24}s_{34} + 1.3483e^{-5}{c_1}^2c_{34}s_{24} + \\
1.3483e^{-5}c_{24}{s_1}^2s_{34} + 1.3483e^{-5}c_{34}{s_1}^2s_{24} + 1.3483e^{-5}c_1{c_2}^2s_1{s_4}^2 + \\
1.3483e^{-5}c_1{c_3}^2s_1{s_2}^2{s_4}^2 - 0.0012c(\theta_2+\theta_3)c_{12}s_3{s_4}^2 - 0.0012c(\theta_2+\theta_3)c_{12}{s_4}^2 - \\
1.9419e^{-9}c(\theta_2+\theta_3)c_2s_{13}{s_4}^2 - 1.9419e^{-9}c(\theta_2+\theta_3)c_3s_{12}{s_4}^2 + \\
0.0012{c_1}^2c_{23}s_{23}{s_4}^2 - 1.7452e^{-7}c_{23}{s_1}^2s_{23}{s_4}^2 + 0.0012c_{124}s_{134} + \\
0.0012c_{134}s_{124} + 2.6967e^{-5}c_{123}s_{123}{s_4}^2 + 0.0029
\end{gathered}
\tag{91}
$$

$$
\begin{aligned}
\boldsymbol{m_{41}} = {} & 3.9045e^{-8}s_1 - 1.9778e^{-6}c(\theta_4 + 1.6029) - 0.0072s(2\theta_1) \\
& + 4.8499e^{-6}c(\theta_2 + \theta_3)^2 - 8.4387e^{-6}c_2c(\theta_4 + 1.6029) \\
& + 4.7749e^{-9}c_2s_3 + 4.7749e^{-9}c_3s_2 + 1.6659e^{-7}c_2s_4 \\
& - 3.0647e^{-4}c_4c(\theta_5 - 1.5843) - 0.0026c_1{}^2 + 3.4167c(\theta_2 \\
& + \theta_3)^2c_1{}^2 - 7.6194e^{-5}c(\theta_2 + \theta_3)^2s_4{}^2 - 8.7259e^{-8}c_1{}^2c_4{}^2 \\
& + 5.8916e^{-4}c_4{}^2s_1{}^2 - 0.0013c_{24}c(\theta_5 - 1.5843) - 1.5618e^{-8}c_2s_{34} \\
& - 1.5618e^{-8}c_3s_{24} - 3.9327e^{-6}c(\theta_4 + 1.6029)s_{23} \\
& - 1.4410e^{-7}s_{234} + 0.0068c(\theta_2 + \theta_3)^2c_1s_1 - 1.3483e^{-5}c_1c_4{}^2s_1 \\
& + 5.6315e^{-4}c_2s_3c(\theta_5 - 1.5843)^2 \\
& + 5.6315e^{-4}c_3s_2c(\theta_5 - 1.5843)^2 \\
& + 0.0032c(\theta_2 + \theta_3)s(\theta_2 + \theta_3)c_1 \\
& - 3.2188e^{-7}c(\theta_2 + \theta_3)s(\theta_2 + \theta_3)s_1 \\
& + 3.9327e^{-6}c_{23}c(\theta_4 + 1.6029) + 1.4410e^{-7}c_{23}s_4 \\
& + 7.911e^{-7}c_2c(\theta_4 + 1.6029)s_3 + 7.911e^{-7}c_3c(\theta_4 + 1.6029)s_2 \\
& + 7.911e^{-7}s(\theta_5 - 1.5843)s_{234} + 5.8916e^{-4}c_1{}^2c_2{}^2s_3{}^2s_4{}^2 \\
& + 5.8916e^{-4}c_1{}^2c_3{}^2s_2{}^2s_4{}^2 - 8.7259e^{-8}c_2{}^2s_1{}^2s_3{}^2s_4{}^2 \\
& - 8.7259e^{-8}c_3{}^2s_1{}^2s_4{}^2s_4{}^2 + 1.9419e^{-9}c(\theta_2 + \theta_3)c_{14}s_4 \\
& - 0.0012c(\theta_2 + \theta_3)c_4s_{14} - 1.1311e^{-5}c_{234}c(\theta_5 - 1.5843) \\
& + 1.2259e^{-4}c_{24}s_3c(\theta_5 - 1.5843) \\
& + 1.2259e^{-4}c_{34}s_2c(\theta_5 - 1.5843) \\
& - 7.1747e^{-7}s(\theta_5 - 1.5843)c_{23}s_4 \\
& + 1.1311e^{-5}c_4s_{23}c(\theta_5 - 1.5843) \\
& - 5.6315e^{-4}s(\theta_5 - 1.5843)c_4s_{23}c(\theta_5 - 1.5843) \\
& - 1.3483e^{-5}c_1{}^2c_{24}s_{34} - 1.3483e^{-5}c_1{}^2c_{34}s_{24} \\
& + 1.3483e^{-5}c_{24}s_1{}^2s_{34} + 1.3483e^{-5}c_{34}s_1{}^2s_{24} \\
& + 5.6315e^{-4}s(\theta_5 - 1.5843)c_{234}c(\theta_5 - 1.5843) \\
& + 1.3483e^{-5}c_{34}s_1{}^2s_{24} + 1.3483e^{-5}c_1c_3{}^2s_1s_2{}^2s_4{}^2 \\
& - 0.0012c(\theta_2 + \theta_3)c_{12}s_3s_4{}^2 - 0.0012c(\theta_2 + \theta_3)c_{13}s_2s_4{}^2 \\
& - 1.9419e^{-9}c(\theta_2 + \theta_3)c_2s_{13}s_4{}^2 - 1.9419e^{-9}c(\theta_2 + \theta_3)c_3s_{12}s_4{}^2 \\
& + 0.0012c_1{}^2c_{23}s_{23}s_4{}^2 - 1.7452e^{-7}c_{23}s_1{}^2s_{23}s_4{}^2 + 0.0012c_{124}s_{134} \\
& + 0.0012c_{134}s_{124} + 2.6967e^{-5}c_{123}s_{123}s_4{}^2 + 0.0029
\end{aligned} \tag{92}
$$

$$
\begin{gathered}
\boldsymbol{m_{42}} = 4.8499e^{-6}c(\theta_2 + \theta_3)^2 - 0.0072s(2\theta_1) - 0.0026c_1{}^2 - \\
593\left(3.8987e^{-29}c_4 + 3.6601e^{-25}s_4c(\theta_5 - 1.5843)\right)(5.4210e^{-2}c_3 - \\
2.3347e^{-26}s(\theta_5 - 1.5843) + 4.6892e^{-26}) + (c_4s_1 + c_{12}s_{34} + \\
c_{13}s_{24})(5.8916e^{-4}c_4s_1 - 6.7417e^{-6}c_{14} - 5.8418e^{-4}c(\theta_2 + \theta_3)s_4 + \\
5.8418e^{-4}c_{12}s_{34} + 5.8418e^{-4}c_{13}s_{24} + 6.7417e^{-6}c_2s_{134} + 6.7417e^{-6}c_3s_{124}) + \\
(c_2s_{134} - c_{14} + c_3s_{124})(8.7259e^{-8}c_{14} + 6.7417e^{-6}c_4s_1 - 9.7093e^{-10}c(\theta_2 + \\
\theta_3)s_4 + 6.7417e^{-6}c_{12}s_{34} + 6.7417e^{-6}c_{13}s_{24} - 8.7259e^{-8}c_2s_{134} - \\
8.7259e^{-8}c_3s_{124}) + 3.4167c(\theta_2 + \theta_3)^2c_1{}^2 - 2.9278e^{-23}s(\theta_4 + \\
1.6029)(8.6736e^{-26}c_3 - 4.0422e^{-26}) + 0.0068c(\theta_2 + \theta_3)^2c_1s_1 - c(\theta_2 + \\
\theta_3)s_4\left(5.8418e^{-4}c_4s_1 - 9.7093e^{-10}c_{14} + 7.6194e^{-5}c(\theta_2 + \theta_3)s_4 + \\
5.8418e^{-4}c_{12}s_{34} + 5.8418e^{-4}c_{13}s_{24} + 9.7093e^{-10}c_2s_{134} + 9.7093e^{-10}c_3s_{124}\right) + \\
0.0032c(\theta_2 + \theta_3)s(\theta_2 + \theta_3)c_1 - 3.2188e^{-7}c(\theta_2 + \theta_3)s(\theta_2 + \theta_3)s_1 + 0.0029
\end{gathered} \tag{93}
$$

$$
\begin{gathered}
\boldsymbol{m_{43}} = 3.9327e^{-6}s(\theta_4 + 1.6029) - 1.4410e^{-7}c_4 - 0.0072s(2\theta_1) + \\
4.8499e^{-6}c(\theta_2 + \theta_3)^2 - 0.0026c_1{}^2 + 7.1747e^{-7}s(\theta_5 - 1.5843)c_4 - \\
1.1311e^{-5}s_4c(\theta_5 - 1.5843) + 3.4167c(\theta_2 + \theta_3)^2c_1{}^2 - 7.6194e^{-5}c(\theta_2 + \\
\theta_3)^2s_4{}^2 - 8.7259e^{-8}c_1{}^2c_4{}^2 + 5.8916e^{-4}c_4{}^2s_1{}^2 + 0.0068c(\theta_2 + \theta_3)^2c_1s_1 + \\
5.6315e^{-4}s(\theta_5 - 1.5843)s_4c(\theta_5 - 1.5843) - 1.3483e^{-5}c_1c_4{}^2s_1 + 0.0032c(\theta_2 + \\
\theta_3)s(\theta_2 + \theta_3)c_1 - 3.2188e^{-7}c(\theta_2 + \theta_3)s(\theta_2 + \theta_3)s_1 + 5.8916e^{-4}c_1{}^2c_2{}^2s_3{}^2s_4{}^2 + \\
5.8916e^{-4}c_1{}^2c_3{}^2s_2{}^2s_4{}^2 - 8.7259e^{-8}c_2{}^2s_1{}^2s_3{}^2s_4{}^2 - 8.7259e^{-8}c_3{}^2s_1{}^2s_2{}^2s_4{}^2 +
\end{gathered} \tag{94}
$$

$$1.9419e^{-9}c(\theta_2+\theta_3)c_{14}s_4 - 0.0012c(\theta_2+\theta_3)c_4s_{14} - 1.3483e^{-5}c_1{}^2c_{24}s_{34} - 1.3483e^{-5}c_1{}^2c_{34}s_{24} + 1.3483e^{-5}c_{24}s_1{}^2s_{34} + 1.3483e^{-5}c_{34}s_1{}^2s_{24} + 1.3483e^{-5}c_1c_2{}^2s_3{}^2s_4{}^2 + 1.3483e^{-5}c_1c_3{}^2s_1s_2{}^2s_4{}^2 - 0.0012c(\theta_2+\theta_3)c_{12}s_3s_4{}^2 - 0.0012c(\theta_2+\theta_3)c_{13}s_2s_4{}^2 - 1.9419e^{-9}c(\theta_2+\theta_3)c_2s_{13}s_4{}^2 - 1.9419e^{-9}c(\theta_2+\theta_3)c_3s_{12}s_4{}^2 + 0.0012c_1{}^2c_{23}s_{23}s_4{}^2 - 1.7452e^{-7}c_{23}s_1{}^2s_{23}s_4{}^2 + 0.0012c_{124}s_{134}s_4{}^2 + 0.0012c_{134}s_{124} + 2.6967e^{-5}c_{123}s_{123}s_4{}^2 + 0.0029$$

$$m_{44} = -5.6315e^{-4}s(\theta_5-1.5843)^2 + 3.4167c(\theta_2+\theta_3)^2c_1{}^2 + 0.0068c(\theta_2+\theta_3)^2c_1s_1 - 7.6194e^{-5}c(\theta_2+\theta_3)^2s_4{}^2 + 4.8499e^{-6}c(\theta_2+\theta_3)^2 - 0.0012c(\theta_2+\theta_3)c_{12}s_3s_4{}^2 - 0.0012c(\theta_2+\theta_3)c_{13}s_2s_4{}^2 + 1.9419e^{-9}c(\theta_2+\theta_3)c_{14}s_4 + 0.0032c(\theta_2+\theta_3)s(\theta_2+\theta_3)c_1 - 1.9419e^{-9}c(\theta_2+\theta_3)c_2s_{13}s_4{}^2 - 1.9419e^{-9}c(\theta_2+\theta_3)c_3s_{12}s_4{}^2 - 0.0012c(\theta_2+\theta_3)c_4s_{14} - 3.2188e^{-7}s(\theta_2+\theta_3)c(\theta_2+\theta_3)s_1 + 5.8916e^{-4}c_1{}^2c_2{}^2s_3{}^2s_4{}^2 + 0.0012c_1{}^2c_{23}s_{23}s_4{}^2 - 1.3483e^{-5}c_1{}^2c_{24}s_{34} + 5.8916e^{-4}c_1{}^2c_3{}^2s_2{}^2s_4{}^2 - 1.3483e^{-5}c_1{}^2c_{34}s_{24} - 8.7259e^{-8}c_1{}^2c_4{}^2 - 0.0026c_1{}^2 + 1.3483e^{-5}c_1c_2{}^2s_1s_3{}^2s_4{}^2 + 2.6967e^{-5}c_{123}s_{12}s_4{}^2 + 0.0012c_{124}s_{134} + 1.383e^{-5}c_1c_3{}^2s_1s_2{}^2s_4{}^2 + 0.0012c_{134}s_{124} - 1.3483e^{-5}c_1c_4{}^2s_1 - 8.7259e^{-8}c_2{}^2s_1{}^2s_3{}^2s_4{}^2 - 1.7452e^{-7}c_{23}s_1{}^2s_{23}s_4{}^2 + 1.3483e^{-5}c_{24}s_1{}^2s_{24} - 8.7259e^{-8}c_3{}^2s_1{}^2s_2{}^2s_4{}^2 + 1.3483e^{-5}c_{34}s_1{}^2s_{24} + 5.8916e^{-4}c_4{}^2s_1{}^2 - 0.0072 + 0.0034 \quad (95)$$

$$m_{45} = 3.4167c(\theta_2+\theta_3)^2c_1{}^2 + 0.0068c(\theta_2+\theta_3)^2c_1s_1 - 7.6194e^{-5}c(\theta_2+\theta_3)^2s_4{}^2 + 4.8499e^{-6}c(\theta_2+\theta_3)^2 - 0.0012c(\theta_2+\theta_3)c_{12}s_3s_4{}^2 - 0.0012c(\theta_2+\theta_3)c_{13}s_2s_4{}^2 + 1.9419e^{-9}c(\theta_2+\theta_3)c_{14}s_4 + 0.0032s(\theta_2+\theta_3)c(\theta_2+\theta_3)c_1 - 1.9419e^{-9}c(\theta_2+\theta_3)c_3s_{13}s_4{}^2 - 1.9419e^{-9}c(\theta_2+\theta_3)c_3s_{12}s_4{}^2 - 0.0012c(\theta_2+\theta_3)c_4s_{14} - 3.2188e^{-7}s(\theta_2+\theta_3)c(\theta_2+\theta_3)s_1 + 5.8916e^{-4}c_1{}^2c_2{}^2s_3{}^2s_4{}^2 + 0.0012c_1{}^2c_{23}s_{23}s_4{}^2 - 1.3483e^{-5}c_1{}^2c_{24}s_{34} + 5.8916e^{-4}c_1{}^2c_3{}^2s_2{}^2s_4{}^2 - 1.3483e^{-5}c_1{}^2c_{34}s_{24} - 8.7259e^{-8}c_1{}^2c_4{}^2 - 0.0026c_1{}^2 + 1.3483e^{-5}c_1c_2{}^2c_2{}^2s_1s_3{}^2s_4{}^2 + 2.6967e^{-5}c_{123}s_{123}s_4{}^2 + 0.0012c_{124}s_{124} + 1.3483e^{-5}c_1c_3{}^2s_1s_2{}^2s_4{}^2 + 0.0012c_{134}s_{124} - 1.3483e^{-5}c_1c_4{}^2s_1 - 8.7259e^{-8}c_2{}^2s_1{}^2s_3{}^2s_4{}^2 - 1.7452e^{-7}c_{23}s_1{}^2s_{23}s_4{}^2 + 1.3483e^{-5}c_{24}s_1{}^2s_{23} - 8.7259e^{-8}c_3{}^2s_1{}^2s_2{}^2s_4{}^2 + 1.3483e^{-5}c_{34}s_1{}^2s_{24} + 5.8916e^{-4}c_4{}^2s_1{}^2 + 7.1747e^{-7}s(\theta_5-1.5843) - 0.0072s(2\theta_1) + 0.0029 \quad (96)$$

$$m_{51} = 4.8499e^{-6}c(\theta_2+\theta_3)^2 - 0.0072s(2\theta_1) - 0.0026c(2\theta_1)^2 + 3.0647e^{-4}s(\theta_5-1.5843)s_4 + 3.4167c(\theta_2+\theta_3)^2c_1{}^2 - 7.6194e^{-5}c(\theta_2+\theta_3)^2s_4{}^2 - 8.7259e^{-8}c_1{}^2c_4{}^2 + 5.8916e^{-4}c_4{}^2s_1{}^2 + 5.6315e^{-4}s_{234} + 7.1747e^{-7}s(\theta_5-1.5843)c_2s_3 + 7.1747e^{-7}s(\theta_5-1.5843)c_3s_2 + 0.0013s(\theta_5-1.5843)c_2s_4 + 0.0068c(\theta_2+\theta_3)^2c_1s_1 - 1.3483e^{-5}c_1c_4{}^2s_1 + 0.0032c(\theta_2+\theta_3)s(\theta_2+\theta_3)c_1 - 3.2188e^{-7}c(\theta_2+\theta_3)s(\theta_2+\theta_3)s_1 - 5.6315e^{-4}c_{23}s_4 - 1.2259e^{-4}s(\theta_5-1.5843)c_2s_{34} - 1.2259e^{-4}s(\theta_5-1.5843)c_3s_{24} - 1.311e^{-5}s(\theta_5-1.5843)s_{234} + 5.8916e^{-4}c_1{}^2c_2{}^2s_3{}^2s_4{}^2 + 5.8916e^{-4}c_1{}^2c_3{}^2s_2{}^2s_4{}^2 - 8.7259e^{-8}c_2{}^2s_1{}^2s_3{}^2s_4{}^2 - 8.7259e^{-8}c_3{}^2s_1{}^2s_2{}^2s_4{}^2 + 1.9419e^{-9}c(\theta_2+\theta_3)c_{14}s_4 - 0.0012(\theta_2+\theta_3)c_4s_{14} - 7.1747e^{-7}c_{234}c(\theta_5-1.5843) + 1.1311e^{-5}s(\theta_5-1.5843)c_{23}s_4 + 7.1747e^{-7}c_4s_{23}c(\theta_5-1.5843) - 1.3483e^{-5}c_1{}^2c_{24}s_{34} - 1.3483e^{-5}c_1{}^2c_{34}s_{24} + 1.3483e^{-5}c_{24}s_1{}^2s_{34} + 1.3483e^{-5}c_{34}s_1{}^2s_{24} + 1.3483e^{-5}c_1c_2{}^2s_1s_3{}^2s_4{}^2 + 1.3483e^{-5}c_1c_3{}^2s_1s_2{}^2s_4{}^2 - 0.0012c(\theta_2+\theta_3)c_{12}s_3s_4{}^2 - 0.0012c(\theta_2+\theta_3)c_{13}s_2s_4{}^2 - 1.9419e^{-9}c(\theta_2+\theta_3)c_2s_{13}s_4{}^2 - 1.9419e^{-9}c(\theta_2+\theta_3)c_3s_{12}s_4{}^2 + 0.0012c_1{}^2c_{23}s_{23}s_4{}^2 - 1.7452e^{-7}c_{23}s_1{}^2s_{23}s_4{}^2 + 0.0012c_{124}s_{134} + 0.0012c_{134}s_{124} + 2.6967e^{-5}c_{123}s_{123}s_4{}^2 + 0.0029 \quad (97)$$

$$m_{52} = 5.6315e^{-4}c_4 - 0.0072s(2\theta_1) + 1.2259e^{-4}c(\theta_5 - 1.5843) + 4.8499e^{-6}c(\theta_2+\theta_3)^2 - 0.0026c_1^2 - 0.0013s_3c(\theta_5 - 1.5843) - 1.1311e^{-5}s(\theta_5 - 1.5843)c_4 - 7.1747e^{-7}s_4c(\theta_5 - 1.5843) + 3.4167c(\theta_2+\theta_3)^2c_1^2 - 7.6194e^{-5}c(\theta_2+\theta_3)^2s_4^2 - 8.7259e^{-8}c_1^2c_4^2 + 5.8916e^{-4}c_4^2s_1^2 - 0.0013s(\theta_5 - 1.5843)c_{34} + 0.0068c(\theta_2+\theta_3)^2c_1s_1 - 1.3483e^{-5}c_1c_4^2s_1 + 0.0032c(\theta_2+\theta_3)s(\theta_2+\theta_3)c_1 - 3.2188e^{-7}c(\theta_2+\theta_3)s(\theta_2+\theta_3)s_1 + 5.8916e^{-4}c_1^2c_2^2s_3^2s_4^2 + 5.8916e^{-4}c_1^2c_3^2s_2^2s_4^2 - 8.7259e^{-8}c_2^2s_1^2s_3^2s_4^2 - 8.7259e^{-8}c_3^2s_1^2s_2^2s_4^2 + 1.9419e^{-9}c(\theta_2+\theta_3)c_{14}s_4 - 0.0012c(\theta_2+\theta_3)c_4s_{14} - 1.3483e^{-5}c_1^2c_{24}s_{34} - 1.3483e^{-5}c_1^2c_{34}s_{24} + 1.3483e^{-5}c_{24}s_1^2s_{34} + 1.3483e^{-5}c_{34}s_1^2s_{24} + 1.3483e^{-5}c_1c_2^2s_1s_3^2s_4^2 + 1.3483e^{-5}c_1c_3^2s_1s_2^2s_4^2 - 0.0012c(\theta_2+\theta_3)c_{12}s_3s_4^2 - 0.0012c(\theta_2+\theta_3)c_{13}s_2s_4^2 - 1.9419e^{-9}c(\theta_2+\theta_3)c_2s_{13}s_4^2 - 1.9419e^{-9}c(\theta_2+\theta_3)c_3s_{12}s_4^2 + 0.0012c_1^2c_{23}s_{23}s_4^2 - 1.7452e^{-7}c_{23}s_1^2s_{23}s_4^2 + 0.0012c_{124}s_{134} + 0.0012c_{134}s_{124} + 2.6967e^{-5}c_{123}s_{123}s_4^2 + 0.0029 \quad (98)$$

$$m_{53} = 5.6315e^{-4}c_4 - 0.0072s(2\theta_1) + 1.2259e^{-4}c(\theta_5 - 1.5843) + 4.8499e^{-6}c(\theta_2+\theta_3)^2 - 0.0026c_1^2 - 1.1311e^{-5}s(\theta_5 - 1.5843)c_4 - 7.1747e^{-7}s_4c(\theta_5 - 1.5843) + 3.4167c(\theta_2+\theta_3)^2c_1^2 - 7.6194e^{-5}c(\theta_2+\theta_3)^2s_4^2 - 8.7259e^{-8}c_1^2c_4^2 + 5.8916e^{-4}c_4^2s_1^2 + 0.0068c(\theta_2+\theta_3)^2c_1s_1 - 1.3483e^{-5}c_1c_4^2s_1 + 0.0032c(\theta_2+\theta_3)s(\theta_2+\theta_3)c_1 - 3.2188e^{-7}c(\theta_2+\theta_3)s(\theta_2+\theta_3)s_1 + 5.8916e^{-4}c_1^2c_2^2s_3^2s_1^2 + 5.8916e^{-4}c_1^2c_3^2s_2^2s_4^2 - 8.7259e^{-8}c_2^2s_1^2s_3^2s_4^2 - 8.7259e^{-8}c_3^2s_1^2s_2^2s_4^2 + 1.9419e^{-9}c(\theta_2+\theta_3)c_{14}s_4 - 0.0012c(\theta_2+\theta_3)c_4s_{14} - 1.3483e^{-5}c_1^2c_{24}s_{34} - 1.3483e^{-5}c_1^2c_{34}s_{24} + 1.3483e^{-5}c_{24}s_1^2s_{34} + 1.3483e^{-5}c_{34}s_1^2s_{24} + 1.3483e^{-5}c_1c_2^2s_1s_3^2s_4^2 + 1.3483e^{-5}c_1c_3^2s_1s_2^2s_4^2 - 0.0012c(\theta_2+\theta_3)c_{12}s_3s_4^2 - 0.0012c(\theta_2+\theta_3)c_{13}s_2s_4^2 - 1.9419e^{-9}c(\theta_2+\theta_3)c_2s_{13}s_4^2 - 1.9419e^{-9}c(\theta_2+\theta_3)c_3s_{12}s_4^2 + 0.0012c_1^2c_{23}s_{23}s_4^2 - 1.7452e^{-7}c_{23}s_1^2s_{23}s_4^2 + 0.0012c_{124}s_{134} + 0.0012c_{134}s_{124} + 2.6967e^{-5}c_{123}s_{123}s_4^2 + 0.0029 \quad (99)$$

$$m_{54} = 3.4167c(\theta_2+\theta_3)^2c_1^2 + 0.0068c(\theta_2+\theta_3)^2c_1s_1 - 7.6194e^{-5}c(\theta_2+\theta_3)^2s_4^2 + 4.8499e^{-6}c(\theta_2+\theta_3)^2 - 0.0012c(\theta_2+\theta_3)c_{12}s_3s_4^2 - 0.0012c(\theta_2+\theta_3)c_{13}s_2s_4^2 + 1.9419e^{-9}c(\theta_2+\theta_3)c_{14}s_4 + 0.0032s(\theta_2+\theta_3)c(\theta_2+\theta_3)c_1 - 1.9419e^{-9}c(\theta_2+\theta_3)c_2s_{13}s_4^2 - 1.9419e^{-9}c(\theta_2+\theta_3)c_3s_{12}s_4^2 - 0.0012c(\theta_2+\theta_3)c_4s_{14} - 3.2188e^{-7}s(\theta_2+\theta_3)c(\theta_2+\theta_3)s_1 + 5.8916e^{-4}c_1^2c_2^2s_3^2s_4^2 + 5.8916e^{-4}c_1^2c_{23}s_{23}s_4^2 - 1.3483e^{-5}c_1^2c_{24}s_{34} + 5.8916e^{-4}c_1^2c_3^2s_2^2s_4^2 - 1.3483e^{-5}c_1^2c_{34}s_{24} - 8.7259e^{-8}c_1^2c_4^2 - 0.0026c_1^2 + 1.3483e^{-5}c_1c_2^2s_1s_3^2s_4^2 + 2.6967e^{-5}c_{123}s_{123}s_4^2 + 0.0012c_{124}s_{134} + 1.3483e^{-5}c_1c_3^2s_1s_2^2s_4^2 + 0.0012c_{134}s_{124} - 1.3483e^{-6}c_1c_4^2s_1 - 8.7259e^{-8}c_2^2s_1^2s_3^2s_4^2 - 1.7452e^{-7}c_{23}s_1^2s_{23}s_4^2 + 1.3483e^{-5}c_{24}s_1^2s_{34} - 8.7259e^{-8}c_3^2s_1^2s_2^2s_4^2 + 1.3483e^{-5}c_{34}s_1^2s_{24} + 5.8916e^{-4}c_4^2s_2^2 + 7.1747e^{-7}s(\theta_5 - 1.5843) - 0.0072 + 0.0029 \quad (100)$$

$$m_{55} = 3.4167c(\theta_2+\theta_3)^2c_1^2 + 0.0068c(\theta_2+\theta_3)^2c_1s_1 - 7.6194e^{-5}c(\theta_2+\theta_3)^2s_4^2 + 4.8499e^{-6}c(\theta_2+\theta_3)^2 - 0.0012c(\theta_2+\theta_3)c_{12}s_3s_4^2 - 0.0012c(\theta_2+\theta_3)c_{13}s_2s_4^2 + 1.9419e^{-9}c(\theta_2+\theta_3)c_{14}s_4 + 0.0032s(\theta_2+\theta_3)c(\theta_2+\theta_3)c_1 - 1.9419e^{-9}c(\theta_2+\theta_3)c_2s_{13}s_4^2 - 1.9419e^{-9}c(\theta_2+\theta_3)c_3s_{12}s_4^2 - 0.0012c(\theta_2+\theta_3)c_4s_{14} - 3.2188e^{-7}s(\theta_2+\theta_3)c(\theta_2+\theta_3)s_1 + 5.8916e^{-4}c_1^2c_2^2s_3^2s_4^2 + 0.0012c_1^2c_{23}s_{23}s_4^2 - 1.3483e^{-5}c_1^2c_{24}s_{23} + 5.8916e^{-4}c_1^2c_3^2s_2^2s_4^2 - 1.3483e^{-5}c_1^2c_{34}s_{24} - 8.7259e^{-8}c_1^2c_4^2 - 0.0026c_1^2 + 1.3483e^{-5}c_1c_1^2s_1s_3^2s_4^2 + 2.6967e^{-5}c_{123}s_{123}s_4^2 + 0.0012c_{124}s_{134} + 1.3483e^{-5}c_1c_3^2s_1s_2^2s_4^2 + 0.0012c_{134}s_{124} - 1.3483e^{-6}c_1c_4^2s_1 - 8.7259e^{-8}c_2^2s_1s_3^2s_4^2 - 1.7452e^{-7}c_{23}s_1^2s_{23}s_4^2 + 1.3483e^{-5}c_{24}s_1^2s_{34} - \quad (101)$$

$$8.7259e^{-8}c_3{}^2s_1{}^2s_2{}^2s_4{}^2 + 1.3483e^{-5}c_{34}s_1{}^2s_{24} + 5.8916e^{-4}c_4{}^2s_2{}^2 - 0.0072 + 0.0034$$

3.4 Friction

Friction is not considered by the Lagrange-Euler dynamics of the robot manipulator joints. Friction is a very complex process and is a nonlinear phenomenon that is unique to each system [39]. Models of friction include dynamic (viscous) friction and static friction. Static and dynamic friction are defined, for a robot manipulator, as the torque necessary to move the fixed joints of the robot. Static friction indicates that a non-zero torque is needed to initiate joint movement, while dynamic friction indicates the amount of frictional torque that increases as joint speed increases.

Modeling friction force is important for control purposes [40], because it can significantly improve the overall performance of the robot manipulator in terms of accuracy and control stability. Torque control algorithms can also be implemented using axial torque data of the motor rotation axis of the robot manipulator [41]. Friction can be affected by several factors such as temperature, speed, force/torque levels, acceleration, position, and lubricant/grease properties. This poses a major challenge to the robot manipulator, which has very complex dynamics [40]. The literature provides numerous identification methods and friction models, more comprehensive models of friction include dependence on factors such as rotational speed, load, and temperature. Through the Equation (102) [39], the friction torque τ can be calculated, which depends on the load torque L, angular velocity $\dot{\varphi}$ and joint temperature T. In this study, robot friction is not modeled; instead, the rotational friction block is employed to simulate the friction block in contact with spinning components. The friction is calculated as a function of the robotic arm's relative velocity and is supposed to represent the sum of the Stribeck, Coulomb, and viscous friction.

$$\tau(L,\dot{\varphi},T)=\tau_L(L)+\tau_S(\dot{\varphi})+\tau_V(\dot{\varphi},T)+\tau_C \qquad (102)$$

Where τ_L is friction component dependent on load, τ_S is Stribeck friction, τ_V is viscous friction, τ_C is Coulomb friction.

3.5 Simulink Model of DC Motor

DC motor modeling is the process of creating equations that clearly define the connection between input (voltage or current) and output (angular velocity or torque) to achieve the required position, velocity, and acceleration. DC motors play an essential role in control and drive systems, and they are widely employed in mechanical systems such as robotics [42]. DC motors transform electrical energy into mechanical rotational energy, which is paired with mechanical elements to produce the necessary angular motion of the link. DC motors can be controlled by controlling the voltage or current. Equation (103) depicts the connection between motor torque and current.

$$\tau_m(t) = K_m i_a(t) \qquad (103)$$

Where $\tau_m(t)$ is the motor torque, K_m is the motor torque constant, and $i_a(t)$ is the motor current. Equation (104) shows the relationship between the back EMF voltage and the motor shaft speed.

$$v_b = k_m \omega_m \qquad (104)$$

Where v_b is the back EMF voltage, and ω_m is the motor shaft speed of the motor. Equation (105) shows the electric current flowing into the motor.

$$i = \frac{v - v_b}{R_a} \tag{105}$$

Where v is the voltage applied to the motor, and R_a is the resistance of the armature. Equation (106) is obtained by putting the back EMF voltage value from Equation (104) into Equation (105).

$$\omega_m = \frac{v - i\,R_a}{k_m} \tag{106}$$

The motor speed ω_m is calculated by controlling the voltage through this equation. From Equation (107) the torque can be calculated.

$$\tau_m = J\ddot{\theta} \tag{107}$$

Where $\ddot{\theta}$ is the maximum acceleration, and J is the moment of inertia. If the inertia is increased, this will reduce the acceleration of the inertia it contains. The inertia of the motor members can be calculated through Equation (108).

$$J = J_m + J_I \tag{108}$$

Where J_m is the inertia of the motor's rotor and J_I is the coupling inertia, which varies depending on setup and load. Equation (109) is the result of combining Equations (103) and (107).

$$I = \frac{J\ddot{\theta}}{k_m} \tag{109}$$

This equation allows the control of the motor by controlling the electric current flowing to it using feedback from a PID controller. In this work, a DC motor was modeled by feeding the current flowing through it into a PID controller. Five DC motors were linked to the manipulator's arm and controlled by the reference CTC by the control algorithm. Fig. 3 depicts the DC motor in a laboratory setting, while Table 4 lists the DC motor characteristics and values used in the simulation.

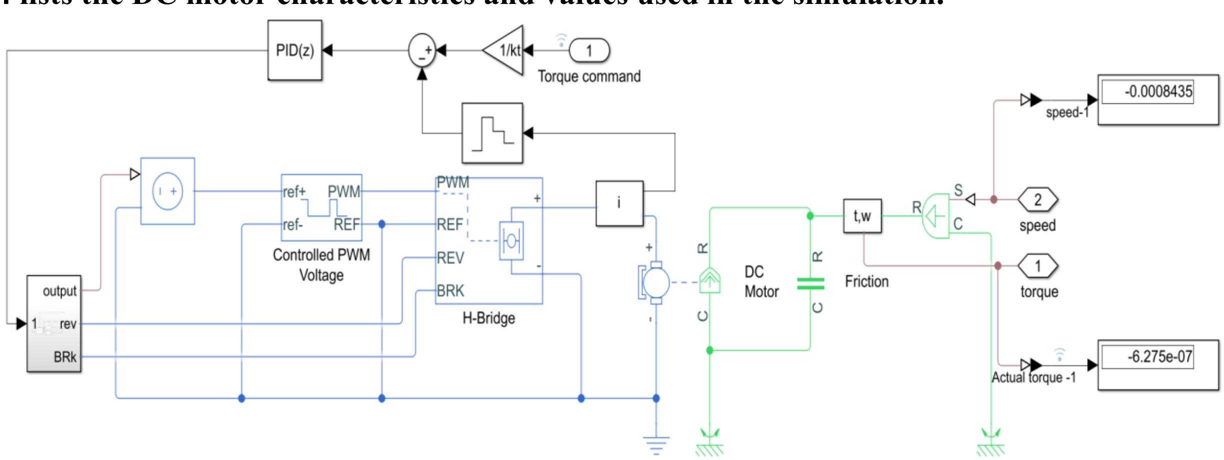

Fig. 3. DC Motor modeling using Simscape Multibody toolbox.

Table 4. Electrical and mechanical parameters of the DC motor used in simulation.

Parameters	Values	Unit
Moment of inertia (Bm)	$47.3e^{-6}$	$N.m/(rad/s)$
Friction coefficient (Jm)	$47.3e^{-6}$	$Kg.m^2$
Back EMF constant (Kb)	0.7	$V/(rad/s)$
Torque constant (Kt)	0.7	Nm/A
Electrical resistance (Ra)	1.5	ohm
Electrical inductance (La)	$170e^{-3}$	H

4 PD/PID CONTROL IN TASK SPACE

The task space is a method for modeling robot manipulator and control dynamics, because its structure provides a dynamic separation between the tasks of the end effector and its dynamics. Control dynamics offer the basis for constructing computational algorithms used in mechanical design, control, and simulation. The goal of mission space control is to control the robot directly within the mission space, and control those errors within that space, that is, instead of choosing q_1, q_2, q_3, q_4, q_5 as the generalized coordinates as in Equation (43), X_1, X_2, X_3, X_4, X_5 are chosen as the generalized coordinates. Equations (110) to (112) [38] represent the differential relationship between the joint coordinates q and the task coordinates of the end effector frame (operational space coordinates) X.

$$x = \mathrm{F(q)} \tag{110}$$

$$\dot{x} = \mathrm{J(q)}.\dot{q} \tag{111}$$

$$\ddot{x} = \mathrm{J(q)}.\ddot{q} + \mathrm{J(q)}.\dot{\mathrm{q}} \tag{112}$$

Where $J(q)$ is the Jacobian matrix, $F(q)$ is the force gradient for the desired position in X, and $q, \dot{q}, \ddot{q}$ represents the position, velocity, and acceleration in the joint space, respectively. $X, \dot{X}, \ddot{X}$ represent the initial position, velocity, and acceleration in the task space. And the desired mission space position, velocity, and acceleration are denoted by $X_d, \dot{X}_d, \ddot{X}_d$ respectively. Equation (43) has been rewritten in task space so that the task dynamics can be determined as in Equation (113) [43]. These dynamics are known as inverse dynamics or CTC. This Equation calculates the force F and multiplies it by $J^T(q)$ to get the torque as in Equation (114). τ is the motor torque for each joint of the robot.

$$M(X)\ddot{X} + \mathrm{C}(\mathrm{X}, \dot{X}) + G(\mathrm{X}) = F \tag{113}$$

$$\tau = J^T(q).F \tag{114}$$

Where $M(X)$ is the mass matrix or the kinetic energy matrix of the end-effector. $C(X, \dot{X})$ is the matrix of the centrifugal force and Coriolis forces of the end-effector. $G(X)$ is the matrix of the gravitational forces of the end-effector. F is the generalized force matrix of the end-effector. $X, \dot{X}, \ddot{X}$ are respectively related to the position, velocity, acceleration and direction of the end-effector. In addition, τ is a matrix related to the robot's torque of the joints. The mass matrix, centrifugal forces matrix, Coriolis forces, and gravitational matrix that were calculated within the joint space are related to the task space as in Equations (115) to (117) [43], respectively.

$$M(X) = (\mathrm{J(q)}M^{-1}(\mathrm{q})J^T(\mathrm{q}))^{-1} \tag{115}$$

$$C(\mathrm{X},\dot{X}) = \left(\mathrm{J}(\mathrm{q})M^{-1}(\mathrm{q})J^{T}(\mathrm{q})\right)^{-1}\left(\mathrm{J}(\mathrm{q})M^{-1}(q) - \dot{J}(q)\dot{q}\right)$$
$$h(q,\dot{q}) = \dot{J}(q)\dot{q} \quad (116)$$

$$G(\mathrm{X}) = \left(\mathrm{J}(\mathrm{q})M^{-1}(\mathrm{q})J^{T}(\mathrm{q})\right)^{-1} J(q)M^{-1}(q)G(q) \quad (117)$$

The control structure can be written as in the Equation (118).

$$F = \widehat{M}(X)F' + \widehat{C}(\mathrm{X},\dot{X}) + \widehat{\mathrm{G}}(X)$$
$$F' = I\ddot{X} \quad (118)$$

Where F' is the input of the end-effector, and $\widehat{M},\widehat{C},\widehat{G}$ refer to the calculated or nominal estimated value of the mass matrix, matrix of the centrifugal force and Coriolis forces, and gravity matrix. It also indicates that feedback linearity in theory cannot be achieved in practice due to the uncertainty in the systems. The site control equation can be written as in Equation (119), and the closed loop of the system is represented as in Equation (120) [37]. The controller of the site will have a linear and discrete behavior, and moving towards the site can be achieved by following this second-order behavior.

$$F' = -K_d(\dot{X} - \dot{X}_d) - K_P(X - X_d) \quad (119)$$

$$I\ddot{X} + K_d(\dot{X} - \dot{X}_d) + K_P(X - X_d) = 0 \quad (120)$$

Where K_p, K_d are the proportional and derivative gain matrices of the PD controller, K_p is the position gain, K_d is the velocity gain, The path tracking equation for the end-effector can be written as in Equation (121), and the closed loop of the system is represented as in Equation (122).

$$F' = I\ddot{X}_d - K_d(\dot{X} - \dot{X}_d) - K_P(X - X_d) \quad (121)$$

$$(\ddot{X} - \ddot{X}_d) + K_d(\dot{X} - \dot{X}_d) + K_P(X - X_d) = 0 \quad (122)$$

This control structure achieves convergent tracking in the task space, as in Equation (123). This equation represents the error dynamics of the linear system. Both error dynamics are highly stable through the appropriate choice of position gain and velocity gain or damping term.

$$\ddot{e} + \dot{K_d}e + K_P e = 0 \quad (123)$$

Where $e, \dot{e}, \ddot{e}$ represent the position error vector of the end-effector, the velocity error, and the acceleration error, respectively, as $e_{(t)} = X - X_d$, $\dot{e}_{(t)} = \dot{X} - \dot{X}_d$, and $\ddot{e}_{(t)} = \ddot{X} - \ddot{X}_d$.

4.1 Simulation of Robot Manipulator

The simulation, control algorithms and mechanical modeling were performed using the MATLAB Simulink environment, by exporting the URDF model of the robot through SolidWorks, and exporting it to the SimScape Multibody environment. Fig. 4 shows the manipulation arm inside MATLAB Simulink.

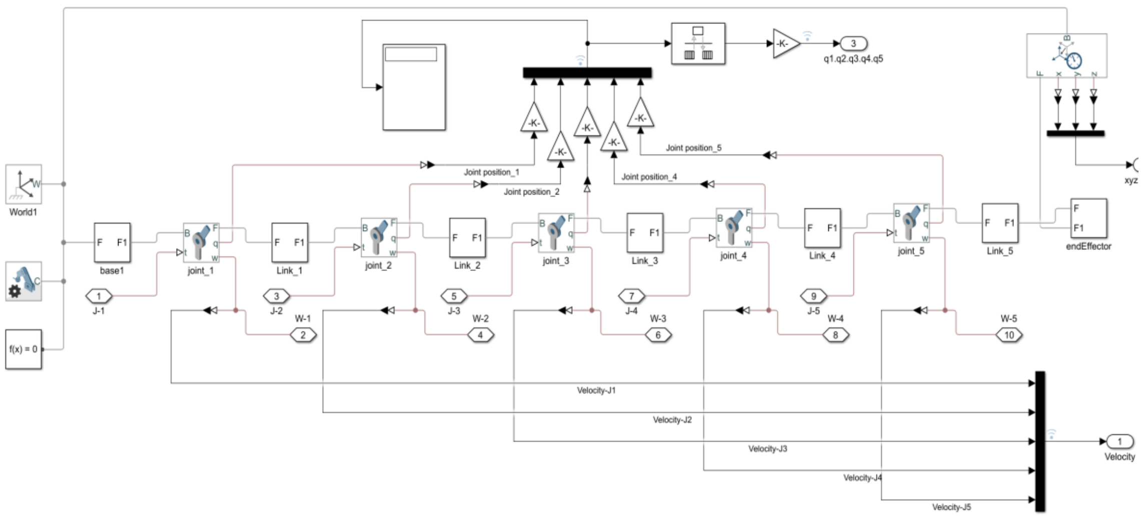

Fig. 4 Dynamics of robot manipulator in the Simscape Multibody Toolbox.

To implement the CTC of the robot in the task space, the control algorithms are created by converting the code created and written in the MLX file into MATLAB functions, and the inputs, outputs, and mathematical relationships between them are defined within each block. Fig. 5 shows the control algorithms in block form that can be used in MATLAB Simulink to simulate the system.

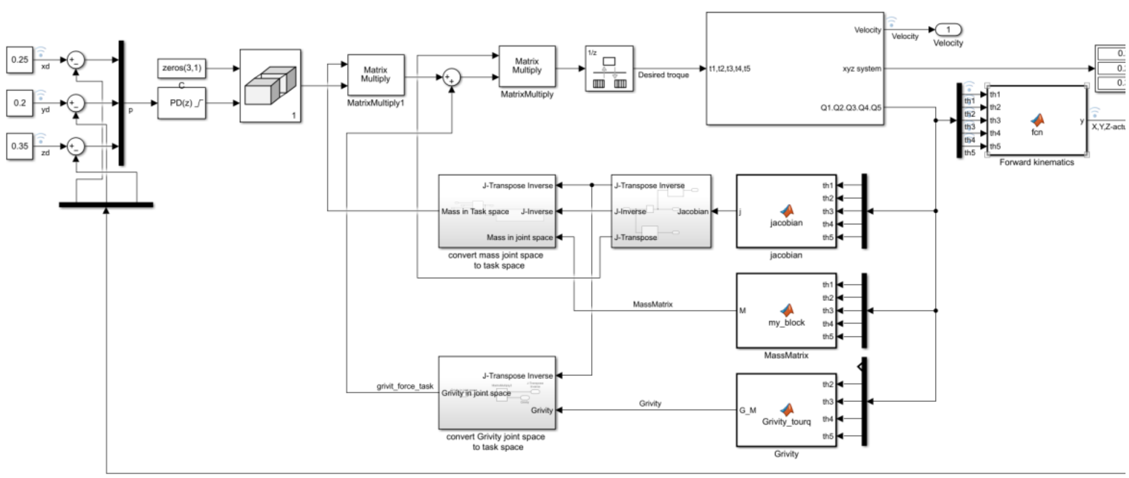

Fig. 5. Simulink model of the Robot controller using PD/PID Computed-Torque Control.

The joint torque is calculated based on the joint angular velocities generated by the control algorithm, and the joint angular velocities measured at the manipulator's joints. This torque is generated using PID controllers, whose parameters are presented in
Table 5. The simulation time in MATLAB is set to stop time simulation at 10 seconds, and the sampling time of the controller is ts = 0.1 sec =10 Hz.

Table 5. PID/PD controllers' gains.

Parameters	P	I	D	Sample time
Link-1 to 4	20	10	0	0.0001
Link-5	20	2	0	-1
PID-Plant gain	20	20	18	0.01
PD-Plant gain	20	0	18	0.01

Note: The simulation time does not match the clock time. The total simulation time depends on many factors such as model complexity, solution step size, and system speed.

In the following figures, simulation results for PD controller are presented as an example. In Fig. 6 the positions reached by the end-effector are shown when using PD controller. The angles of the robot joints are shown in Fig. 7 for the PD controller. The measured torques of the joints for the PD control algorithm are shown in Fig. 8. The linear and angular velocities of the end-effector are shown in Fig. 9. Finally, Fig. 10 shows the linear and angular accelerations of the end-effector for the PD controller.

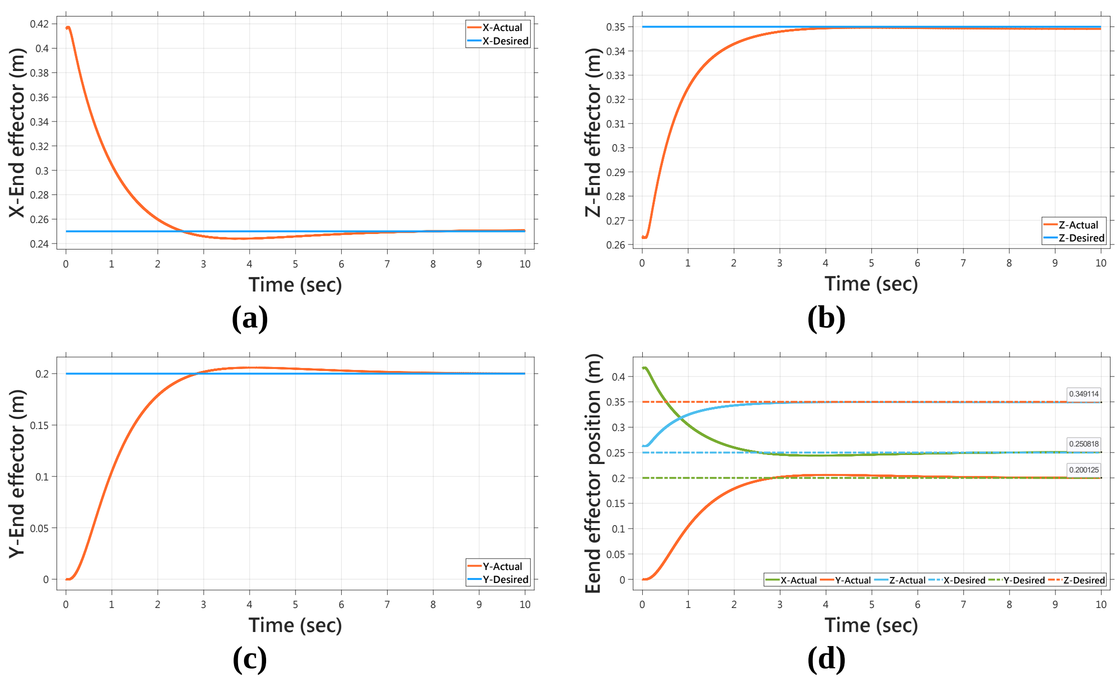

Fig. 6 Simulation results of the position of the end-effector using the PD controller: (a) X-end effector, (b) Z-end effector, (c) Y-end effector, (d) End effector position.

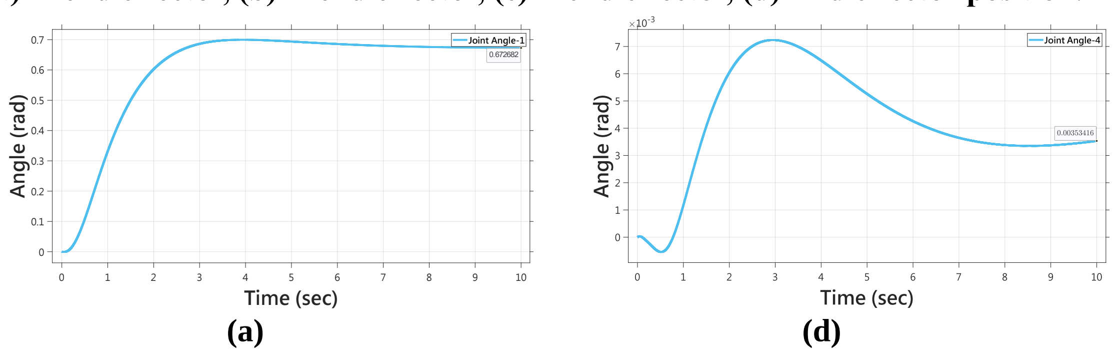

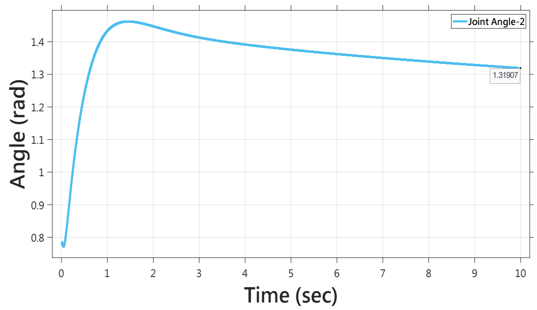

(b)

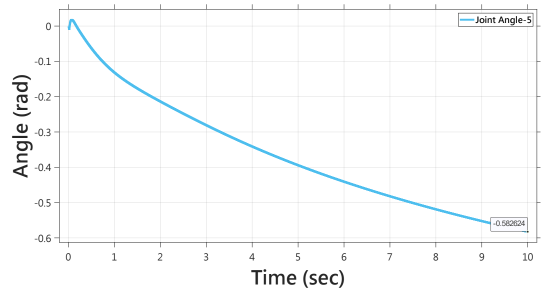

(e)

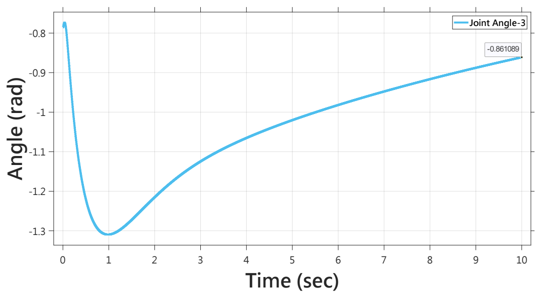

(c)

Fig. 7 Simulation results of robot angles for PD controller: (a) Joint angle 1, (b) Joint angle 2, (c) Joint angle 3, (d) Joint angle 4, (e) Joint angle 5.

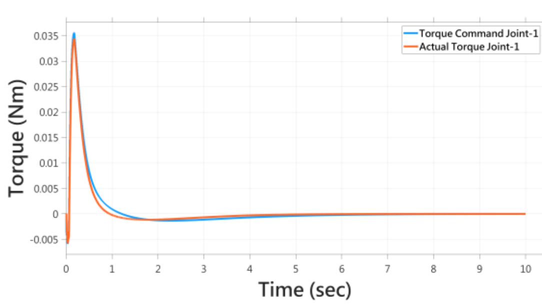

(a)

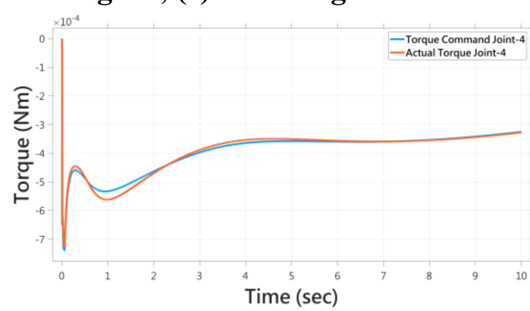

(d)

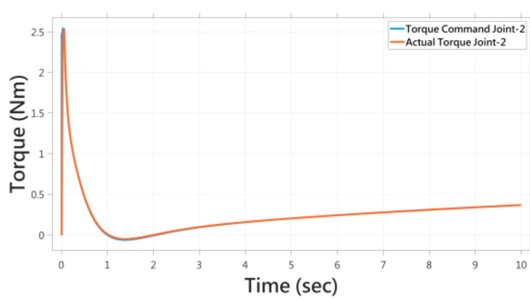

(b)

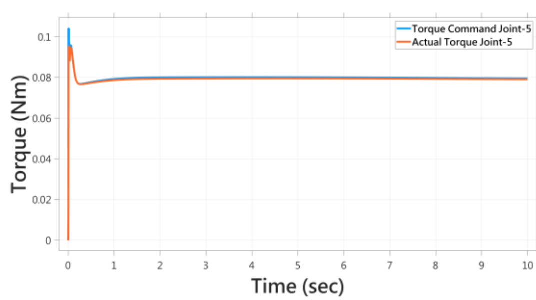

(e)

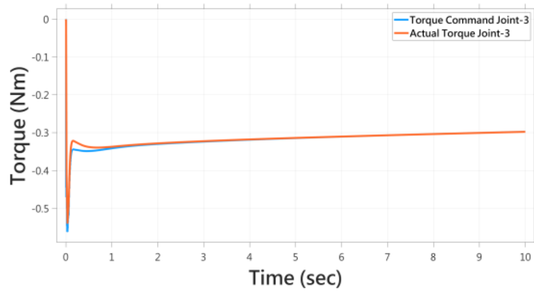

(c)

Fig. 8 Simulation results of the torque of the robot joints for the PD controller: (a) Joint 1, (b) Joint 2, (c) Joint 3, (d) Joint 4, (e) Joint 5.

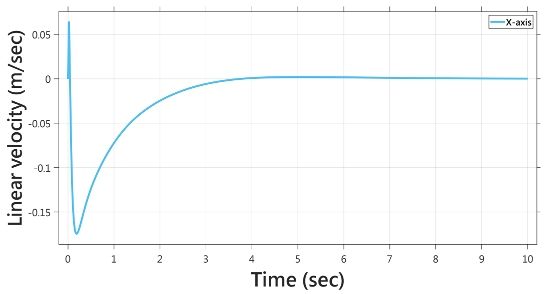

(a)

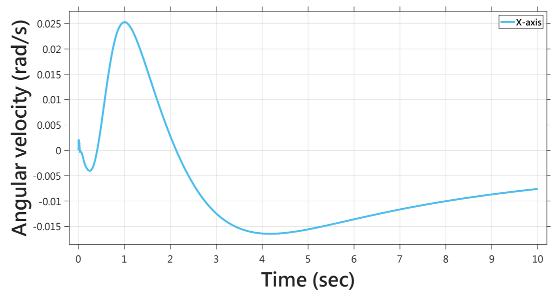

(b)

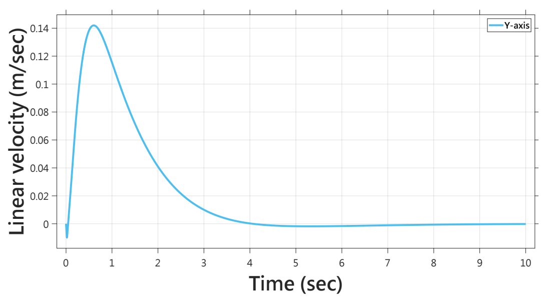

(c)

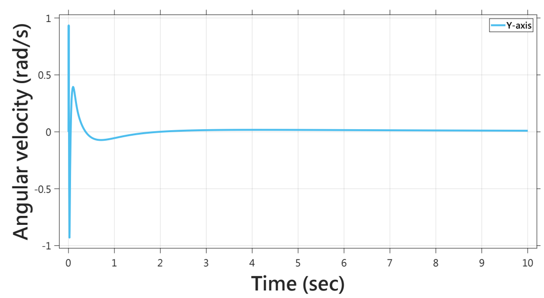

(d)

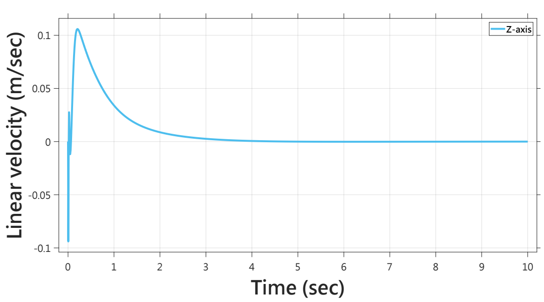

(e)

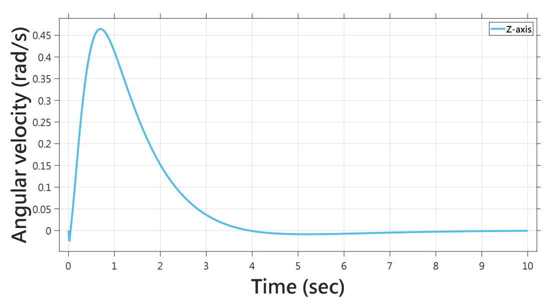

(f)

Fig. 9 Simulation results of linear velocity and angular velocity of the end-effector of the PD controller:(a) linear velocity of x-axis, (b) angular velocity of x-axis, (c) linear velocity of y-axis, (d) angular velocity of y-axis, (e) linear velocity of z-axis, (f) angular velocity of z-axis.

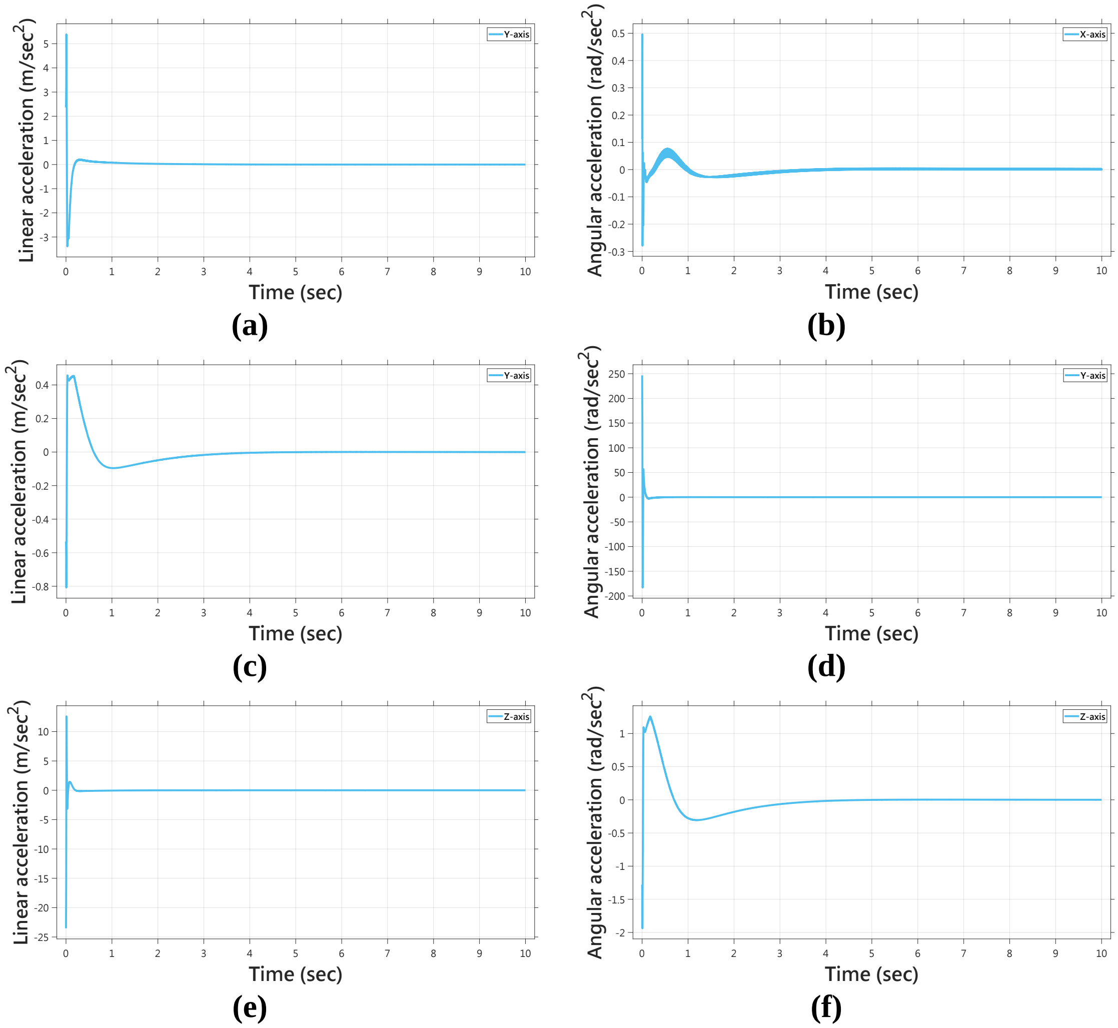

Fig. 10 Simulation results of linear acceleration and angular acceleration of the end-effector of the PD controller: (a) linear velocity of x-axis, (b) angular velocity of x-axis, (c) linear velocity of y-axis, (d) angular velocity of y-axis, (e) linear velocity of z-axis, (f) angular velocity of z-axis.

RESULTS AND DISCUSIONS

The CTC by PID controller and PD controller were tested for the response of positions $x, y, and\ z$. Fig. 11 shows the position of the robot end-effector in Cartesian coordinates. It represents the y-axis versus time representing the x-axis using PID-CTC and PD-CTC without any external load.

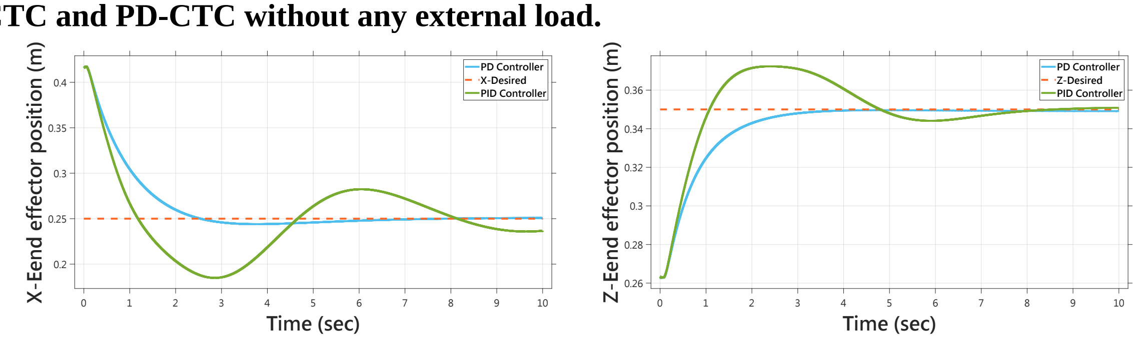

(a) **(c)**

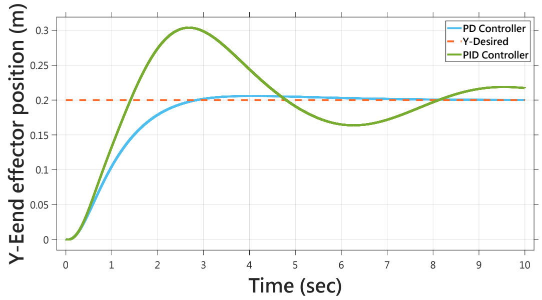

(b)

Fig. 11 Simulation results of the end-effector position of the PD/PID controller: (a) x-end effector position, (b) y-end effector position, (c) z-end effector position.

Based on Fig. 11, by comparing the position of the end-effector, the overshoot of PD-CTC is about (0%) and is less than the overshoot of PID-CTC (6.5%, 10.4%, 2.2%) for $x, y, and\ z$ respectively. The rise time of PD-CTC (1.9 sec, 2.8 sec, 2.48 sec) is slower than PID-CTC (1.11sec, 1.4 sec, 1sec). In addition, the steady-state error of PD-CTC (1mm, 0, 1mm) is less than PID-CTC (13 mm, 17 mm, -1 mm). It is observed that the error of PD-CTC is less than that of PID-CTC. In addition, the settling time of PD-CTC (7.3 sec, 7 sec, 9.14 sec) is faster than PID-CTC (8.13 sec, 9 sec, 9.14 sec). The results show that the position performance of PD-CTC has better accuracy than PID-CTC, but PID-CTC has faster rise time. These results confirm the superiority of PD-CTC over PID-CTC, the maximum error of the y-axis is 17 mm.

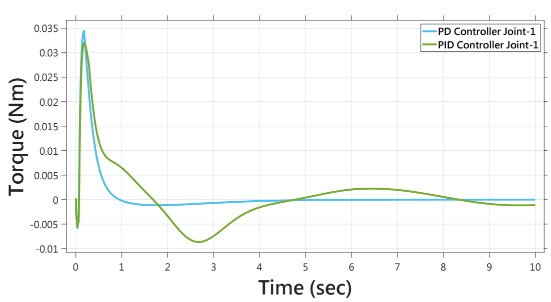

(a)

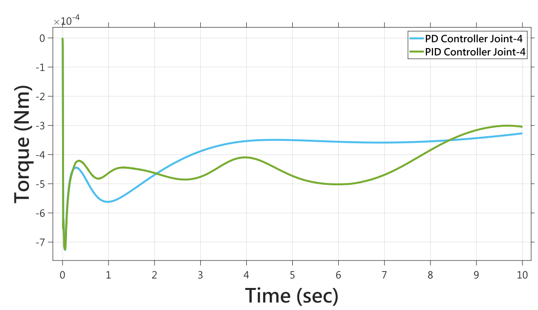

(d)

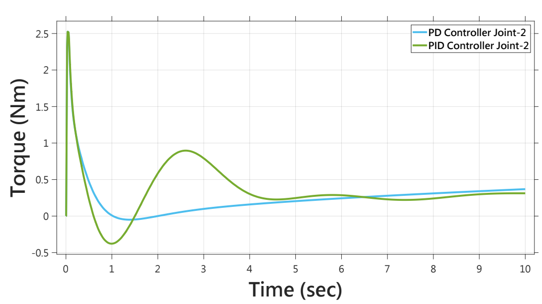

(b)

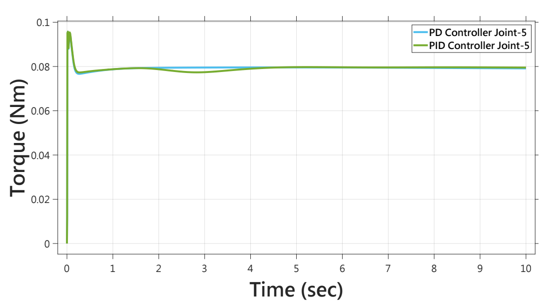

(e)

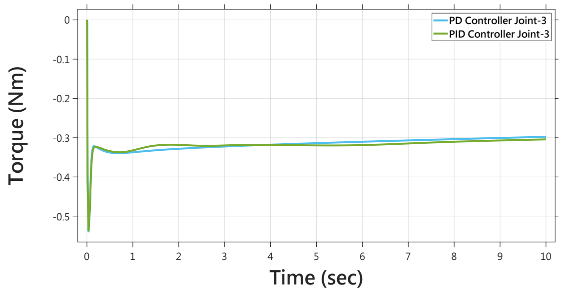

(c)

Fig. 12 Results of simulation of robot joint torque for PD/PID controller: (a) Joint 1, (b) Joint 2, (c) Joint 3, (d) Joint 4, (e) Joint 5.

Figure 12 shows the joint's torque of the robot generated by PD and PID controllers, and it represents the y-axis versus time representing the x-axis. The use of PID-CTC results in higher joint's torque at the first, second, and fourth joints and is significantly applied at the third and fifth joints. The end-acting position is better in the case of PD-CTC.

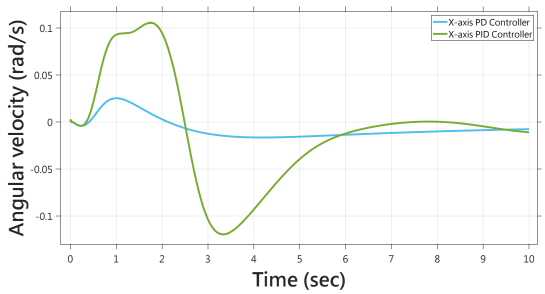

(a)

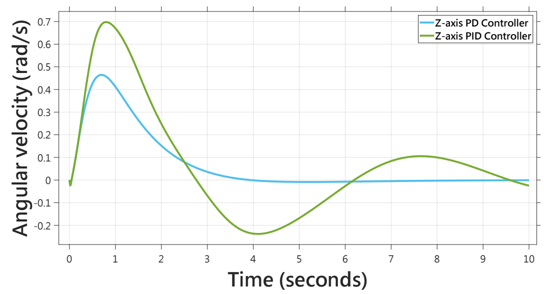

(c)

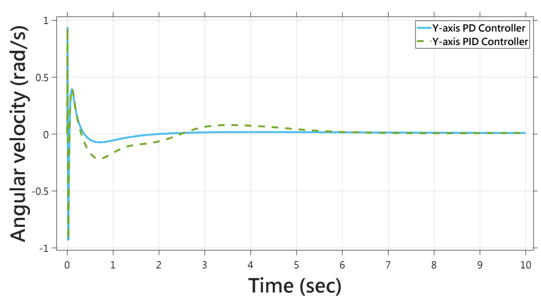

(b)

Fig. 13 Results of simulation of angular velocity of end-effector of PD/PID controller in: (a) x-axis, (b) y-axis, (c) z-axis.

Figure 13 shows the angular velocity of the end effector in $x, y, and\ z$ coordinates respectively, generated by the PD and PID controllers, with the y-axis versus time represented by the x-axis. In the case of PD-CTC (-0.008 rad/sec, 0.01 rad/sec, 0) it is less than PID-CTC (-0.011 rad/sec, 0.01 rad/sec, -0.02 rad/sec), which makes PD-CTC more accurate in reaching the position. In the case of PID-CTC, the robot was faster in the x, and y coordinates by (9.7%, and 24%) respectively, which makes reaching the position faster in the case of PID-CTC.

CONCLUSIONS

This paper provides a 5-degree-of-freedom robot dynamics modeling, simulation, and control using MATLAB. The computed-torque control technique, which is a control technique based on the dynamics of the robot manipulator (model), is used to design a feedback loop, which can approximate the system dynamics as a linear system and eliminate the nonlinearity of the system to take advantage of the linear control techniques PD and PID to achieve the desired response from the end-effector. To model and simulate the robot dynamics, the forward kinematics of the manipulator arm, are calculated. By partial derivation, the Jacobi matrix is calculated to compute the velocity of the manipulator end effector. Again, the Jacobin of the center of mass is calculated to derive the dynamic equations using the Lagrange-Euler equation. The mass matrix and the gravity matrix are calculated, and the calculations are verified by comparing them with the blocks in the MATLAB Library Browser. The equations of motion are formulated in the task space and the PD and PID controllers are designed using the calculated torque control. Simulations are performed using Simscape Multi-body, the data is modeled and analyzed, a comparison is made between PD-CTC and PID-CTC on the same system and under the same simulation conditions. The results prove that PD-CTC is more efficient in reaching the position of the end-effector than PID-CTC, because PD-CTC has a lower steady-state error, overshoot, and settling time while PID-CTC has a lower rise time. The designed platform has great potential in the field of research and academic activities. In future work, computed-torque control will be implemented on a real platform and integrating it with advanced and more complex nonlinear controllers.

REFERENCES

1. Tola D. and Corke P., "Understanding URDF: A Dataset and Analysis," Aug. (2023), [Online]. Available: http://arxiv.org/abs/2308.00514
2. wei Yu Z., feng Liu X., and ping Cai G., "Dynamics modeling and control of a 6-DOF space robot with flexible panels for capturing a free floating target," *Acta Astronaut*, vol. 128, pp. 560–572, Nov. (2016), doi: 10.1016/j.actaastro.2016.08.012.
3. Afzal A., Katz D. S., Le Goues C., and Timperley C. S., "Simulation for robotics test automation: Developer perspectives," in *2021 14th IEEE conference on software testing, verification and validation (ICST)*, IEEE, (2021), pp. 263–274.
4. Feng C., Chen Z., Jin W., and Guo W., "Motion Control and Simulation Analysis of a Manipulator Based on Computed Torque Control Method," in *Lecture Notes in Computer Science (including subseries Lecture Notes in Artificial Intelligence and Lecture Notes in Bioinformatics)*, Springer Science and Business Media Deutschland GmbH, (2023), pp. 10–22. doi: 10.1007/978-981-99-6483-3_2.
5. Urrea C., Saa D., and Kern J., "Automated Symbolic Processes for Dynamic Modeling of Redundant Manipulator Robots," *Processes*, vol. 12, no. 3, Mar. (2024), doi: 10.3390/pr12030593.
6. Zhou Z., Yang X., Wang H., and Zhang X., "Coupled dynamic modeling and experimental validation of a collaborative industrial mobile manipulator with

human-robot interaction," ***Mech Mach Theory*****, vol. 176, Oct. (2022), doi: 10.1016/j.mechmachtheory.2022.105025.**

7. **Gale S., Rahmati H., Gravdahl J. T., and Martens H., "Improvement of a Robotic Manipulator Model Based on Multivariate Residual Modeling,"** ***Front Robot AI*****, vol. 4, Jul. (2017), doi: 10.3389/frobt.2017.00028.**
8. **George Thuruthel T., Renda F., and Iida F., "First-Order Dynamic Modeling and Control of Soft Robots,"** ***Front Robot AI*****, vol. 7, Jul. (2020), doi: 10.3389/frobt.2020.00095.**
9. **Duan H., Dao J., Green K., Apgar T., Fern A., and Hurst J., "Learning Task Space Actions for Bipedal Locomotion," Nov. (2020), [Online]. Available: http://arxiv.org/abs/2011.04741**
10. **Cardona M., Serrano F. E., and García Cena C. E., "Dynamic Modeling and Passivity-Based Control of an RV-3SB Robot,"** ***Actuators*****, vol. 12, no. 9, Sep. (2023), doi: 10.3390/act12090339.**
11. **Le H. N. and Vo N. T., "Modeling and analysis of an RUU Delta Robot using SolidWorks and SimMechanics,"** ***Int J Dyn Control*****, vol. 12, no. 7, pp. 2467–2479, Jul. (2024), doi: 10.1007/s40435-023-01377-1.**
12. **Nguyen-Tuong D., Seeger M., and Peters J., "Computed Torque Control with Nonparametric Regression Models."**
13. ***IROS Madrid 2018 : 2018 IEEE/RSJ International Conference on Intelligent Robots and Systems : Towards a Robotic Society : October, 1-5, 2018, Madrid, Spain, Madrid Municipal Conference Centre*****. IEEE, (2018).**
14. **Tanner H. G. and Kyriakopoulos K. J., "Mobile manipulator modeling with Kane's approach," (2001).**
15. **Korayem M. H., Rahimi H. N., and Nikoobin A.,"Mathematical modeling and trajectory planning of mobile manipulators with flexible links and joints,"** ***Appl Math Model*****, vol. 36, no. 7, pp. 3229–3244, Jul. (2012), doi: 10.1016/j.apm.2011.10.002.**
16. **Dubowsky S., Gu P.-Y., and Deck J. F., "THE DYNAMIC ANALYSIS OF FLEXIBILITY IN MOBILE ROBOTIC MANIPULATOR SYSTEMS," (1991).**
17. **Choi J., Kwon W., Lee Y. S., and Han S., "Adaptive time-delay estimation error compensation for application to robot manipulators,"** ***Control Eng Pract*****, vol. 151, Oct. 2024, doi: 10.1016/j.conengprac.2024.106029.**
18. **Minh Nguyet N. T. and Ba D. X., "A neural flexible PID controller for task-space control of robotic manipulators,"** ***Front Robot AI*****, vol. 9, Jan. (2023), doi: 10.3389/frobt.2022.975850.**
19. **Hadi Barhaghtalab M., Meigoli V., Golbahar Haghighi M. R., Nayeri S. A., and Ebrahimi A., "Dynamic analysis, simulation, and control of a 6-DOF IRB-120 robot manipulator using sliding mode control and boundary layer method,"** ***J Cent South Univ*****, vol. 25, no. 9, pp. 2219–2244, Sep. (2018), doi: 10.1007/s11771-018-3909-2.**
20. **Yu W., "Preliminaries," in** ***PID Control with Intelligent Compensation for Exoskeleton Robots*****, Elsevier, (2018), pp. 1–12. doi: 10.1016/B978-0-12-813380-4.00001-3.**

21. **Sridhar Reddy A., Satish Chembuly V. V. M. J., and Kesava Rao V. V. S., "Dynamic Analysis and Control of Redundant Manipulator for Agricultural Applications in a Virtual Environment,"** ***International Journal of Mathematical, Engineering and Management Sciences*****, vol. 8, no. 4, pp. 710–737, Aug. (2023), doi: 10.33889/IJMEMS.2023.8.4.041.**
22. **Belda K. and Rovný O., "Predictive control of 5 DOF robot arm of autonomous mobile robotic system motion control employing mathematical model of the robot arm dynamics," in** ***2017 21st International Conference on Process Control (PC)*****, IEEE, (2017), pp. 339–344.**
23. **Wang Z., "PREDICTION AND ANALYSIS OF ROBOTIC ARM TRAJECTORY BASED ON ADAPTIVE CONTROL,"** ***Mechatronic Systems and Control*****, vol. 51, no. 10, (2023), doi: 10.2316/J.2023.201-0349.**
24. **Kern J., Marrero D., and Urrea C., "Fuzzy control strategies development for a 3-DoF robotic manipulator in trajectory tracking,"** ***Processes*****, vol. 11, no. 12, p. 3267, (2023).**
25. **Zhou J. and Zhang Q , "Adaptive Fuzzy Control of Uncertain Robotic Manipulator,"** ***Math Probl Eng*****, vol. 2018, (2018), doi: 10.1155/2018/4703492.**
26. **Yu W , "Stable PID Control and Systematic Tuning of PID Gains," in** ***PID Control with Intelligent Compensation for Exoskeleton Robots*****, Elsevier, (2018), pp. 13–33. doi: 10.1016/b978-0-12-813380-4.00002-5.**
27. **Yu W , "PID Control in Task Space," in** ***PID Control with Intelligent Compensation for Exoskeleton Robots*****, Elsevier, (2018), pp. 35–53. doi: 10.1016/b978-0-12-813380-4.00003-7.**
28. **Verma V., Gupta A., Gupta M. K., and Chauhan P., "Performance estimation of computed torque control for surgical robot application,"** ***Journal of Mechanical Engineering and Sciences*****, vol. 14, no. 3, pp. 7017–7028, Sep. (2020), doi: 10.15282/jmes.14.3.2020.04.0549.**
29. **Imran Ullah M., Ali Ajwad S., Ul Islam R., Iqbal U., and Iqbal J., "Modeling and Computed Torque Control of a 6 Degree of Freedom Robotic Arm," (2014).**
30. **Hashemi S. M., Abbas H. S., and Werner H., "Low-complexity linear parameter-varying modeling and control of a robotic manipulator,"** ***Control Eng Pract*****, vol. 20, no. 3, pp. 248–257, Mar. (2012), doi: 10.1016/j.conengprac.2011.11.002.**
31. **Tatjewski P., "Effective Nonlinear Predictive and CTC-PID Control of Rigid Manipulators,"** ***Journal of Automation, Mobile Robotics and Intelligent Systems*****, pp. 1–16, (2024).**
32. **Tola D. and Corke P., "Understanding URDF: A Dataset and Analysis," Aug. (2023), [Online]. Available: http://arxiv.org/abs/2308.00514**
33. **Bellicoso C. D., Buonocore L. R., Lippiello V., and Siciliano B., "Design, modeling and control of a 5-DoF light-weight robot arm for aerial manipulation," in** ***2015 23rd Mediterranean Conference on Control and Automation (MED)*****, IEEE, (2015), pp. 853–858.**
34. **Iliukhin V. N., Mitkovskii K. B., Bizyanova D. A., and Akopyan A. A., "The modeling of inverse kinematics for 5 DOF manipulator,"** ***Procedia Eng*****, vol. 176, pp. 498–505, (2017).**

35. Dikmenli S., "Forward & inverse kinematics solution of 6-dof robots those have offset & spherical wrists," *Eurasian Journal of Science Engineering and Technology*, vol. 3, no. 1, pp. 14–28, (2022).
36. Abdolmalaki R. Y., "Geometric Jacobians derivation and kinematic singularity analysis for smokie robot manipulator & the Barrett WAM," *arXiv preprint arXiv:1707.04821*, (2017).
37. Siciliano B., Sciavicco L.,Villani L., and Oriolo G., *Force control*. Springer, (2009).
38. Siciliano B. and Khatib O. , "Robotics and the Handbook," in *Springer Handbook of Robotics*, Springer, (2016), pp. 1–6.
39. Nevmerzhitskiy M. N., Notkin B. S., Vara A. V., and Zmeu K. V., "Friction model of industrial robot joint with temperature correction by example of KUKA KR10," *Journal of Robotics*, vol. 2019, no. 1, p. 6931563, (2019).
40. Bittencourt A. C., Wernholt E., Sander-Tavallaey S., and Brogårdh T., "An extended friction model to capture load and temperature effects in robot joints," in *2010 IEEE/RSJ international conference on intelligent robots and systems*, IEEE, (2010), pp. 6161–6167.
41. Bittencourt A. C. and Gunnarsson S., "Static friction in a robot joint-modeling and identification of load and temperature effects," (2012).
42. Rashidifar M. A., Rashidifar A. A., and Ahmadi D., "Modeling and Control of 5DOF robot arm using fuzzy logic supervisory control," *IAES International Journal of Robotics and Automation*, vol. 2, no. 2, p. 56, (2013).
43. Nakanishi J., Cory R., Mistry M., Peters J., and Schaal S., "Operational space control: A theoretical and empirical comparison," *Int J Rob Res*, vol. 27, no. 6, pp. 737–757, (2008).